CANADIAN THESES ON MICROFICHE

I.S.B.N.

THESES CANADIENNES SUR MICROFICHE

National Library of Canada
Collections Development Branch

Canadian Theses on
Microfiche Service

Ottawa, Canada
K1A 0N4

Bibliothèque nationale du Canada
Direction du développement des collections

Service des thèses canadiennes
sur microfiche

NOTICE

The quality of this microfiche is heavily dependent upon the quality of the original thesis submitted for microfilming. Every effort has been made to ensure the highest quality of reproduction possible.

If pages are missing, contact the university which granted the degree.

Some pages may have indistinct print especially if the original pages were typed with a poor typewriter ribbon or if the university sent us a poor photocopy.

Previously copyrighted materials (journal articles, published tests, etc.) are not filmed.

Reproduction in full or in part of this film is governed by the Canadian Copyright Act, R.S.C. 1970, c. C-30. Please read the authorization forms which accompany this thesis.

THIS DISSERTATION
HAS BEEN MICROFILMED
EXACTLY AS RECEIVED

AVIS

La qualité de cette microfiche dépend grandement de la qualité de la thèse soumise au microfilmage. Nous avons tout fait pour assurer une qualité supérieure de reproduction.

S'il manque des pages, veuillez communiquer avec l'université qui a conféré le grade.

La qualité d'impression de certaines pages peut laisser à désirer, surtout si les pages originales ont été dactylographiées à l'aide d'un ruban usé ou si l'université nous a fait parvenir une photocopie de mauvaise qualité.

Les documents qui font déjà l'objet d'un droit d'auteur (articles de revue, examens publiés, etc.) ne sont pas microfilmés.

La reproduction, même partielle, de ce microfilm est soumise à la Loi canadienne sur le droit d'auteur, SRC 1970, c. C-30. Veuillez prendre connaissance des formules d'autorisation qui accompagnent cette thèse.

LA THÈSE A ÉTÉ
MICROFILMÉE TELLE QUE
NOUS L'AVONS REÇUE

NL-339 (r. 82/08)

Canada

267

0-315-12578-0

National Library of Canada | Bibliothèque nationale du Canada

Canadian Theses Division | Division des thèses canadiennes

Ottawa, Canada
K1A 0N4

60489

PERMISSION TO MICROFILM — AUTORISATION DE MICROFILMER

• Please print or type — Écrire en lettres moulées ou dactylographier

Full Name of Author — Nom complet de l'auteur

JOHN ROBINSON

Date of Birth — Date de naissance
28/8/1955

Country of Birth — Lieu de naissance
IRELAND

Permanent Address — Résidence fixe
5 PORTMAHON DRIVE RIALTO
DUBLIN (8) IRELAND

Title of Thesis — Titre de la thèse
GLYCEROL-3-PHOSPHATE DEHYDROGENASE AND FUMARATE REDUCTASE OF ESCHERICHIA COLI.

University — Université
UNIVERSITY OF ALBERTA

Degree for which thesis was presented — Grade pour lequel cette thèse fut présentée
PH.D.

Year this degree conferred — Année d'obtention de ce grade
1982

Name of Supervisor — Nom du directeur de thèse
DR JOEL WEINER

Permission is hereby granted to the NATIONAL LIBRARY OF CANADA to microfilm this thesis and to lend or sell copies of the film.

The author reserves other publication rights, and neither the thesis nor extensive extracts from it may be printed or otherwise reproduced without the author's written permission.

L'autorisation est, par la présente, accordée à la BIBLIOTHÈQUE NATIONALE DU CANADA de microfilmer cette thèse et de prêter ou de vendre des exemplaires du film.

L'auteur se réserve les autres droits de publication; ni la thèse ni de longs extraits de celle-ci ne doivent être imprimés ou autrement reproduits sans l'autorisation écrite de l'auteur.

Date
23/6/82

Signature
John Robinson

NL-91 (4/77)

THE UNIVERSITY OF ALBERTA

Studies on Glycerol-3-Phosphate Dehydrogenase and Fumarate Reductase of *Escherichia coli*

by

© John J Robinson

A THESIS

SUBMITTED TO THE FACULTY OF GRADUATE STUDIES AND RESEARCH

IN PARTIAL FULFILMENT OF THE REQUIREMENTS FOR THE DEGREE

OF Doctor of Philosophy

Department of Biochemistry

University of Alberta

Fall, 1982

Microfilming

THE UNIVERSITY OF ALBERTA

RELEASE FORM

NAME OF AUTHOR John J Robinson

TITLE OF THESIS Studies on Glycerol-3-Phosphate Dehydrogenase and Fumarate Reductase of *Escherichia coli*

DEGREE FOR WHICH THESIS WAS PRESENTED Doctor of Philosophy

YEAR THIS DEGREE GRANTED Fall, 1982

Permission is hereby granted to THE UNIVERSITY OF ALBERTA LIBRARY to reproduce single copies of this thesis and to lend or sell such copies for private, scholarly or scientific research purposes only.

The author reserves other publication rights, and neither the thesis nor extensive extracts from it may be printed or otherwise reproduced without the author's written permission.

(SIGNED) John Robinson

PERMANENT ADDRESS:

5 PORTMAHON DRIVE
RIALTO DUBLIN 8
IRELAND

DATED June 23rd 19

THE UNIVERSITY OF ALBERTA

FACULTY OF GRADUATE STUDIES AND RESEARCH

The undersigned certify that they have read, and recommend to the Faculty of Graduate Studies and Research, for acceptance, a thesis entitled Studies on Glycerol-3-Phosphate Dehydrogenase and Fumarate Reductase of *Escherichia coli* submitted by John J Robinson in partial fulfilment of the requirements for the degree of Doctor of Philosophy.

Joel H Weiner
Supervisor

External Examiner

Date Dec. 8th 1982

To my family and my friends.

ABSTRACT

The activation of many purified intrinsic and extrinsic membrane proteins by amphipaths has been well documented. This phenomenon has been studied using the purified aerobic glycerol-3-phosphate dehydrogenase of *E.coli*. This primary dehydrogenase supplies reducing equivalents to the electron transport chain during aerobic growth on glycerol or glycerol-3-phosphate. A broad range of nonionic detergents and phospholipids were found to activate the phenazine methosulfate (PMS)-coupled 3-(4,5-dimethylthiazolyl-2)-2,5-diphenyltetrazolium bromide (MTT) reductase activity while the ferricyanide reductase activity was unaffected. The nonionic detergent Brij 58 was found to be the best activator. Activation was not accompanied by any significant change in quaternary structure or in the affinity of the enzyme for its substrate L-glycerol-3-phosphate. Also, the pH dependence of both activities was identical. However, the reductase activities were differentially inhibited by Cu^{+2} and Zn^{+2}. Cupric sulfate inhibited the PMS/MTT activity while zinc sulfate inhibited the ferricyanide reductase activity. In addition, whereas the apparent Km for DL-glycerol-3-phosphate, as measured by either reductase assay was unaffected by activation, the apparent Km for PMS decreased upon activation while the apparent Km for ferricyanide remained unaffected. Amphipaths appear to be acting at the level of PMS and seem to be enhancing the interaction between this

electron acceptor and the enzyme.

E.coli fumarate reductase, a terminal electron transferring enzyme induced by anaerobic growth in the presence of fumarate, has been characterized. The purified enzyme was shown to exist as an $\alpha\beta$ dimer of 69,000 and 25,000 dalton subunits and bound only 0.15 mg of Triton X-100/mg of protein. The enzyme contained 4-5 moles each of nonheme iron and acid labile sulfur and was inhibited by sulfhydryl reagents. Further investigation of the sensitivity to sulfhydryl reagents revealed a single sensitive sulfhydryl group which was located in the 69,000 dalton subunit. The topology of the 69,000 and 25,000 dalton subunits in the membrane was studied by lactoperoxidase-catalysed ^{125}I-iodination and by antibody titration experiments. The results suggested that both subunits were located on the cytoplasmic side of the plasma membrane.

Further characterization of the purified enzyme revealed that both catalytic activity and stability at alkaline pH or elevated temperatures were enhanced by anions. The effectiveness of anions as activators appeared to correlate with their charge density. Also, reducing agents potentiated the activating effects of anions. Anions appeared to mediate their effects through a direct interaction with the enzyme as indicated by a) a change in the circular dichroic spectrum and b) a decreased susceptibility to inhibition by the sulfhydryl reagent

5,5'-dithiobis(2-nitrobenzoic acid) upon activation.

Investigation of the membrane-bound and Triton X-100 extracted fumarate reductase suggested that it consisted of four subunits of molecular weights 69,000, 25,000, 15,000 and 14,100 present in a molar ratio of 1:1:1:1. The properties of the membrane-bound and Triton X-100 solubilized enzymes were quite similar to the purified, anion activated two subunit form of the enzyme. Anions may be altering the properties of the purified two subunit enzyme in such a way that it more closely resembles the structurally more complex membrane-bound form.

Acknowledgements

I would like to thank my supervisor, Dr Joel Weiner, for his guidance through the course of my graduate studies. His enthusaism was a constant source of encouragement. I would also like to thank Bernie Lemire, Tony Schryvers, Peter Dickie, Elke Lohmeier, Mark Ehrman, Scott Hagen, Heather Dettman, Kelly Dabbs and David Latour for many hours of useful discussion.

I am indepted to many members of the Department of Biochemistry for their willingness to make their research facilities available to me and in many cases for providing assistance in performing experiments. In particular I would like to thank Dr. L. Smillie, M. Natriss and M. Carpenter for help with the amino acid analyses and Dr. C. Kay, K. Oikawa and M. Aarbo for help with the circular dichroic and sedimentation equilibrium analysis. I am grateful to R. Bradley and P d'OBrenan for the photography and graphics in this thesis. I would especially like to thank Dr. W. Bridger for many hours of informative discussions.

Financial support from the Department of Biochemistry and the Alberta Heritage Foundation For Medical Research is gratefully acknowledged.

Table of Contents

Chapter — Page

I. Introduction 1

A. Mechanisms of Energy Coupling. 1

1) Chemiosmotic Coupling Hypothesis. 3

2) Other Models for Energy Coupling. 9

B. Electron Transport Chains of *E.coli*. 10

1) Aerobic Electron Transport Chains. 11

2) Anaerobic Electron Transport Chains. ...16

3) Primary Dehydrogenases. 21

4) Terminal Reductases. 31

C. Thesis Problem. 35

II. General Materials and Methods. 38

A. Materials. 38

1) Chemicals. 38

2) Enzymes. 38

3) Strains. 39

4) Growth Media. 39

B. Methods. 41

1) Purification of the Aerobic Glycerol-3-Phosphate Dehydrogenase. 41

2) Purification of Fumarate Reductase. 43

3) Cholate Depletion of Purified Fumarate Reductase. 45

4) Enzyme Assays. 45

5) Preparation of Kaback Vesicles. 47

6) Preparation of Everted Membrane

Vesicles. 47

7) Preparation of Spheroplasts. 48

8) SDS-Polyacrylamide Gel Electrophoresis. 48

III. The Effect of Amphipaths on the Flavin-Linked Aerobic Glycerol-3-Phosphate Dehydrogenase of *Escherichia coli*. 50

A. Introduction. 50

B. Methods 51

1) Removal of Detergent. 51

2) Phospholipid Titrations. 52

3) Fluorescence Measurements. 52

4) Thermal Stability. 52

5) Chemical Cross-Linking. 53

6) Sedimentation Equilibrium Analysis. 53

7) Circular Dichroic Measurements. 53

8) Ion Effects. 54

9) Km and Vmax Measurements. 54

C. Results. 54

1) Activation by Phospholipids and Detergents. 54

2) Effect of Activation on Quaternary Structure. 58

3) Effect of Activation on Secondary Structure. 64

4) Effect of Activation on Substrate Binding. 64

5) Effect of pH on the Reductase Activities of Activated G3PD. 65

6) Selective Inhibition of the PMS/MTT and Ferricyanide Reductase Activities. 68

7) Effect of Activation on the Apparent

Michaelis-Menten Constants. 73

D. Discussion. 75

IV. Molecular Properties of Fumarate Reductase. 82

A. Introduction. 82

B. Methods. 82

1) Dimethyl Suberimidate Cross-Linking of Fumarate Reductase. 82

2) Isolation of Subunits for Amino Acid Analysis. 83

3) Amino Acid Analysis. 83

4) Two Dimensional Polyacrylamide Gel Electrophoresis. 84

5) Triton X-100 Binding. 85

6) Treatment of Fumarate Reductase with Sulfhydryl Reagents. 86

7) Identification of the Subunit containing the Essential Sulfhydryl Group. 87

8) Effect of p-Chloromercuriphenylsulfonate on the Visible Absorption Spectrum of Fumarate Reductase. 89

9) Iron-Sulfur Content. 89

C. Results. 89

1) Quaternary Structure of Fumarate Reductase. 89

2) Amino Acid Composition and N-Termini of the Separated Subunits. 91

3) Two Dimensional Electrophoretic Analysis of Fumarate Reductase. 94

4) Triton X-100 Binding. 96

5) Inhibition of Fumarate Reductase by Sulfhydryl Reagents. 98

6) Quantitation of Sulfhydryl Groups

Essential for Activity. 101

7) Subunit Localization of the Essential Sulfhydryl. 101

8) Visible Absorption Spectrum and Iron-Sulfur Content. 103

D. Discussion. 108

V. The Sidedness of Fumarate Reductase in the Cytoplasmic membrane of *Escherichia coli*. 110

A. Introduction. 110

B. Methods. 112

1) Preparation of Broken Cells. 112

2) Lactoperoxidase Catalysed Iodination. .112

3) Preparation and Purification of Anti-Fumarate Reductase Gamma Globulin. ..114

4) Titration of Fumarate Reductase with Anti-Fumarate Reductase Gamma Globulin. ..114

C. Results. 115

1) Sidedness of the Active Site of Fumarate Reductase. 115

2) ^{125}I-Iodide Labelling of Everted Membrane Vesicles and Spheroplasts. 116

3) Inhibition of Fumarate Reductase Activity by Antibody. 118

D. Discussion. 121

VI. Effects of Anions on Fumarate Reductase. 123

A. Introduction. 123

B. Methods. 124

1) Titration of Fumarate Reductase with Anions. 124

2) Thermostability of Fumarate Reductase. 124

3) Stability of Fumarate Reductase at Alkaline pH. 124

4) Effect of Alkaline pH on the Visible Absorption Spectrum of Fumarate Reductase. 125

5) Circular Dichroic Spectra of Fumarate Reductase. 125

6) Titration of Fumarate Reductase with DTNB. 126

7) Measurement of the Michaelis-Menten Constants and Maximal Velocities. 126

C. Results. 126

1) Stimulation of Fumarate Reductase Activity by Anions. 126

2) Effect of Anions on Thermostability. ..134

3) Effect of Anions on the Stability of Fumarate Reductase at Alkaline pH. 134

4) Effect of Anions on the Circular Dichroic Spectrum of Fumarate Reductase. .142

5) Effect of Anions on the Sulfhydryl Sensitivity of Fumarate Reductase. 144

6) Effect of Anions on the Catalytic Parameters of Fumarate Reductase. 147

D. Discussion. 150

VII. The Effects of Anions on Membrane-Bound and Triton X-100 Solubilized Fumarate Reductase. ...154

A. Introduction. 154

B. Methods. 155

1) Preparation of Membrane Vesicles and Triton X-100 Extracts. 155

2) Growth of *E.coli* HB101/pfrd63. 156

3) Chemical Cross-Linking. 157

C. Results. 158

1) Anaerobic and Aerobic Expression of Fumarate Reductase in *E.coli* HB101/pfrd63. 158

2) PAGE-SDS Analysis of a Triton X-100 Extract of HB101/pfrd63 Plasma Membranes. 160

3) Chemical Cross-Linking of the Triton X-100 Extract. 162

4) Effect of Anions on Catalytic Activity. 164

5) Effect of Anions on Stability at Alkaline pH. 164

6) Effect of Anions on Thermostability. ..166

D. Discussion. 166

VIII. Conclusions. 172

BIBLIOGRAPHY 177

Appendix I. 186

Appendix II. 187

Appendix III. 189

List of Tables

TABLE 1. *E.coli* strains utilized. 40

TABLE 2. Effect of detergents on G3PD activity. 56

TABLE 3 Effects of amphipaths on the kinetic constants of G3PD. 73

Table 4. The amino acid composition of *E.coli* fumarate reductase and succinate dehydrogenase from beef heart mitochondria and *Rhodospirillum rubrum* chromatophores. 92

TABLE 5. Stimulation of fumarate reductase by anions. ...127

TABLE 6. Dependence of activation of fumarate reductase on the order of addition. 131

TABLE 7. Stability of fumarate reductase at alkaline pH in the absence of anions. 138

TABLE 8. Effect of phosphate on the Km and Vmax for succinate and fumarate. 148

TABLE 9. Aerobic and anaerobic expression of fumarate reductase in HB101/pfrd63. 159

TABLE 10. Effect of anions on the catalytic activity of membrane-bound and Triton X-100 solubilized fumarate reductase. 165

List of Figures

Figure 1. Energy transduction in membrane systems. 7

Figure 2. The aerobic electron transport chain of *E.coli* as proposed by Haddock and Jones. 13

Figure 3. The aerobic electron transport chain of *E.coli* as proposed by Downie and Cox. 15

Figure 4. The *E.coli* anaerobic electron transport chain to nitrate reductase. 17

Figure 5. The *E.coli* anaerobic electron transport chain to fumarate reductase. 20

Figure 6. The effect of fatty acyl chain length on the PMS-coupled MTT reducing activity of G3PD. 55

Figure 7. Correlation between Brij 58 mediated quenching of tryptophan fluorescence and stimulation of PMS-coupled MTT reduction. 59

Figure 8. Thermal stability of G3PD in the presence and absence of Brij 58. 60

Figure 9. Densitometric scan of the SDS-PAGE electrophoretic pattern of G3PD cross-linked by dimethyl suberimidate. 62

Figure 10. Lactoperoxidase catalysed iodination of G3PD in Brij buffer. 63

Figure 11. Fluorescence titration curves of G3PD. 66

Figure 12. The pH dependence of the PMS/MTT and ferricyanide reductase activities of G3PD. 67

Figure 13. Inhibition of G3PD activity by cupric sulfate. 69

Figure 14. Inhibition of G3PD activity by zinc sulfate. ..70

Figure 15. Densitometric scan of the SDS-PAGE electrophoretic pattern of cross-linked and non cross-linked cholate-depleted fumarate reductase. 90

Figure 16. Amino terminal sequence of the 25,000 dalton subunit of fumarate reductase. 93

Figure 17. Two dimensional electrophoresis of purified fumarate reductase. 95

Figure 18. Binding of Triton X-100 to cholate-depleted fumarate reductase. 97

Figure 19. Sulfhydryl sensitivity of fumarate reductase. .99

Figure 20. Sulfhydryl sensitivity of fumarate reductase. 100

Figure 21. Quantitation of the sensitive sulfhydryl group of cholate-depleted fumarate reductase. 102

Figure 22. Localization of the essential sulfhydryl group of fumarate reductase. 104

Figure 23. The visible absorption spectrum of fumarate reductase before and after treatment with p-CMS. 105

Figure 24. Comparison of the probable iron-sulfur centre(s) of fumarate reductase with those of a ferredoxin from *Peptococcus aerogenes*. 107

Figure 25. Lactoperoxidase catalysed iodination of spheroplasts and everted membrane vesicles. 117

Figure 26. Inhibition of fumarate reductase activity with anti-fumarate reductase antibody. 119

Figure 27. Stimulation of fumarate reductase activity by phosphate and dithiothreitol. 129

Figure 28. Stimulation of cholate-depleted fumarate reductase by phosphate esters. 132

Figure 29. Thermostability of fumarate reductase. 135

Figure 30. Stability of fumarate reductase at alkaline pH. 136

Figure 31. Effect of alkaline pH on the visible absorption spectrum of fumarate reductase. 140

Figure 32. The far ultraviolet circular dichroic spectrum of cholate-depleted fumarate reductase. 143

Figure 33. Sensitivity of fumarate reductase to inhibition by DTNB. 145

Figure 34. Lineweaver-Burk plots of the succinate dehydrogenase activity of fumarate reductase. 149

Figure 35. Densitometric scan of an 8-22% (w/v) gradient Laemmli gel of a Triton X-100 extract of HB101/pfrd63 plasma membranes. 161

Figure 36. First and second dimension gels of the cross-linked Triton X-100 extract of HB101/pfrd63 plasma membranes. 163

Figure 37. Stability of membrane-bound and Triton X-100 extracted fumarate reductase at alkaline pH. 167

Figure 38. Thermostability of membrane-bound and Triton X-100 extracted fumarate reductase. 168

List of Abbreviations

ADP	adenosine-5'-diphosphate
AMP	adenosine-5'-monophosphate
ATP	adenosine-5'-triphosphate
DCPIP	dichlorophenolindophenol
DTNB	5,5'-dithiobis-(-2 nitrobenzoic acid)
DTT	dithiothreitol
EDTA	ethylenediamine tetraacetic acid
FAD	flavin adenine dinucleotide
Fe/S	iron-sulfur protein(s)
FMN	flavin mononucleotide
Fp	flavoprotein
G3PD	aerobic glycerol-3-phosphate dehydrogenase
Hepes	N-2-hydroxyethyl-piperazine-N'-2-ethanesulfonic acid
HOQNO	2-N-heptyl-4-hydroxyquinoline-N-oxide
MTT	3-(4,5-dimethylthiazolyl-2)-2,5-diphenyltetrazolium bromide
MK	menaquinone

NAD^+	nicotinadide adenine dinucleotide, oxidized form
NADH	nicotinamide adenine dinucleotide, reduced form
p-CMB	p-chloromercuribenzoic acid
p-CMS	p-chloromercuriphenylsulfonic acid
PMS	phenazine methosulfate
Q	ubiquinone
SDS	sodium dodecyl sulfate
SDS-PAGE	sodium dodecyl sulfate polyacrylamide gel electrophoresis
TEMED	tetramethylethylenediamine

I. Introduction

A. Mechanisms of Energy Coupling.

All living organisms require energy for the following functions: a) mechanical work, b) biosynthetic processes and c) transport of metabolites across cellular and sub-cellular membranes. In other words living organisms maintain their complex low entropy structures by consuming energy from their environment. Waste energy in the form of heat is then returned to the environment where it has a randomizing effect. Plants and some bacteria convert solar energy into chemical energy in the form of glucose. Subsequent degradation of glucose generates ATP and NADPH. Similarily, in animals and some bacteria, degradation of catabolites generates ATP and NADPH. Thus all forms of life use ATP and NADPH, transportable and immediately useable forms of chemical energy, to maintain life. The question of how cells make ATP and NADPH from glucose was partially answered when the pathways of intermediary metabolism were elucidated. NADPH can be generated by the oxidation of glucose in the Pentose Phosphate Pathway as well as by the action of the enzyme transhydrogenase. ATP can be synthesized by the substrate level phosphorylation of ADP and GDP during glycolysis and the Krebs cycle respectively. In animal tissues the GTP generated during the Krebs cycle can be used to phosphorylate ADP while in *E.coli* ATP is generated directly from ADP during substrate level phosphorylation.

However, despite the discovery of substrate level phosphorylation it was realized that this process alone could not meet the energy requirements of aerobic organisms. Since the discovery of ATP in 1929 the mechanism of its synthesis has been a major area of biochemical research. In 1940 Ochoa (1), while studying the P/O ratio for the oxidation of pyruvate, proposed that phosphorylation must occur not only when the substrate is oxidized during glycolysis but also during the passage of hydrogen atoms along the respiratory chain to oxygen. In 1951 Gale and Paine (2) demonstrated that glumatate transport in *Staphylococcus aureus* was inhibited by such compounds as sodium azide and 2,4-dinitrophenol. This observation established a link between electron transport and/or oxidative phosphorylation and the active transport of glutamate. With the development of methodology for the preparation of closed membrane vesicles (3) it has become apparent that electron flow down the respiratory chain drives the transport of many different metabolites across the bacterial plasma membrane.

Although research during the past forty years has shown that a number of cellular processes are dependent upon a functioning electron transport chain, the mechanism by which the free energy released by electron transport is conserved and used has remained controversial. Indeed, it is only in the past ten years that the chemiosmotic coupling hypothesis, proposed by Peter Mitchell in 1961 (4), has

gained wide acceptance. This hypothesis will be discussed in detail in this chapter. The other major hypotheses of energy coupling will only be briefly discussed here.

1) Chemiosmotic Coupling Hypothesis.

The chemiosmotic coupling hypothesis of Peter Mitchell developed from his interest in the coupling between metabolic energy and membrane transport. The hypothesis consists of the following postulates (5);

1) The ATP synthetase is a membrane-bound reversible proton translocating ATPase, having a characteristic H^+/P stoichiometry.

2) Respiratory and photoredox chains are membrane-bound vectorial metabolic proton translocating systems, having characteristic $H^+/2e$ stoichiometries and having the same polarity for proton translocation across the membrane during normal forward redox activity as the ATPase has for ATP hydrolysis.

3) There are proton-linked solute porter systems for osmotic stabilization and metabolite transport.

4) Systems 1-3 are plugged through a topologically closed insulating membrane, called the coupling membrane, that has a non-aqueous osmotic barrier phase of low permeability to solutes in general and to protons and hydroxyl ions in particular.

Postulate 2 was expanded to define electron transport chains as consisting of alternating hydrogen and electron carriers arranged asymmetrically across the membrane in loops.

Essentially the chemiosmotic coupling hypothesis can be summarized by pathway 1;

(1) Oxidation $\longrightarrow \Delta\bar{\mu}_{H^+} \longleftrightarrow$ ATP

oxidation and phosphorylation are coupled via a transmembrane electrochemical potential of protons. The electrochemical potential or proton motive force is made up of an electrical component $\Delta\psi$ and a chemical component, ΔpH, as defined in equation 2;

(2) $$\Delta\bar{\mu}_{H^+} = \Delta\psi - Z\Delta pH$$

$Z=2.3RT/F$ and has a value of 58.8 mV at room temperature.

The basic postulates of the chemiosmotic hypothesis have been rigorously tested in the twenty years since its conception. Moyle and Mitchell (6) and Thayer and Hinkle (7) have shown that ATP hydrolysis by beef heart mitochondrial ATPase results in extrusion of protons. In these experiments an H^+/P value of 2 was obtained. Furthermore, *E.coli* plasma membranes containing an ATPase mutated in the α subunit (uncA mutants), do not show ATP dependent membrane energization (8). The proton pumping activity of yeast ATPase, reconstituted into liposomes, has also been demonstrated (9). Mitchell and Moyle (10,11) have also shown proton extrusion during mitochondrial electron transport. By measuring the acidification of the suspending medium following the addition of pulses of oxygenated saline to an anaerobic suspension of mitochondria, they estimated that two protons were extruded per redox loop. An electrochemical potential of 230 mV has been measured in rat liver

mitochondria oxidizing β-hydroxybutyrate in the absence of phosphate (12).

The role of the proton motive force in energizing bacterial transport systems has been reviewed (12,13). In general the results agree with Mitchell's hypothesis (14) of transport being driven by one of the following; a) a symport with protons, b) an antiport with protons or c) in response to the electrical potential component of the proton motive force. However, for symport systems the stoichiometry of protons/solutes transported has not been completely resolved (15).

The key requirement of the chemiosmotic hypothesis is that the membrane should be largely impermeable to protons and hydroxyl ions. Mitchell has measured a conductance of 0.5 μmho cm^{-2} for the inner mitochondrial membrane. This conductance is compatable with the chemiosmotic hypothesis. The inability of opponents to demonstrate oxidative phosphorylation in soluble preparations has added credence to Mitchell's hypothesis.

In my opinion the single most convincing piece of evidence in favour of ATP synthesis being driven by a gradient of protons comes from an experiment of Racker and Stockenius (16). In an elegant experiment they reconstituted the mitochondrial F_oF_1 ATPase and the light driven proton pump, bacteriorhodopsin, into liposomes. They were then able to demonstrate ATP synthesis in response to a light pulse. A similar experiment has been performed using the yeast F_oF_1

ATPase (9). These experiments clearly demonstrated that a proton gradient could drive the synthesis of ATP by the ATPase complex. In addition, these experiments showed that ATP synthesis did not require a physical interaction between the respiratory chain components and the ATPase.

Although it is now largely accepted that the high energy intermediate coupling the redox reactions of electron transport to the performance of energy requiring membrane functions such as ATP synthesis and membrane transport is an electrochemical gradient of protons, Figure 1, there is a considerable amount of controversy surrounding the mechanisms of generation and utilization of the proton motive force. Inherent in Mitchell's hypothesis is the requirement for alternating hydrogen and electron carriers arranged asymmetrically across the energy transducing membrane in a series of redox loops. Such an arrangement would facilitate charge separation between protons and electrons and lead to the extrusion of protons from the cell or organelle and the generation of a gradient of protons. Mitchell suggests a $H^+/2e$ ratio of 6; two protons being ejected at each of three redox loops. However, topology studies on the inner mitochondrial membrane have not confirmed the existance of three loops (17) and Mitchell has since modified his views to accomodate this finding. He now proposes a special role for ubiquinone and cytochrome b in what has become known as the Q cycle (18). This cycle accounts for only two redox loops while still maintaining a

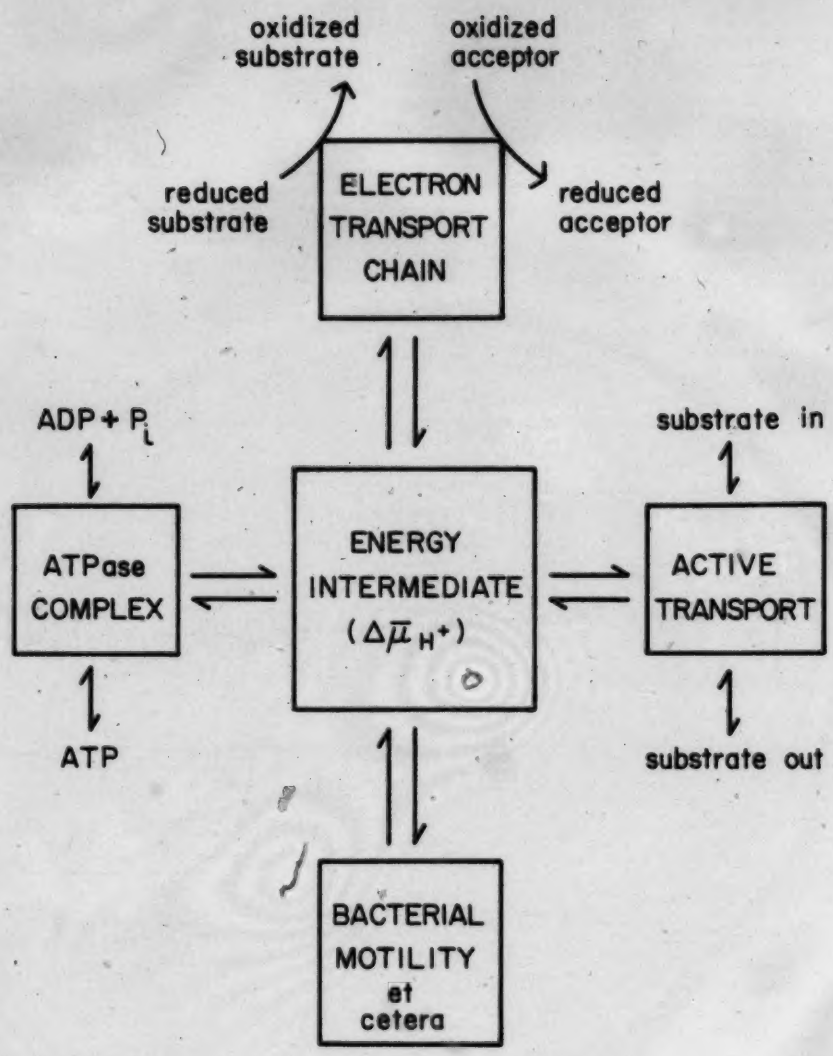

Figure 1. Energy Transduction in Membrane Systems. The above figure is a schematic representation of a general energy transduction scheme.

$H^+/2e$ ratio of 6. However, the discovery of the proton pumping activity of bacteriorhodopsin (19) and the mitochondrial cytochrome oxidase (20) has led to the suggestion that the proton motive force may be generated by a proton pumping activity of the components of the respiratory chain (21).

Another point of contention is Mitchell's H^+/site ratio of 2. Brand *et al* (22) have measured a H^+/site ratio of 3-4 and suggest that Mitchell's ratio may be low due to the uptake of a proton with inorganic phosphate during mitochondrial respiration.

The mechanism by which a proton gradient drives the synthesis of ATP is also unresolved. Three mechanisms have been proposed:

a) As proposed by Mitchell (23) ATP synthesis is a result of the protonation of a phosphate molecule by two protons followed by a nucleophilic attack by ADP.

b) Racker (24) has proposed that an interaction between the F_1 component of the ATPase and Mg^{+2} induces a conformational change in F_1 which leads to the formation of a high energy phosphoenzyme intermediate. Interaction between the phosphoenzyme and ADP leads to the formation of ATP and a dephosphorylated F_1. Protons then displace the Mg^{+2} ions and allow the F_1 to return to the deactivated conformation ready for another cycle of ATP synthesis. This mechanism is based on the known mechanisms of Ca^{+2} and Na^+/K^+ ATPases, enzymes which are structurally much simpler

than the F_0F_1 ATPase complexes of energy transducing membranes.

c) The third mechanism was proposed by Boyer and his colleagues (25,26,27). As a result of the effect of uncouplers on various exchange reactions catalysed by mitochondria, Boyer has suggested that the energized state of the membrane regulates ADP and Pi binding to and ATP release from the F_0F_1 ATPase. According to the alternating catalytic site model energy is required for the binding of ADP and Pi to the ATPase in a manner which favours ATP formation while release of preformed ATP at a second catalytic site also requires the input of energy. ATP synthesis *per se* does not require the input of energy. This model is indirectly supported by the finding of tightly bound ADP and ATP on the ATPases from mitochondria, chloroplasts and bacteria.

2) Other Models for Energy Coupling.

As originally proposed by Boyer (28) the conformational coupling hypothesis requires a physical interaction between the electron transport proteins and the ATPase complex. Boyer suggested that the free energy of electron transport reactions is conserved in the form of high energy protein conformations. This conformational energy is transmitted to the ATPase with the resultant synthesis of ATP. There has never been more than circumstantial evidence for conformational coupling and the hypothesis has been adapted as a mechanism of ATP synthesis, as described above.

The first model of oxidative phosphorylation was the chemical coupling hypothesis of Slater (29). The proposed mechanism is analogous to the substrate level phosphorylation of ADP during glycolysis. Essentially, Slater postulated that redox energy is conserved in the form of a high energy covalently modified electron carrier. Synthesis of ATP is then driven, through a series of high energy intermediates, by hydrolysis of this high energy bond. Extensive research has failed to find any of the postulated high energy intermediates and the hypothesis has been largely abandoned.

Williams (30) has postulated that during electron transport protons, generated within the membrane, are transmitted via channels to the site of ATP synthesis. Transmission would be by hydronium ion formation using water molecules within the proton channels. ATP formation would be driven by the removal of water, a product of the condensation of ADP and Pi, by the need to hydrate the high energy protons in the vicinity of the ATPase. Although this model is difficult to evaluate it has not been entirely discarded.

B. Electron Transport Chains of *E.coli*.

E.coli is a facultative anaerobe, being able to grow both aerobically and anaerobically. Energy for growth can be derived both fermentatively, via glycolysis, and oxidatively, using either oxygen, nitrate or fumarate as

terminal electron acceptors. A variety of substrates can be used to provide reducing equivalents for the respiratory chain. Thus, NADH, succinate, malate, D- and L-lactate, α-hydroxybutyrate, L-glycerol-3-phosphate, formate, dihydroorotate and pyruvate can all be oxidized by primary dehydrogenases which serve as components of electron transport chains. The compositions of these chains vary with the carbon sources available for growth, the growth phase and the terminal electron acceptor present. At present the function of all the redox components found in the *E.coli* plasma membrane is not known. Also, the involvement of some electron transport proteins in more than one chain is uncertain at present. Finally, the sidedness of the cytochrome components in the aerobic and anaerobic electron transport chains of *E.coli* has been deduced largely from the sequence of components and the chemiosmotic requirement for alternating hydrogen and electron carriers arranged asymmetrically across the membrane.

In this section the aerobic and anaerobic electron transport chains will be described and then the properties of the primary dehydrogenases and terminal reductases will be discussed.

1) Aerobic Electron Transport Chains.

The *E.coli* aerobic electron transport chain contains nonheme iron, acid labile sulfur, ubiquinone, flavoproteins and cytochromes b_{558}, b_{562}, b_{595}, a_1, o and d (31). Cytochromes c_{550} and c_{552} are also present but are

considered to be minor components. Cytochromes o and d are the major terminal oxidases, while cytochrome a, appears not to be kinetically competent as a terminal electron transfer enzyme (32). Although the factors regulating the levels of the different cytochromes are poorly understood, it seems clear that in exponentially growing cells, the major cytochromes are b_{558}, b_{562} and o (31). As cells enter stationary phase cytochromes b_{558}, d and a, appear (31). Also, Poole and Haddock (33) have found that exponentially growing *E.coli*, under conditions of sulfate limitation, contain cytochromes b_{558}, d and a, in addition to b_{558}, b_{562} and o. The factors responsible for the increased synthesis of cytochromes b_{558}, d and a, as stationary phase is approached or when growth is limited by sulfate are not clear.

Figure 2 is a schematic representation of the aerobic electron transport chain as envisaged by Haddock and Jones (34). The solid lines represent the pathway that operates during exponential growth, while the broken lines represent the pathway that would operate, along with the second redox loop from a flavoprotein dehydrogenase to cytochrome o, during stationary phase or when sulfate is limiting. The flavo- and iron-sulfur proteins represented by the box would vary depending on the carbon source available for growth. The scheme in Figure 2 suggests that under certain limiting conditions, such as low oxygen or sulfate in the growth medium, the segment of the chain between the NADH

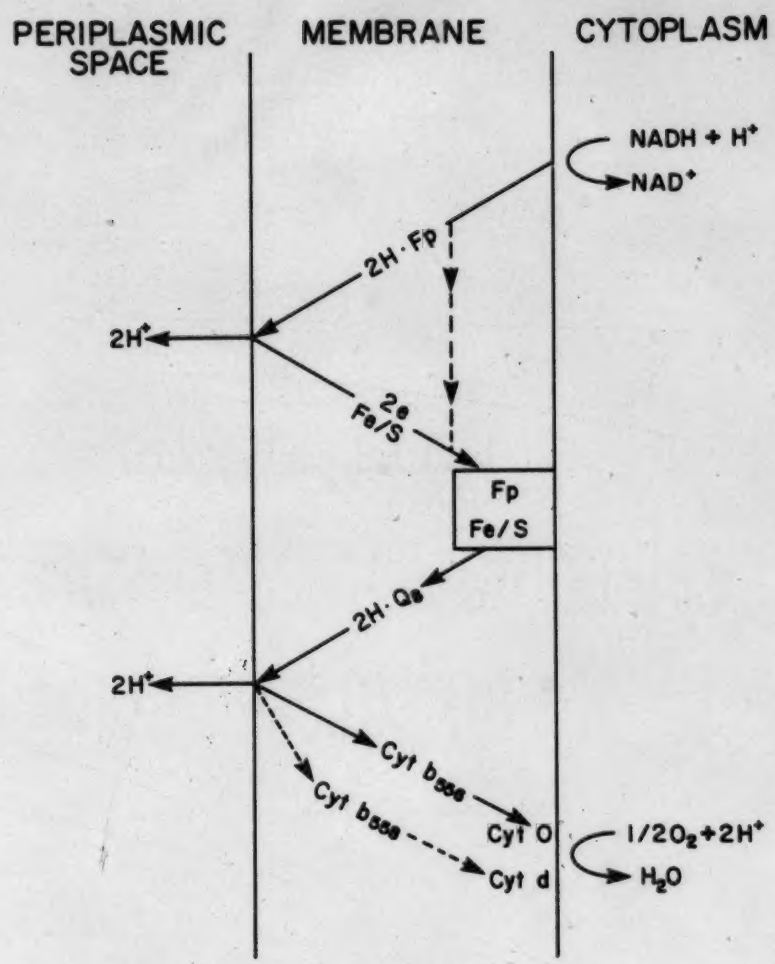

Figure 2. The aerobic electron transport chain of *E.coli* as proposed by Haddock and Jones (34). The nature of the flavoprotein, Fp, will vary depending on the carbon source available. Cyt=cytochrome; Q_8=ubiquinone-8; Fe/S=iron-sulfur protein(s); H =hydrogen atom.

dehydrogenase and the flavoprotein dehydrogenase ceases to be a proton translocating redox loop. When this happens reducing equivalents are passed directly from the NADH dehydrogenase to the flavoprotein dehydrogenase. Evidence for this uncoupled pathway comes from the demonstration by Poole and Haddock (33) that ATP dependent, uncoupler sensitive reduction of NAD by succinate, DL-glycerol-3-phosphate or D-lactate does not occur in electron transport particles prepared from cells grown in the presence of limiting sulfate.

A different electron transport chain has been proposed by Downie and Cox (35), Figure 3. Again the flavo- and iron-sulfur proteins represented in the box would vary depending on the carbon source available. The main difference between the two proposed pathways is in the role of ubiquinone. In the second scheme, Figure 3, ubiquinone is involved in both redox loops. Evidence for such an involvement has come from the demonstration of Poole and Haddock (36) of a requirement for ubiquinone in the energy linked reduction of NAD by succinate, L-glycerol-3-phosphate or D-lactate. In other words energy dependent reversed electron flow through redox loop 1 required ubiquinone. However, in the same study it was shown that reversed electron flow through loop 1 was not cytochrome dependent. Measurement of the H^+/O ratio for cells grown aerobically on different carbon sources indicated a ratio of 4 for NAD-linked respiratory substrates such as malate and a ratio

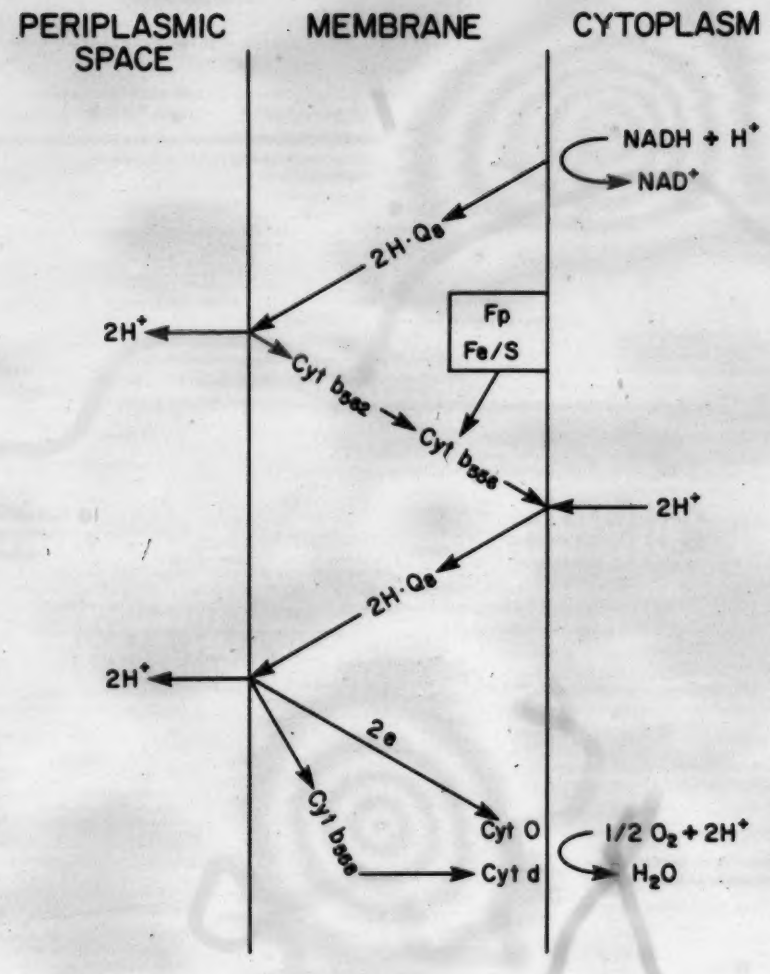

Figure 3. The aerobic electron transport chain of *E.coli* as proposed by Downie and Cox (35). The symbols used are as described in the legend to Figure 2.

of 2 for flavin linked respiratory substrates such as succinate (37). These results suggest that the overall arrangement in Figures 2 and 3 are correct although the exact sequence of carriers is uncertain at present.

2) Anaerobic Electron Transport Chains.

a) Electron Transport to Nitrate Reductase.

Anaerobic growth of *E.coli* on nitrate, molybdenum and a nonfermentable carbon source results in the induction of an electron transport chain which exhibits NADH, D- or L-lactate, L-glycerol-3-phosphate or succinate dependent nitrate reduction (34,38). If growth is in the presence of potassium selenite then a formate dependent reduction of nitrate also appears. The formate-nitrate reductase pathway is the best studied electron transport chain in *E.coli*. Figure 4 is a schematic representation of the anaerobic electron pathway to nitrate as envisaged by Haddock and Jones (34). The pathway consists of two proton translocating Mitchell loops. Using spheroplasts prepared from cells grown anaerobically in the presence of nitrate, Garland *et al* (39) measured H^+/NO_3^- ratios of 4 for L-malate oxidation and 2 for succinate, D-lactate and DL-glycerol-3-phosphate oxidation. Unfortunately, because of technical difficulties, an accurate H^+/NO_3^- ratio for formate could not be measured. However, it was determined that the value was greater than 2.

E.coli grown anaerobically in the presence of nitrate contain an NADH-oxidase activity and Figure 4 suggests that

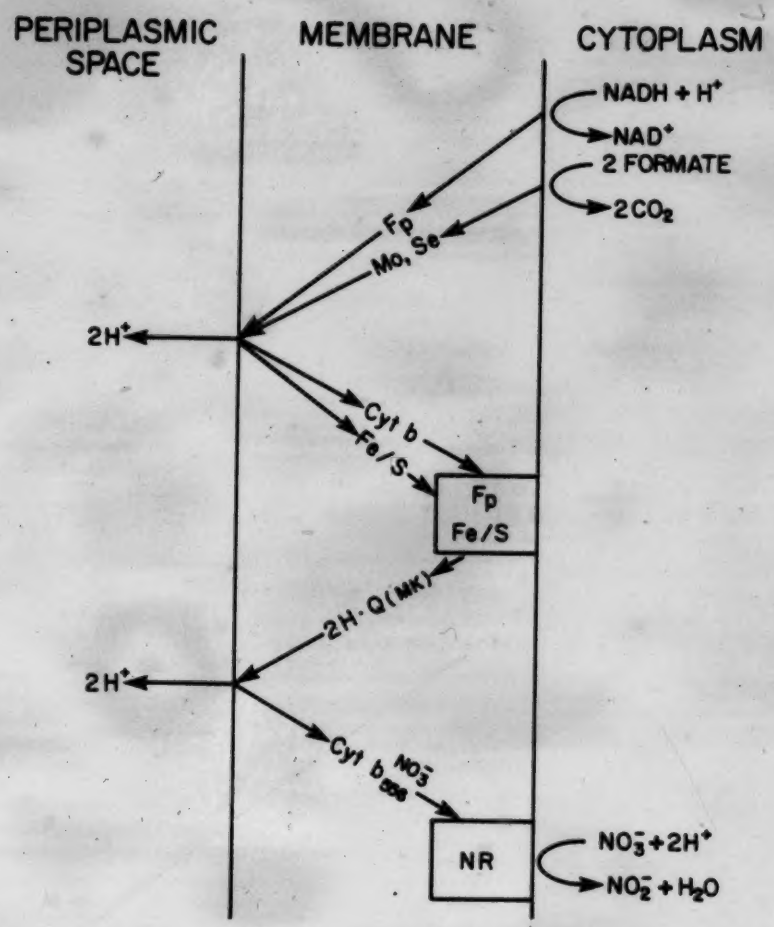

Figure 4. The *E.coli* anaerobic electron transport chain to nitrate reductase (taken from 34). Mo,Se is the molybdenum and selenium containing formate dehydrogenase; MK=Menaquinone; NR=Nitrate Reductase. The other symbols used are as described in the legend to Figure 2.

the NADH-nitrate reductase pathway uses components of both the NADH-oxidase and formate-nitrate reductase pathways. Measurement of the H^+/O and H^+/NO_3^- ratios for NADH dependent oxygen and nitrate reduction gave values of approximately 4. This result suggests that malate oxidation by both oxygen and nitrate involves proton translocation in the NADH dehydrogenase region of the chain.

Enoch and Lester (40) have purified formate dehydrogenase and nitrate reductase and found that both enzymes have a b-type cytochrome associated with them. Polyacrylamide gel electrophoresis in the presence of SDS indicated that the purified enzymes did not share a common subunit. This result suggests that two different cytochromes were involved. Interestingly, in the same study it was shown that formate-nitrate reductase activity could be reconstituted with preparations of formate dehydrogenase, nitrate reductase and ubiquinone-6. When cytochrome free nitrate reductase was used no reconstitution of activity occured. Menaquinone could replace ubiquinone-6 but was only 30% as effective.

Cytochrome $b_{558}^{NO_3^-}$, often referred to as the γ subunit of nitrate reductase, is quite different from the other cytochromes found in *E.coli*. In general, heme mutants of *E.coli* will synthesise apocytochromes in the absence of heme biosynthesis. However, Kemp *et al* (41) have found that heme mutants will not synthesize apocytochrome $b_{558}^{NO_3^-}$ in the absence of 5-aminolevulinic acid. It therefore seems that

heme biosynthesis plays a role in regulating the synthesis of this cytochrome. The scheme in Figure 4 conforms reasonably well with the present evidence available on the composition and organization of the electron transport chain to nitrate.

b) Electron Transport to Fumarate.

Anaerobic growth of *E.coli* on glycerol (or glycerol-3-phosphate) and fumarate results in the induction of an electron transport chain that utilizes glycerol-3-phosphate dehydrogenase (G3PD) as a primary dehydrogenase and fumarate reductase as a terminal electron transferring enzyme (34,38). The anaerobic G3PD has been purified and characterized and is distinct from the aerobic G3PD (42). In addition to glycerol-3-phosphate oxidation, fumarate reduction can be coupled with the oxidation of NADH, lactate, formate, hydrogen and dihydrooratate.

Figure 5 is a schematic representation of the chain from the flavoprotein G3PD to fumarate reductase (34). Miki and Lin (43) have demonstrated glycerol-3-phosphate dependent reduction of fumarate in membrane particles prepared from anaerobically grown *E.coli*. The coupling reaction was abolished by Triton X-100, suggesting the existance of an organised glycerol-3-phosphate dehydrogenase-fumarate reductase complex in the *E.coli* plasma membrane. Singh and Bragg (44,45) have shown that cytochromes, although not required for glycerol-3-phosphate dependent reduction of fumarate, are required for membrane

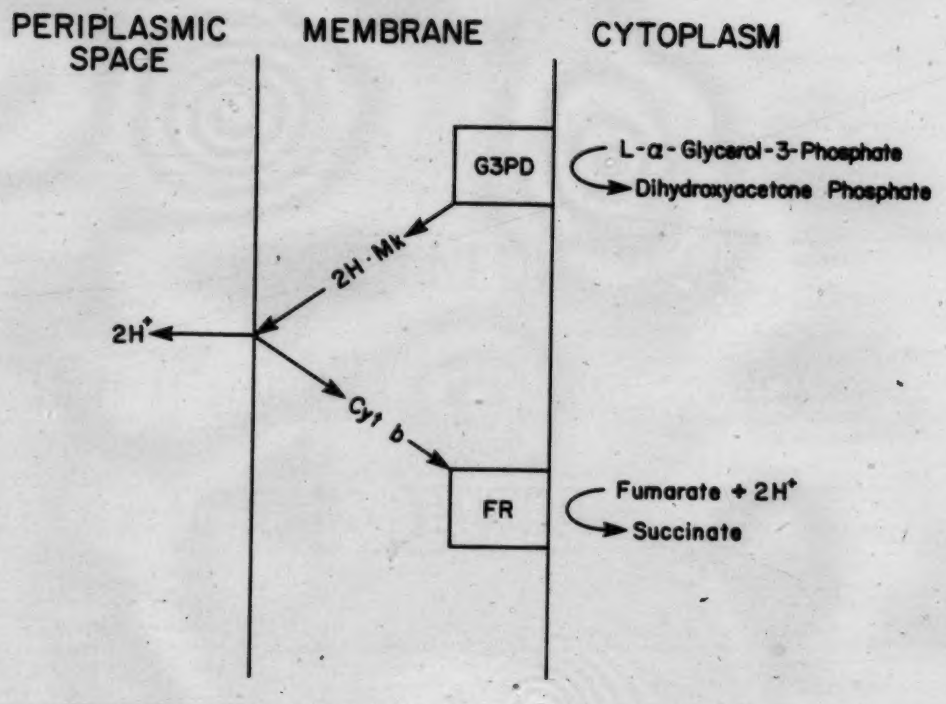

Figure 5. The *E.coli* anaerobic electron transport chain to fumarate reductase (taken from 34).
G3PD=glycerol-3-phosphate dehydrogenase; FR=Fumarate Reductase. The other symbols are as described in the legends to Figures 2 and 4.

energization. The inhibition of electron transport by HOQNO, a reagent which inhibits electron transfer between formate and nitrate by interacting with the b-type cytochromes in the chain, has led to the suggestion that a b-type cytochrome is involved in the glycerol-fumarate chain (38). However, little is known about the properties of this cytochrome. The scheme in Figure 5 is further supported by the measurement of a $H^+/2e$ ratio of 2 for the glycerol-3-phosphate-fumarate electron transport chain (46).

3) Primary Dehydrogenases.

a) The Aerobic and Anaerobic Glycerol-3-Phosphate Dehydrogenases.

The aerobic glycerol-3-phosphate dehydrogenase (G3PD) was initially purified and partially characterized by Weiner and Heppel (47). Following extraction with 0.1% (w/v) sodium deoxycholate the enzyme was purified by DEAE-cellulose and phosphocellulose chromatography. The native molecular weight was estimated to be 80,000 while PAGE-SDS analysis revealed one major band of molecular weight 35,000 suggesting that the native enzyme was a dimer. The purified protein showed a typical flavoprotein absorption spectrum with a peak at 450 nm. Using membrane permeable and impermeable electron acceptors as well as the effect of glycerol-3-phosphate on amino acid uptake in whole cells, spheroplasts and Kaback vesicles, it was deduced that the active site of G3PD was exposed on the cytoplasmic face of the membrane (48).

In a more rigorous investigation, homogenous enzyme, purified in the presence of 0.2% (w/v) Brij 58 was extensively characterized (49). The purified material migrated as a single band corresponding to a molecular weight of 58,000 on polyacrylamide gels in the presence of SDS. Analytical gel filtration suggested a dimeric structure for the native enzyme. Quantitation of the flavin content indicated 0.5 moles of FAD/mole of 58,000 dalton polypeptide. The purified enzyme was shown to be capable of utilizing a number of electron acceptors; PMS, DCPIP, ferricyanide, methylene blue and menadione were all effective while Q_6 and Q_{10} were ineffective. MTT was not directly reduced by the enzyme but PMS, methylene blue and menadione served as intermediate electron acceptors and coupled to MTT reduction.

Enzyme activity was inhibited 60% by 10 mM ATP but was slightly activated by 0.5 mM ATP suggesting that activity may be regulated by the level of ATP in the cell. Quantitative inhibition (93%) was obtained with 0.3 mM p-chloromercuribenzoate while removal of Brij 58 resulted in a seven fold loss of activity. Activity could be reconstituted by the addition of Brij 58, Triton X-100 or phospholipids. This requirement for amphipaths will be discussed further in Chapter III. Throughout this study activity was measured by the PMS/MTT reductase assay. Interestingly, it was also shown that the detergent-depleted enzyme could reconstitute with Kaback vesicles

prepared from a glpD$^-$ (the aerobic G3PD) strain, which then showed glycerol-3-phosphate dependent proline uptake.

E.coli possess a second G3PD which functions during growth under anaerobic conditions. Kistler and Lin (50), using an *E.coli* mutant missing the aerobic G3PD, found that anaerobic growth on glycerol with either nitrate or fumarate was normal but that growth was halted by the admission of oxygen. Under the same conditions growth of wild type cells continued smoothly. Mutants lacking the anaerobic enzyme but with normal levels of the aerobic G3PD grew on glycerol aerobically and anaerobically on glycerol plus nitrate but not fumarate. These results suggest that the aerobic enzyme is also present under anaerobic conditions and can couple with the electron transport chain to nitrate reductase but not fumarate reductase. On the other hand, the anaerobic enzyme appears not to be able to couple with the electron transport chain to oxygen. The level of the anaerobic G3PD was found to be the same in cells grown either aerobically or anaerobically with nitrate. With fumarate as the terminal electron acceptor the level was elevated several fold.

The initial investigation of the anaerobic G3PD was carried out by Kistler and Lin (51). Following lysis of mutant *E.coli* which lacked the aerobic enzyme, the anaerobic G3PD was found in the soluble rather than the particulate fraction. Approximately 30% purification was achieved by a combination of $(NH_4)_2SO_4$ precipitation, Sephadex G-75 and DEAE-cellulose chromatography. Enzyme activity was

stimulated by FMN and FAD. FMN was the better activator although maximal activation required the presence of both nucleotides. A native molecular weight of approximately 80,000 was determined.

Despite the partial purification and characterization of the anaerobic enzyme, its relationship to the aerobic enzyme was not clear. In order to establish the differences between these two enzymes, Schryvers and Weiner (42) have carried out an extensive purification and characterization of the anaerobic enzyme. By using an *E.coli* strain harboring a ColE1:*E.coli* plasmid which carries the glpA gene (anaerobic G3PD) they have been able to obtain levels of enzyme activity 10 fold greater than that found in the wild type. By using a combination of $(NH_4)_2SO_4$ precipitation, Phenyl Sepharose CL-4B and Hydroxylapatite chromatography they have been able to purify the enzyme to homogeneity. The native enzyme exists as an $\alpha\beta$ dimer of 62,000 and 43,000 dalton subunits. Ethylene glycol was required to prevent excessive losses of activity during purification. The stabilizing effect of ethylene glycol was shown to be related to its ability to prevent dissociation of the native enzyme into its subunits. The purified enzyme contains one mole of FAD/mole of dimer and one iron-sulfur centre of the Fe_2S_2 type. In agreement with the results of Kistler and Lin (51), Schryvers and Weiner found that enzyme activity was stimulated by both FMN and FAD. Again, FMN was the better activator.

b) NADH Dehydrogenase.

Respiratory NADH dehydrogenase has been purified from aerobically grown *E.coli* (52). By cloning the *ndh* gene into the multicopy plasmid pSF2124 and incubating transformed cells in the presence of chloramphenicol, an inhibitor of protein synthesis which stops cell division while allowing replication of the plasmid to occur, it was possible to amplify the level of NADH dehydrogenase activity 50-60 fold over that found in wild type cells. All of the enzyme activity was found in the membrane fraction. However, upon further amplification of activity to approximately 80-100 fold over that found in the wild type, a small but variable amount af activity appeared in the cytoplasm. Purification was achieved by a combination of cholate extraction and hydroxylapatite chromatography, yielding a homogenous enzyme with an NADH-ubiquinone oxidoreductase specific activity of 500-600 units mg^{-1} and a NADH-ferricyanide oxidoreductase specific activity of 130-150 units mg^{-1}.

The purified enzyme has been characterized (53). SDS-PAGE analysis revealed a single species of molecular weight 45,000 while lipid analysis indicated 2g of phospholipid/g of protein and one mole of ubiquinone-8/mole of enzyme subunit. The major phospholipid was phosphatidylethanolamine. Gel filtration in the presence of SDS removed the bound phospholipid. Quantitation of flavin content indicated one mole of noncovalently bound FAD/mole of subunit and no iron or acid labile sulfur was found

associated with the enzyme. By comparison of the amino acid sequence of the purified enzyme with the nucleotide sequence of the *ndh* gene it was concluded that apart from posttranslational cleavage of a N-formylmethionine residue, the mature enzyme corresponds to the entire coding sequence of the gene. Thus, NADH dehydrogenase appears not to be synthesized as a precursor containing a signal peptide. A cyanide sensitive NADH-oxidase activity could be reconstituted in membranes, prepared from a *ndh*$^-$ mutant, by incubation of the membranes with purified enzyme.

c) Formate Dehydrogenase.

Formate dehydrogenase, induced by anaerobic growth on formate and nitrate, has been purified and characterized (54). Solubilization with deoxycholate and ammonium sulfate followed by chromatography on Bio-Gel A-1.5m and DEAE-Bio-Gel A yielded a preparation of formate dehydrogenase which was 93-95% pure. In order to retain activity it was essential to maintain anaerobic conditions during the purification. The purified enzyme consists of three subunits, α, β and γ, of molecular weights 110,000, 32,000 and 20,000 respectively in a molar ratio of 1:1:0.2-1. A native molecular weight of 590,000±59,000 was determined by sedimentation velocity measurements. Compositional analysis indicated that the enzyme contained, 1 mole of selenium, 1 mole of heme, 1 mole of molybdenum, 14 moles of nonheme iron and 13 moles of acid labile sulfur per mole of enzyme. The absorption spectrum indicated the

presence of a b-type cytochrome in the preparation. No flavin, ubiquinone or menaquinone were detected. Activity could be measured using a number of electron acceptors; PMS, DCPIP, methylene blue, ferricyanide and nitroblue tetrazolium were all effective. Cyanide and azide were found to inhibit the different reductase activities to different extents leading Enoch and Lester (54) to conclude that formate dehydrogenase contains a number of different catalytic sites for interaction with artificial electron acceptors.

d) Lactate Dehydrogenases.

Bennett *et al* (55) have demonstrated the existance of two distinct membrane-bound lactate dehydrogenases in *E.coli*. Both enzymes can couple with the respiratory chain and one is specific for D-lactate and the second is specific for L-lactate. Both dehydrogenases were present under aerobic and anaerobic conditions but whereas the level of the D-lactate enzyme was constant during growth on various carbon sources the L-lactate enzyme was repressed by growth on glucose, pyruvate or succinate. Furthermore, the membrane-bound enzymes could be distinguished by a) their thermal stability and b) their sensitivity to sulfhydryl reagents. Heating at 60°C for 1.5 mins caused complete loss of the D-lactate dehydrogenase activity while the L-lactate dehydrogenase was only slightly inhibited. The D-lactate enzyme was inhibited 65% by 0.03 mM p-chloromercuribenzoate while the L-lactate enzyme was only inhibited 15%. Neither

enzyme was NAD$^+$ dependent.

Futai and Kimura (56) have purified and characterized the L-lactate dehydrogenase. A combination of sodium cholate extraction, $(NH_4)_2SO_4$ precipitation and DEAE-cellulose and Bio-Gel A-0.5m chromatography yielded 95% pure enzyme. PAGE-SDS analysis indicated a single polypeptide of molecular weight 43,000. Both L-lactate and DL-α-hydroxybutyrate were rapidly oxidized while D-lactate was oxidized at only 0.1% the rate of L-lactate oxidation. The enzyme was found to contain 1 mole of FMN/mole of 43,000 dalton subunit. Incubation of inside-out vesicles with specific anti-body against the purified enzyme caused 80% inhibition of L-lactate dependent oxygen uptake. This result suggests that the dehydrogenase is located on the cytoplasmic side of the membrane and is indeed a part of the respiratory chain.

D-lactate dehydrogenase has also been purified and characterized (57,58,59). As purified by Futai (57), the enzyme consists of a single subunit of molecular weight 72,000. The enzyme was specific for D-lactate but oxidized L-lactate at about 14% and DL-α-hydroxybutyrate at about 10% the rate of D-lactate oxidation. The enzyme was a flavoprotein containing 1 mole of noncovalently bound FAD/72,000 dalton subunit. Kohn and Kaback (58) have also purified D-lactate dehydrogenase. Their results are in general agreement with those of Futai (57). However, Kohn and Kaback (58) found that Triton X-100 alters the enzyme's

pH optimum and apparent Km for D-lactate. Triton X-100 shifted the pH optimum from 7.5 to 8.5 and decreased the apparent Km from 1.4×10^{-3} to 9×10^{-4} M. Pratt *et al* (59) have found that the PMS/MTT reductase activity of the detergent-depleted enzyme was stimulated 5-6 fold by amphipaths. The phenomenon of activation of membrane-bound enzymes by amphipaths will be discussed further in Chapter III.

e) Pyruvate Oxidase.

Pyruvate oxidase was originally purified by Williams and Hager (60). The native enzyme exists as a tetramer of identical subunits each of molecular weight 66,000. Each subunit contains one mole of noncovalently-bound FAD. Thiamine pyrophosphate was also shown to be a required cofactor. Enzyme activity, as measured with artificial electron acceptors, could be stimulated by trypsin proteolysis or by the presence of surface-active agents. Also, in this early study it was found that oxygen could act as an electron acceptor only when a cytochrome-containing particulate fraction was present. This requirement suggested an involvement of pyruvate oxidase in the respiratory chain. More recently an improved procedure for purifying pyruvate oxidase has been reported (61). This procedure involves the use of a thiamine pyrophosphate affinity column. The properties of the enzyme purified by this procedure were essentially the same as reported previously (60).

Shaw-Goldstein *et al* (62) have shown that membrane-bound pyruvate oxidase can feed reducing equivalents into the electron transport chain to oxygen. These workers showed that oxidation of pyruvate to acetate and CO_2 can drive the uptake of phenylalanine by Kaback vesicles. As part of the same study the localization of pyruvate oxidase on the cytoplasmic side of the membrane was demonstrated.

e) Succinate Dehydrogenase.

Kim and Bragg (63) have solubilized and partially purified succinate dehydrogenase. The activity of the solubilized enzyme was found to be very labile but the membrane-bound enzyme could be activated four-fold by incubation at 38°C for 15 mins in the presence of phosphate and succinate. The solubilized enzyme was inactivated by this treatment. Malonate was a competitive inhibitor of the membrane-bound enzyme while sodium azide and o-phenanthroline were without effect. A molecular weight of 100,000 was determined.

More recently succinate dehydrogenase has been investigated using crossed immunoelectrophoresis (64,65,66). Jones *et al* (64) have identified two polypeptides of molecular weights 73,000 and 26,000 as the components of succinate dehydrogenase. They also found nonheme iron associated with the enzyme. Owen and Condon (65) and Condon and Owen (66) also carried out an immunoelectrophoretic analysis of Triton X-100 extracts of *E.coli* membranes

containing succinate dehydrogenase. However, their analysis revealed seven polypeptides associated with the succinate dehydrogenase staining precipitin band. Two of the polypeptides had molecular weights of 71,500 and 27,000 in agreement with the results of Jones *et al* (64). By growing cells in the presence of ^{14}C-riboflavin it was shown that the 71,500 dalton polypeptide had covalently-bound FAD. The reason for the discrepency between the results of these studies is not obvious since essentially the same methodology was used in both cases.

4) Terminal Reductases.

a) Fumarate Reductase.

Cole and Guest (67,68) have described the cloning and expression of the fumarate reductase gene (frd gene). Using lambda transducing phages, into which a 4.9 kb *Hind III* fragment of the *E.coli* chromosome had been inserted, Cole and Guest were able to complement frd mutants. Following infection, fumarate reductase activity was elevated 5 fold and two polypeptides of molecular weights 72,000 and 26,500 appeared in the membrane of the infected cells.

In another study, Cole and Guest (69) found a 32 fold amplification of fumarate reductase activity in ampicillin-hyperresistant mutants of *E.coli*. The frd gene lies at 92.8 mins on the *E.coli* map and adjacent to the ampA and ampC genes which are the regulatory and structural genes respectively for β-lactamase. These hyperresistant mutants contain multiple repeats of the amp-frd region of the *E.coli*

genome. Following anaerobic growth, polypeptides of molecular weights 97,000, 80,000, 72,000, 49,000, 33,000 and 26,500 were amplified over the wild type level. Interestingly, the 72,000 and 26,500 dalton polypeptides were found in both the membrane and soluble fractions. Ultracentrifugation on a 10-50% (w/w) sucrose gradient at 150,000g for 16 hrs at 4°C could not pellet the soluble activity. Both the 72,000 and 26,500 dalton polypeptides cosedimentated together suggesting a functional association. The authors concluded that amplification of fumarate reductase saturates the membrane binding sites and results in the accumulation of a cytoplasmic form of the enzyme.

Fumarate reductase has been purified to homogeneity and partially characterized (70,71,72). By a combination of Triton X-100 extraction and Phenyl Sepharose CL-4B chromatography, enzymatically active fumarate reductase has been purified from wild type *E.coli* and shown to consist of two polypeptides of molecular weights 69,000 and 25,000 present in a molar ratio of 1:1. (70). The apparent Michaelis-Menten constants for the membrane-bound and purified enzymes were 470 and 410 *uM* respectively. The optical properties of the pure enzyme were those of a flavoprotein having absorption maxima at 350 and 465 nm. The presence of an FAD cofactor, covalently attached to the large subunit, was subsequently demonstrated (71). Lohmeier *et al* (72) have succeeded in amplifying the level of fumarate reductase activity 10 fold over that found in wild

type cells by identifying plasmids that code for fumarate reductase in the Clark and Carbon colony bank. Two plasmids were found to complement frd mutants, pLC16-43 and pLC43-46. Restriction analysis indicated that both plasmids contained a *Hind III* fragment 7.7 kb in length. Isolation and partial characterization of enzyme from the plasmid carrying strains (MV12/pLC16-43 and CSR603/pLC16-43) indicated that the amplified enzyme was identical to the enzyme isolated from the wild type strain.

Recently the fumarate reductase operon has been sequenced (73,74,75). This analysis indicated that the operon codes for four polypeptides of molecular weights 70,000 (73), 27,000 (74), 15,000 and 13,000 (75). The 70,000 and 27,000 dalton polypeptides are the catalytically active subunits. The function(s) of the 15,000 and 13,000 dalton polypeptides is uncertain at present. As a result of the elucidation of the nucleotide sequence of the large subunit it appears that the sequence of nine amino acids, surrounding the covalently attached FAD, is identical to the sequence around the covalently attached FAD moiety of beef heart mitochondrial succinate dehydrogenase (76). Other similarities between these two enzymes will be discussed in Chapter IV. The gene coding for the 13,000 dalton polypeptide lies adjacent to and partially overlaps the ampC or β-lactamase structural gene. Sequence analysis indicates that the C-terminal region of the 13,000 dalton polypeptide is coded for by nucleotides in the promoter region of the

ampC gene and that the stop codon lies in the attenuator region of the ampC gene (75). Also, the nucleotide sequences of the small polypeptides indicates that they contain 70% hydrophobic amino acids.

b) Nitrate Reductase.

Nitrate reductase has been purified in a number of laboratories (77,78,79,54). The subunit composition of the purified enzyme appears to depend on the method of solubilization used. If the enzyme is released by heat treatment of membranes and subsequently purified it consists of two subunits, one of molecular weight 142-155,000 (depending on the laboratory) and a second subunit which varies in molecular weight from 47,000 to 67,000. The heterogeneity in this second polypeptide is thought to be due to proteolytic degradation during the heat treatment. On the other hand if the enzyme is solubilized by Triton X-100 then three polypeptides of molecular weights 142,000 (α), 60,000 (β), and 20,000 (γ) are obtained (78). The γ subunit is thought to contain heme (40) and may be cytochrome $b_{556}^{NO_3^-}$. The two subunit form of the enzyme appears to exist as a tetramer of molecular weight 800,000 (77) in equilibrium with a 200,000 dalton monomeric form (79). The tetrameric form contains 4 moles of molybdenum/mole of enzyme. De Moss (80) has shown that tryptic digestion of the β subunit to a subunit of molecular weight 43,000 can cause dissociation of the tetramer to the monomer.

In a detailed study, MacGregor has examined the release of enzyme by heat treatment of membranes (81,82). Heat treatment or the absence of $cyt_{552}^{NO_3^-}$ resulted in proteolytic cleavage of the β subunit. Also, cleavage of this subunit resulted in the release of the α subunit from the membrane. These results have been interpreted to mean that nitrate reductase is anchored to the membrane through its β subunit and that an interaction between the β and γ subunits occurs within the membrane which prevents proteolysis of the β subunit. In a later study (83) it was shown that $cytb_{558}^{NO_3^-}$ was required for quantitative incorporation of the α and β subunits into the membrane. Antibody raised against the heat solubilized subunits ($\alpha+\beta$) precipitated all three subunits from Triton X-100 membrane extracts. The stoichiometries in Triton extracts were $\alpha_1:\beta_1:\gamma_2$. Recently, it has been shown that $cytb_{558}^{NO_3^-}$ and nitrate reductase are under the control of the same operator-promoter region (84). This result lends further support to the results of MacGregor which suggest that normal incorporation and function of nitrate reductase requires the presence of $cytb_{558}^{NO_3^-}$.

C. Thesis Problem.

Our approach to understanding the structure and function of *E.coli* electron transport proteins has been to purify and characterize individual components with the long term goal of reconstituting a coupled electron transport system. In order to facilitate purification and

characterization we have amplified the levels of fumarate reductase 10-20 fold over that found in wild type *E.coli*. This amplification has been achieved by two approaches: a) by introducing a ColE1:*E.coli* plasmid, which codes for fumarate reductase, into a recipient strain of *E.coli* and b) by cloning the fumarate reductase operon into the vector pBR322 and introducing this modified plasmid into a transformable strain of *E.coli*. The former approach has resulted in an 8-10 fold amplification of activity while the latter approach has increased fumarate reductase levels 15-20 fold over the wild type level. Much of the work presented in this thesis was simplified by the enhanced levels of activity in these strains.

In Chapter III I describe the results of a study of the interaction between the aerobic glycerol-3-phosphate dehydrogenase and amphipaths. The importance of understanding such interactions is obvious. Amphipaths allow us to partially reproduce the membrane environment and afford us a simpler system to study. By understanding how proteins behave in this relatively simple system we can begin to understand how they function in the membrane.

The bulk of this thesis presents the results of a study of the terminal electron transferring enzyme, fumarate reductase. Chapter IV describes the characterization of the purified, 100,000 dalton form of the enzyme, which is composed of 69,000 and 25,000 dalton catalytically active subunits. Chapter V deals with the question of the sidedness

of these subunits in the cytoplasmic membrane. This question is of interest in order to critically evaluate Mitchell's chemiosmotic requirement for an asymmetrical arrangement of electron transport components. In Chapter VI I describe the results of an investigation of the activation of the purified enzyme by anions.

At the time of these studies the fumarate reductase operon had not been sequenced and we were unaware of the existence of the 15,000 and 13,000 dalton polypeptides. Sequence analysis indicated that these polypeptides contained 70% hydrophobic amino acids and when we analysed membrane polypeptides and Triton X-100 extracts of plasma membranes on 15% Laemmli gels a species of molecular weight 13,000-15,000 was amplified along with the 69,000 and 25,000 dalton catalytic subunits. When Triton X-100 extracts were run on 8-22% (w/v) Laemmli gels this low molecular weight species was shown to consist of two polypeptides of molecular weights 15,000 and 14,100 present in an approximate molar ratio of 1:1. We hypothesised that membrane-bound fumarate reductase consisted of three-four dissimilar subunits of molecular weights 69,000, 25,000 and 13,000-15,000. In Chapter VII I report some data on the properties of membrane-bound and Triton X-100 solubilized fumarate reductase. This latter study helped to explain some puzzling results obtained during the characterization of the purified 100,000 dalton form of the enzyme.

II. General Materials and Methods.

A. Materials.

1) Chemicals.

^{3}H-Triton X-100 (1 mCi/μmole), sodium ^{14}C-cyanide (7.9mCi/mmole), and sodium ^{3}H-cholic acid (14 Ci/mmole) were obtained from New England Nuclear, Boston, Ma. Sodium (^{125}I)-iodide was obtained from the Edmonton Radiopharmaceutical Centre, Edmonton, Alberta. Acrylamide, bis-acrylamide, DTT, SDS, TEMED, Coomassie Brilliant Blue R-250, ammonium persulphate and Bio-Rex 70 were obtained from Bio-Rad Laboratories, Richmond, Ca. DTNB, ATP, ADP, and AMP were obtained from PL Biochemicals Inc, Milwaukee, Wis. Dimethyl suberimidate, PMS, MTT, potassium ferricyanide, methyl viologen, benzyl viologen, iodoacetamide, p-chloromercuriphenlysulphonate and nonionic detergents were from Sigma Chemical Co, St Louis, Mo. DTSP was obtained from Pierce Chemical Co, Rockford, Ill. Phenyl Sepharose CL-4B and Sephadex G-25 were from Pharmacia Fine Chemicals, Dorval, Quebec. Hydroxyapatite was from Clarkson Chemical Co, Williamsport, Pa and Whatman Phosphocellulose, P-11 was from H. Reeve Angel and Co, Clifton, N.J. LKB ampholytes were from Fisher Scientific Co, Edmonton, Alberta. All common reagents were of the highest grade available.

2) Enzymes.

Lactoperoxidase (200 units/mg) and ribonuclease were from Miles Laboratories Ltd, Rexdale Ontario.

Deoxyribonuclease (410 units/mg) and lysozyme (42,700 units/mg) were from Sigma Chemical Co, St Louis, Mo.

3) Strains.

The strains listed in Table 1 were used.

4) Growth Media.

All strains were subcultured aerobically in Luria Broth (85) before inoculation into the medium of choice. Stock strains were stored frozen at -80°C in Luria Broth made 8% (v/v) in dimethyl sulfoxide. For purification of the aerobic glycerol-3-phosphate dehydrogenase an overnight culture of strain 7 was inoculated into a medium containing 10g of K_2HPO_4, 1.85g of KH_2PO_4, 10g of Difco yeast extract and 50 mg of thiamin per litre. Glycerol, 0.5% (v/v) was the carbon source. Cells were allowed to grow aerobically in a 300 litre fermentator to early stationary phase, harvested in a CEPA continuous flow centrifuge and the cell paste was frozen immediately in liquid nitrogen and stored at -80°C.

For purification of fumarate reductase, MV12/pLC16-43, CSR603/pLC16-43 or Pfrd63 were inoculated from overnight cultures into a medium containing 5.44g of KH_2PO_4, 10.49g of K_2HPO_4, 2g of $(NH_4)_2SO_4$, 3.75g of NaOH, 4.64g of fumaric acid, 48μg of $MgSO_4$, 5.5μg of $MnSO_4.4H_2O$, 0.5μg of $Fe_2(SO_4)_3$, 5μg of $CaCl_2$, 0.7% (v/v) glycerol and 0.05% (w/v) casamino acids (glycerol/fumarate medium). When MV12/pLC16-43 was grown the medium was supplementated with threonine, leucine and tryptophan at a level of 20μg/ml each. Growth of Pfrd63 was on medium supplemented with

Table 1

E.coli Strains Utilized.

Strain	Genotype
7	HfrC,glpR,phoA,relA,tonA22.
MV12	$F^{'}$,recA,trpD,thr,leu.
CSR603	F^{-},recA,thr,leu,pro, arg,thi,phr,ara,lac,gal,tyr, mtl,strA,tsx,SupE44.
HB101	F^{-},pro,leu,gal,lac, thi,recA,strR,r_B^{-},m_B^{-}.

proline, leucine and thiamin at 20 ug/ml each. Growth was anaerobic in 19 litre carboys which were filled to the top with medium and tightly sealed with a rubber stopper. Each carboy was stirred gently to ensure no sedimentation of cells occured. The subcultures of CSR603 and MV12 contained 1 unit/ml of colicin E1 while both the subcultures and 19 litre cultures contained 100 ug/ml ampicillin when Pfrd63 was grown. Growth of CSR603 and MV12 was allowed to continue to early stationary phase while Pfrd63 was allowed to grow to late stationary phase. Cells were harvested by centrifugation in a Sorvall RC-3 centrifuge and the cell paste frozen immediately in liquid nitrogen and stored at -80°C.

B. Methods.

1) Purification of the Aerobic Glycerol-3-Phosphate Dehydrogenase.

Step 1 Broken Cell Fraction

One hundred grams of frozen cell paste were thawed at room temperature in 550 ml of 50 mM Tris-HCl, pH 8.0, containing 50 mg/litre phenylmethylsulfonylfluoride (buffer A). To this was added EDTA to 10 mM and lysozyme to 0.5 mg/ml. The lysozyme was allowed to act for 20 mins at 37°C and then the sample was diluted to 900 ml with buffer A. The suspension was frozen in liquid nitrogen and immediately thawed in a water bath at 37°C. Magnesium chloride was added to 25 mM followed by deoxyribonuclease and ribonuclease to

10ug/ml each. The suspension was incubated a further 30 mins at 37°C then centrifuged at 40,000g for 30 mins at 2°C. The supernatant was discarded and the broken cells resuspended by homogenization in 800 ml of buffer A and centrifuged as before. The washed preparation was resuspended by homogenization in 700 ml of 50 mM Tris-HCl, pH 7.5, containing 10% (v/v) glycerol and 0.25 M NaCl to yield fraction 1.

Step 2 Deoxycholate Extraction

Sodium deoxycholate was added to 0.2% (w/v) to Fraction 1 and the suspension was stirred at room temperature for 20 mins. If the sample became viscous 10 mM $MgCl_2$ and 10 ug/ml deoxyribonuclease were added. The deoxycholate extract was centrifuged at 40,000g for 60 mins at 2°C. The pellet was discarded and the supernatant (Fraction 2) was made 20% in ethylene glycol and 0.2% (w/v) in Brij 58 (Fraction 2A).

Step 3 Bio-Rex 70 Chromatography

Fraction 2A was immediately diluted 1 to 3 with 50 mM Imidazole-HCl, pH 6.8, 20% ethylene glycol, 0.2% (w/v) Brij 58 (Buffer B) and applied to a 6x12 cm (350 ml) column of Bio-Rex 70 equilibrated in Buffer B. The column was washed with 600 ml of buffer B containing 0.35 M NaCl and activity was eluted with 1 litre of Buffer B containing 0.65 M NaCl. Active fractions were pooled to yield Fraction 3.

Step 4 Phosphocellulose Chromatography

Fraction 3 was diluted 1 to 6 with 20 mM potassium phosphate, pH 6.6, containing 20% (v/v) ethylene glycol,

0.2% (w/v) Brij 58 (Buffer C) and was applied to a 6x7 cm (200 ml) column of phosphocellulose P-11 equilibrated in Buffer C. Activity was eluted with a linear gradient of 0.35 to 0.8 M NaCl in Buffer C. Active fractions were pooled to yield Fraction 4.

Step 5 Hydroxyapatite Chromatography

Fraction 4 was diluted 1 to 4 with 20% (v/v) ethylene glycol and applied to a 2x9 cm (30 ml) column of hydroxyapatite. The column was washed with 60 ml of 5 mM potassium phosphate, pH 7.5, 20% (v/v) ethylene glycol, 0.2% (w/v) Brij 58 and then eluted with a linear gradient of 6 to 60 mM potassium phosphate, pH 7.5, in 20% (v/v) ethylene glycol, 0.2% (w/v) Brij 58. Active fractions were pooled and stored at -70°C (Fraction 5). Fraction 5 was then reapplied to a phosphocellulose column and eluted with either Brij or Perchlorate buffers, as described in Chapter III, to give the Brij or Perchlorate forms of the enzyme respectively. Both forms of the enzyme were stable at -70°C for up to 2 years.

2) Purification of Fumarate Reductase.

The procedure described below is a slight modification of that described in (70) and is based on 60g wet weight of *E.coli* paste.

Step 1 Preparation of Membrane Fraction

Sixty grams of *E.coli* paste were resuspended in 300 ml of 50 mM Tris-HCl, pH 7.5, containing 50 mM NaCl, 50 ug/ml phenylmethylsulfonylfluoride, 25 mM $MgCl_2$, and 10 ug/ml each

of deoxyribonuclease and ribonuclease The resuspended cells were passed twice through a French Pressure Cell, prechilled to 4°C, at 16,000 psi. The lysate was centrifuged at 15,000g for 15 mins at 2°C and the membranes collected by ultracentrifugation of the supernatant at 100,000g for 2 hr at 2°C. The membranes were washed once with 50 mM Tris-HCl, pH 8.0, 0.15 M KCl, 0.25 M sucrose and 10 mM EDTA, collected by ultracentrifugation and resuspended by homogenization in 50 mM Tris-HCl, pH 8.0, to a density of 0.2g of pellet/ml (Fraction 1).

Step 2 Solubilization of Enzyme Activity

Fraction 1 was made 0.5% (v/v) in Triton X-100 and stirred on ice for 60 mins. Insoluble debris was removed by centrifugation at 26,000g for 30 mins at 2°C. The amber supernatant (Fraction 2) was made 17.5% (w/v) in ammonium acetate, stirred at 0°C for 45 mins and the solution clarified by centrifugation at 16,000g for 10 mins at 2°C to give Fraction 3.

Step 3 Phenyl Sepharose Chromatography

Fraction 3 was applied to a 4x16 cm (200 ml) column of Phenyl Sepharose CL-4B equilibrated at 4°C with 50 mM Tris-SO_4, pH 8.0, containing 17.5% (w/v) ammonium acetate and 1 mM EDTA. The column was then washed with 1 litre of equilibration buffer containing 0.5% (w/v) sodium cholate. This washing step removed a peak of protein which contained a low level of fumarate reductase activity. Fumarate reductase was then eluted with a 2 litre decreasing

concentration gradient from 17.5 to 2% (w/v) ammonium acetate in 50 mM Tris-SO_4, pH 8.0, 0.5% (w/v) sodium cholate and 1 mM EDTA. Enzyme activity began to elute towards the end of the gradient and was complete after washing the column with 500 ml of 2% (w/v) ammonium acetate in 50 mM Tris-SO_4, pH 8.0, 0.5% (w/v) sodium cholate and 1 mM EDTA (Fraction 4). A flow chart for the purification is shown in appendix I.

3) Cholate Depletion of Purified Fumarate Reductase.

Purified enzyme was depleted of cholate as follows: the enzyme solution was made 35% saturated in $(NH_4)_2SO_4$. After stirring for 60 mins at 0°C, the precipitated cholate was removed by centrifugation at 48,000g for 20 mins. The protein was then precipitated by making the solution 60% saturated in $(NH_4)_2SO_4$ and stirring for 30 mins at 0°C. After centrifugation as described above, the dark amber pellet of fumarate reductase was dissolved in either 0.4 M potassium phosphate, pH 6.8, or 25 mM Hepes [N-(2-hydroxyethyl)N-2-piperazine-ethane sulfonic acid], pH 6.8 (to give anion-depleted enzyme). This procedure removed up to 96% of the cholate present, as judged by the removal of ^{3}H-cholate.

4) Enzyme Assays.

All assays were carried out at room temperature.

a) Assays of Glycerol-3-Phosphate Dehydrogenase

i) Activity was measured by following the PMS-coupled reduction of MTT at 570 nm. The assay mixture (1 ml)

contained the following; 43 mM Imidazole-HCl, pH 7.0, 1 mM PMS, 0.144 mM MTT and the reaction was initiated by the addition of DL-glycerol-3-phosphate to a concentration of 50 mM. When Brij 58 was used it was present at a concentration of 0.01% (w/v). The millimolar extinction coefficient for reduced MTT was taken to be 17 mM^{-1} cm^{-1} (48).

ii) The reaction conditions for the second assay were the same as those above except that PMS and MTT were replaced by potassium ferricyanide at a concentration of 1 mM. The millimolar extinction coefficient of reduced ferricyanide at 420 nm was taken to be 1 mM^{-1} cm^{-1} (86). One unit of enzyme activity is defined as the amount of enzyme which will catalyse the reduction of 1 micromole of MTT or ferricyanide per min at room temperature.

b) Assay of D-Lactate Dehydrogenase Activity.

Activity was measured by following the PMS-coupled reduction of MTT at 570 nm. The assay mixture (1 ml) contained; 0.1 M potassium phosphate, pH 8.0, 0.4 mM PMS, 0.144 mM MTT, 0.01% (w/v) Brij 58 and the reaction was initiated by the addition of 10 mM D-lactate.

c) Assay of Fumarate Reductase Activity.

i) Enzyme activity was measured by following the fumarate dependent oxidation of reduced methyl- or benzyl viologen at 600 or 550 nm respectively, in a Gilford Model 250 spectrophometer equipped with a chart recorder. The standard assay mixture (2.9 ml) contained; 200 mM sodium phosphate, pH 6.8, 0.5 mM dithiothreitol, 0.21 mM methyl- or

benzyl viologen, 0.7 mM sodium dithionite and 35 mM sodium fumarate. The reaction was initiated by the addition of sodium fumarate. The millimolar extinction coefficients for reduced methyl- and benzyl viologen were taken as 13 and 7.8 mM^{-1} cm^{-1} respectively (87,88). One unit of enzyme activity is defined as the amount of enzyme which catalyzes the oxidation of 1 micromole of reduced benzyl- or methyl viologen per min at room temperature.

ii) The succinate dehydrogenase activity of fumarate reductase was measured by the PMS- coupled MTT reduction assay. The assay mixture (1 ml) contained; 1 mM PMS, 0.07 mM MTT, 0.01% (v/v) Triton X-100 and the reaction was initiated by the addition of various concentrations of sodium succinate. The assay buffer was sodium phosphate, pH 6.8, of various concentrations. This assay was used to measure the Michaelis-Menten constant for succinate as a function of phosphate concentration.

5) Preparation of Kaback Vesicles.

Kaback vesicles were prepared from strain 7 or CSR603/pLC16-43 as described by Kaback (89).

6) Preparation of Everted Membrane Vesicles.

CSR603/pLC16-43 cells were resuspended to a concentration of 1g (wet wgt) per 5 ml in 0.1 M potassium phosphate, pH 6.6, containing 10 mM Na_2EDTA and passed twice through a French Pressure Cell, prechilled to 4°C, at 10,000 psi. The lysate was centrifuged at 15,000g for 15 mins at 2°C and the everted membrane vesicles isolated from the

supernatant by ultracentrifugation at 100,000g for 2 hrs at 2°C. The vesicles were stored at -70°C in 50 mM Tris-SO_4, pH 8.0, containing 10 mM $MgCl_2$.

7) Preparation of Spheroplasts.

Freshly harvested CSR603/pLC16-43 cells were resuspended in 50 mM Tris-HCl, pH 8.0, to a concentration of 0.2 g/5 mls. Na_2EDTA and lysozyme were added to a concentration of 10 mM and 0.5 mg/ml respectively and incubated at room temperature for 30 mins. The spheroplasts were harvested by centrifugation at 1,000g for 5 mins at room temperature, resuspended in 0.1 M potassium phosphate, pH 7.5, containing 23% (w/v) sucrose and used immediately.

8) SDS-Polyacrylamide Gel Electrophoresis.

SDS-polyacrylamide gel electrophoresis was performed using the discontinuous gel system of Laemmli (90). Slab gels, 26.5x16.5 cm were used with a 20 cm running gel and a 2 cm stacking gel. When gradient gels were used the stacking gel was omitted. Samples for PAGE-SDS analysis were added to an equal volume of solubilizing solution (0.1 M Tris-HCl, pH 6.8, 100 mM DTT, 2% (w/v) SDS, 32% (w/v) glycerol and 0.01% (w/v) bromophenol blue) and boiled for 3 mins before being applied to the gel. Electrophoresis was at a constant current of 20 mA in the stacking gel and 30 mA in the running gel. When gradient gels were used electrophoresis was at a constant current of 30 mA.

Alternatively, the fast running gel system of Jovin *et al* (91) was used. Samples were solubilized by addition to an

equal volume of solubilizing solution (59 mM Tris, 59 mM glycine, pH 8.8, 55 mM DTT, 1.1% (w/v) SDS, 45% (w/v) glycerol and 0.01% (w/v) bromophenol blue) and boiled for 3 mins before application to the gel. Electrophoresis was at a constant current of 30 mA.

After electrophoresis, gels were stained with 0.25% (w/v) Coomassie Brilliant Blue R-250 in methanol-acetic acid-water (5:1:5 v/v) and destained in methanol-acetic acid water (7:10:83 v/v). The following proteins were used as molecular weight standards; cytochrome c, 12,300, β-lactoglobulin, 18,400, α-chymotrypsinogen, 25,700, ovalbumin, 43,000, bovine serum albumin, 68,000, phosphorylase B, 92,500, and myosin heavy chain, 200,000 daltons.

III. The Effect of Amphipaths on the Flavin-Linked Aerobic Glycerol-3-Phosphate Dehydrogenase of *Escherichia coli*.

A. Introduction.

The aerobic glycerol-3-phosphate dehydrogenase (G3PD) isolated from the cytoplasmic membrane of *Escherichia coli* has been purified and extensively studied in this laboratory (49). During this study a number of electron acceptors were identified which coupled with G3PD and could therefore be used to assay enzyme activity. These included DCPIP, PMS, MTT and Ferricyanide. The two assays most commonly used involved either the PMS-coupled reduction of MTT (a two electron acceptor) or the direct reduction of potassium ferricyanide (a one electron acceptor). Both reductase activities could readily be measured when enzyme purified in the presence of the nonionic detergent Brij 58 (denoted as the Brij form) was used and resulted in similar turnover numbers. However, when the enzyme was depleted of Brij 58 by replacing the detergent with the chaotropic agent sodium perchlorate (denoted as the perchlorate form) a dramatic loss of the PMS/MTT reductase activity occured while the ferricyanide reductase activity remained largely unaffected. The loss of activity was reversible and could be restored by addition of detergent or phospholipid. Although the phenomenon of activation of membrane-bound enzymes by amphipaths has been well documented (92,93,94,95), the mechanism(s) is still poorly understood. Therefore the

differential activation of G3PD was studied in detail. The approach taken was to systematically measure a number of physical and enzymatic parameters of the Brij and perchlorate forms of the enzyme in the hope of gaining a molecular understanding of amphipath activation.

B. Methods

1) Removal of Detergent.

As a final step in the purification, the enzyme was eluted from a phosphocellulose column at 4°C with 20 mM potassium phosphate, pH 7.5, 20% (v/v) ethylene glycol, 0.2% (w/v) Brij 58 and 0.65 M sodium chloride (Brij buffer). This enzyme preparation was diluted with two volumes of 20% (v/v) ethylene glycol and 0.2 % (w/v) Brij 58 and reapplied to a phosphocellulose column equilibrated at 4°C with 20 mM potassium phosphate, pH 7.5, 20% (v/v) ethylene glycol and 0.2% (w/v) Brij 58. After standing at room temperature for 15 mins to allow the column to thermoequilibrate the column was washed with 10 column volumes of 20 mM potassium phosphate, pH 7.5, and 20% (v/v) ethylene glycol. The enzyme was then eluted with 20 mM potassium phosphate, pH 7.5, 20% (v/v) ethylene glycol and 0.25 M sodium perchlorate (perchlorate buffer). The efficiency of detergent depletion was measured by assaying the dependence of enzyme activity on 0.01% (w/v) Brij 58 in the PMS-coupled MTT reduction assay.

2) Phospholipid Titrations.

Phospholipids were dried under nitrogen, resuspended in water and sonicated for 1-5 mins in 30 sec bursts at maximum power with the microprobe of a Bronson sonifier. Sonicated phospholipids were added directly to the assay mixture to the indicated final concentration (based on weight).

3) Fluorescence Measurements.

For measurement of detergent quenching of tryptophan fluorescence 10 ug of detergent-depleted enzyme were added to 2 ml of 10 mM potassium phosphate, pH 7.5, and titrated with Brij 58. Excitation was at 280 nm and the fluorescence spectrum between 300 and 400 nm was measured with a Turner Model 340 spectrofluorimeter equipped with a scanning device. At the operating sensitivity of the fluorimeter there was no fluorescence contribution by Brij 58. For measurement of the effect of substrate on endogenous flavin fluorescence, 25 ug of enzyme in 50 ul of either Brij or perchlorate buffers were added to 2 ml of 10 mM potassium phosphate, pH 7.5, and titrated with DL-glycerol-3-phosphate. Excitation was at 280 nm and the fluorescence spectrum was measured between 400 and 600 nm.

4) Thermal Stability.

One hundred ul aliquots of G3PD in either Brij (0.35 mg/ml) or perchlorate (0.55 mg/ml) buffers were incubated at 46°C and samples were withdrawn at various times for assay of the PMS/MTT reductase activity. All assays were performed in the presence of 0.01% (w/v) Brij 58.

5) Chemical Cross-Linking.

Cross-linking was performed, using dimethyl suberimidate as the crosslinker, essentially as described by Davies and Stark (96). Before cross-linking, the appropriate form of the enzyme was dialysed against either Brij or perchlorate buffers in which the potassium phosphate had been replaced with 0.2 M Triethanolamine-HCl, pH 8.5. Dimethyl suberimidate was dissolved in 0.2 M Triethanolamine-HCl, pH 8.5, and allowed to react with an equal volume of enzyme at room temperature for 3 hrs. The enzyme was cross-linked at a final concentration of 0.5 mg /ml, while the final concentrations of cross-linker was either 0.5 or 4 mg/ml.

6) Sedimentation Equilibrium Analysis.

Sedimentation equilibrium analysis of the enzyme in perchlorate buffer was performed at 7.5°C in a Beckman Spinco Model E analytical ultracentrifuge at a rotor speed of 8,000 rpm. The protein concentration was 1 mg/ml and a partial specific volume of 0.73 ml/g was assumed.

7) Circular Dichroic Measurements.

The circular dichroic spectrum of the enzyme in Brij or perchlorate buffers was measured between 200 and 250 nm at 27°C in a Cary 60 spectrophotometer with a 6001 CD attachment. Brij and perchlorate buffers were used to establish the baselines for the spectra. Protein concentrations were 0.34 and 0.55 mg/ml for the enzyme in Brij and perchlorate buffers respectively. Molar

ellipticities were calculated as described by Oikawa *et al* (97) and the α-helix β-sheet and random coil components were determined as described by Chen *et al* (98), see appendix II.

8) Ion Effects.

Stocks of zinc- and cupric sulfate at 1 and 0.1 mM respectively, were used. Salts were added directly to the assay mixture, before the addition of enzyme, to the indicated final concentrations.

9) Km and Vmax Measurements.

Km and Vmax values were obtained from the Wilkinson statistical fit (99) of initial rate measurements at varying concentrations of either DL-glycerol-3-phosphate, PMS or ferricyanide.

C. Results.

1) Activation by Phospholipids and Detergents.

Early experiments, performed by Elke Lohmeier and summarized in Figure 6 and Table 2 , were designed to test the effectiveness of a number of phospholipids and detergents as activators. Figure 6 shows the effects of a series of phosphatidylcholines on the PMS-coupled MTT reducing activity of the detergent-depleted form of the enzyme. Only dioleoyl- and dilaurylphosphatidylcholine activated effectively. At the temperature of the assay, 24°C, dipalmitoyl- and distearylphosphatidylcholine would be in the gel state while dimyristoylphosphatidylcholine would be close to its transition temperature. Additional

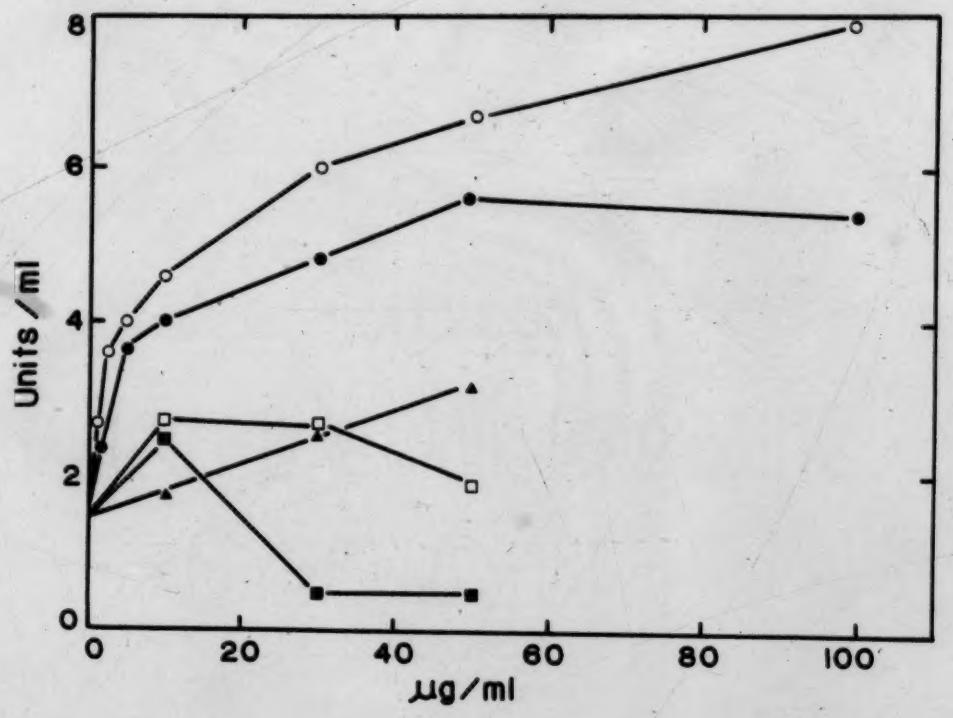

Figure 6. The effect of fatty acyl chain length on the PMS-coupled MTT reductase activity. Activity was measured as described in Chapter II with the appropriate phospholipids added.
○-○, dilaurylphosphatidylcholine;
●-●, dioleoylphosphatidylcholine;
▲-▲, dimyristoylphosphatidylcholine;
■-■, dipalmitoylphosphatidylcholine;
□-□, distearoylphosphatidylcholine.

Table 2

Effect of Detergents on the PMS/MTT Reductase Activity of G3PD.

Detergent	10 ug/ml	100 ug/ml
None	1.1	
Tween 20	2.2	7.5
Tween 40	2.7	8.8
Tween 60	4.8	8.9
Tween 80	2.7	9.4
Tween 85	3.0	10.4
Triton X-100	6.8	12.5
Triton X-114	2.6	14.4
Triton X-165	3.1	7.2
Triton X-102	2.8	5.8
Triton X-305	3.2	5.5
Triton X-45	3.0	0.8
Brij 96	10.7	14.1
Brij 58	17.0	20.0
SDS	1.3	0.15
Sodium cholate	1.8	1.6
Sodium deoxycholate	0.9	0

Assays were performed as described in Chapter II. Detergents were added directly to the assay cuvette followed by 1 ug of detergent-depleted enzyme. Activity is expressed in units/mg.

experiments, performed by Elke Lohmeier, indicated that there was no particular head group requirement for activation. These results indicated that fluid fatty acyl chains were required for activation. Table 2 lists a broad range of detergents which were tested for their ability to activate. While most of the nonionic detergents activated, the ionic detergents tested did not activate. The best activator was found to be Brij 58 and this was selected to study the mechanism of activation. In a similar series of experiments it was shown that the ferricyanide reductase activity was not affected by amphipaths. During this survey of activators Elke Lohmeier showed that replacing MTT with the more readily soluble electron acceptor DCPIP did not abolish the activation by Brij 58. This eliminated the possibility that amphipaths were acting by simply solubilizing the reduced form of MTT which is poorly soluble in aqueous solution.

Although the work of Elke Lohmeier, summarized above, firmly established the ability of amphipaths to selectively activate the PMS/MTT reductase activity of G3PD the mechanism of this activation was still uncertain. To test whether the effect involved a direct interaction between enzyme and activator, endogenous tryptophan fluorescence, which is a good probe of environment in the vicinity of this chromophore, was measured as a function of activator concentration. Quenching of fluorescence was seen in the same concentration range of Brij 58 as activation occured,

Figure 7. No shift in the emission maximum (350 nm) was seen. The decrease in fluorescence may have been due to a direct interaction between G3PD and Brij 58 which resulted in the exposure of a normally buried tryptophan to a more polar environment (100). However, the possibility that the quenching was due to a change in the environment of a surface exposed tryptophan cannot be ruled out. Further evidence of a direct interaction between G3PD and Brij 58 came from thermal stability studies. Incubation of G3PD, in perchlorate buffer, at 46°C resulted in 50% inhibition after 29 mins, Figure 8. On the other hand, G3PD in Brij buffer was not inhibited by 50% until after 80 mins incubation at 46°C. Interestingly, a break occured in the activity versus time profile for the enzyme in perchlorate buffer. The break occured after 21% of the activity had been lost. The break suggested two species of G3PD with different thermal stabilities: the more stable species may represent aggregrated G3PD which may be dissociated to the less thermally stable dimeric G3PD. The perchlorate form of the enzyme used in this study had a 4 fold dependence on Brij 58. Typically, detergent depletion resulted in a 3-5 fold dependence of the PMS/MTT reductase activity on Brij 58.

2) Effect of Activation on Quaternary Structure.

Purified G3PD migrates as a single band corresponding to a molecular weight of 58,000 on polyacrylamide gel electrophoresis in the presence of sodium dodecyl sulphate. Sedimentation equilibrium analysis of the perchlorate form

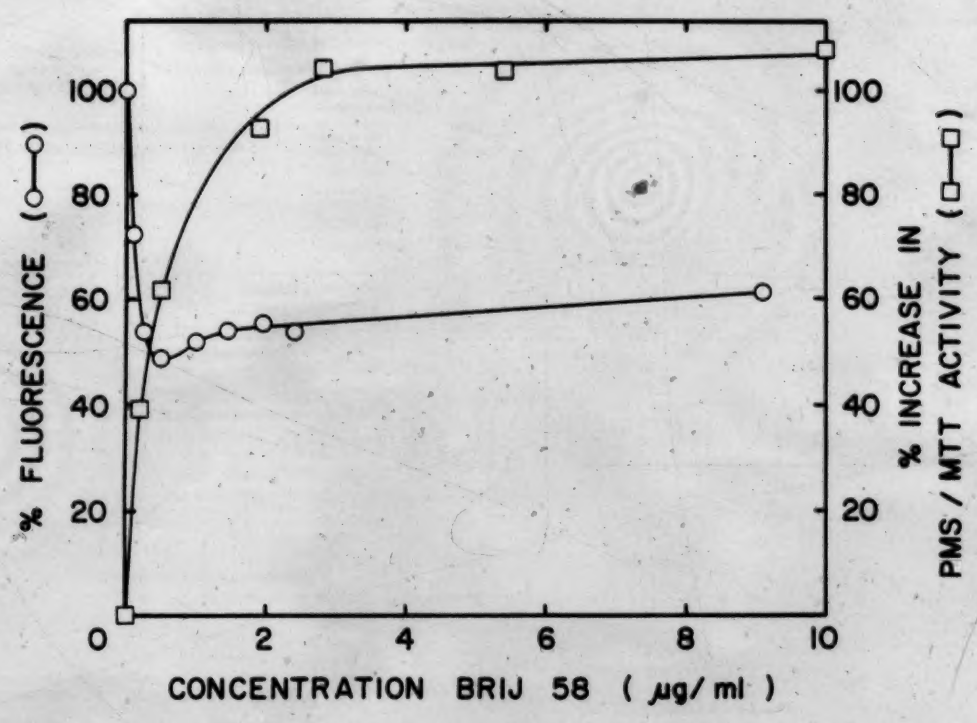

Figure 7. Correlation between Brij 58 mediated quenching of tryptophan fluorescence and stimulation of PMS-coupled MTT reduction. Quenching of tryptophan fluorescence was determined as described in the methods section by measuring the relative fluorescence at 350 nm. Actiyity is plotted as 3 percent stimulation above a base of 2.5 units/mg.

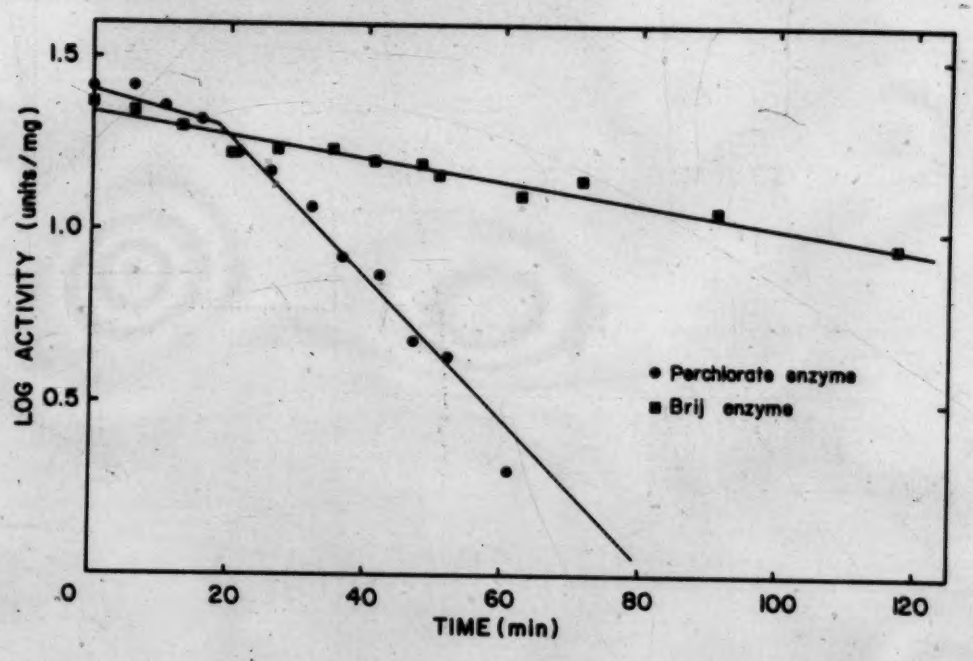

Figure 8. Thermal stability of G3PD at 46°C in the presence and absence of 0.2% (w/v) Brij 58. The protein concentrations were 0.35 mg/ml in the presence and 0.55 mg/l in the absence of Brij 58.

of the enzyme indicated a native molecular weight of 119,000, suggesting an α_2 dimeric structure. Elke Lohmeier, using analytical gel filtration, estimated the native molecular weight of the perchlorate form of G3PD to be 120,000. Since sedimentation equilibrium and gel filtration data are anamolous for proteins containing bound detergent, the effect of activation on quaternary structure was probed using the bifunctional cross-linking reagent dimethyl suberimidate. Dimethyl suberimidate is a bis alkylimidate which cross-links primary amino groups separated by 11 Å or less (101). Figure 9 shows the cross-linking pattern obtained using dimethyl suberimidate at 0.4 and 5 mg/ml and a protein concentration of 0.5 mg/ml. Identical patterns were obtained for the perchlorate and Brij forms of the enzyme. Suprisingly a major band of 177,000 daltons appeared in addition to the 125,000 dalton dimeric G3PD. A possible explanation for this high molecular weight band came from a study of lactoperoxidase catalysed iodination of purified G3PD followed by electrophoresis on a 20% polyacrylamide fast running gel in the presence of sodium dodecyl sulfate (91). This experiment revealed two bands of radioactivity, Figure 10. One band corresponded to G3PD with a molecular weight of 58,000 while the other labelled band corresponded to a polypeptide of approximate molecular weight 12,000. This low molecular weight band stained poorly with Coomassie Brilliant Blue. The 177,000 dalton species may result from cross-linking of several molecules of this low molecular

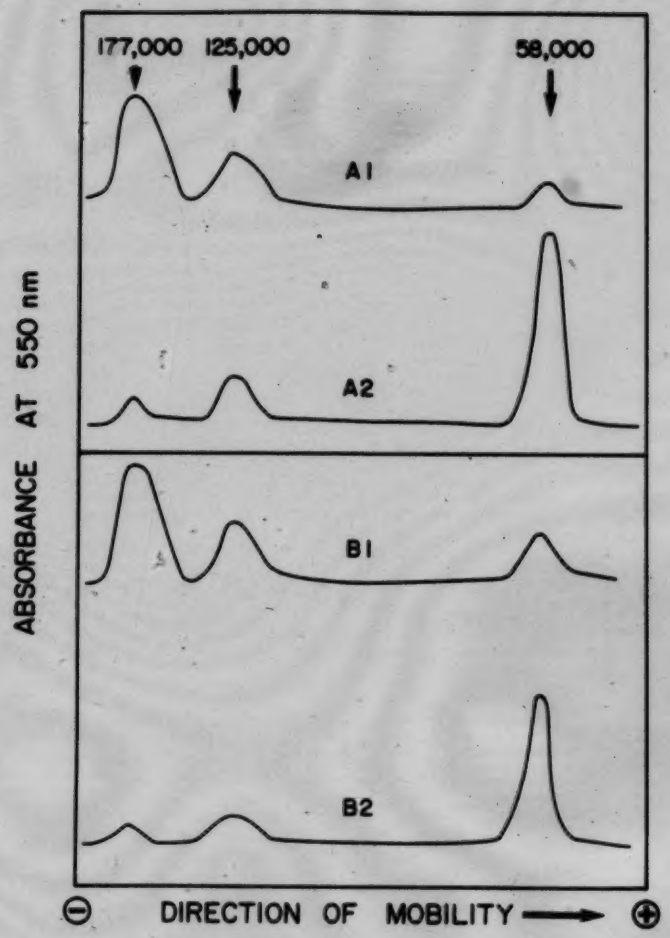

Figure 9. Densitometric scan of the SDS-PAGE electrophoretic pattern of G3PD cross-linked by dimethyl suberimidate. (A1) Enzyme in Brij buffer cross-linked at 4 mg/ml dimethyl suberimidate. (A2) Enzyme in Brij buffer cross-linked at 0.5 mg/ml dimethyl suberimidate. (B1) Enzyme in perchlorate buffer cross-linked at 4 mg/ml dimethyl suberimidate. (B2) Enzyme in perchlorate buffer cross-linked at 0.5 mg/ml dimethyl suberimidate. The protein concentration was 0.5 mg/ml.

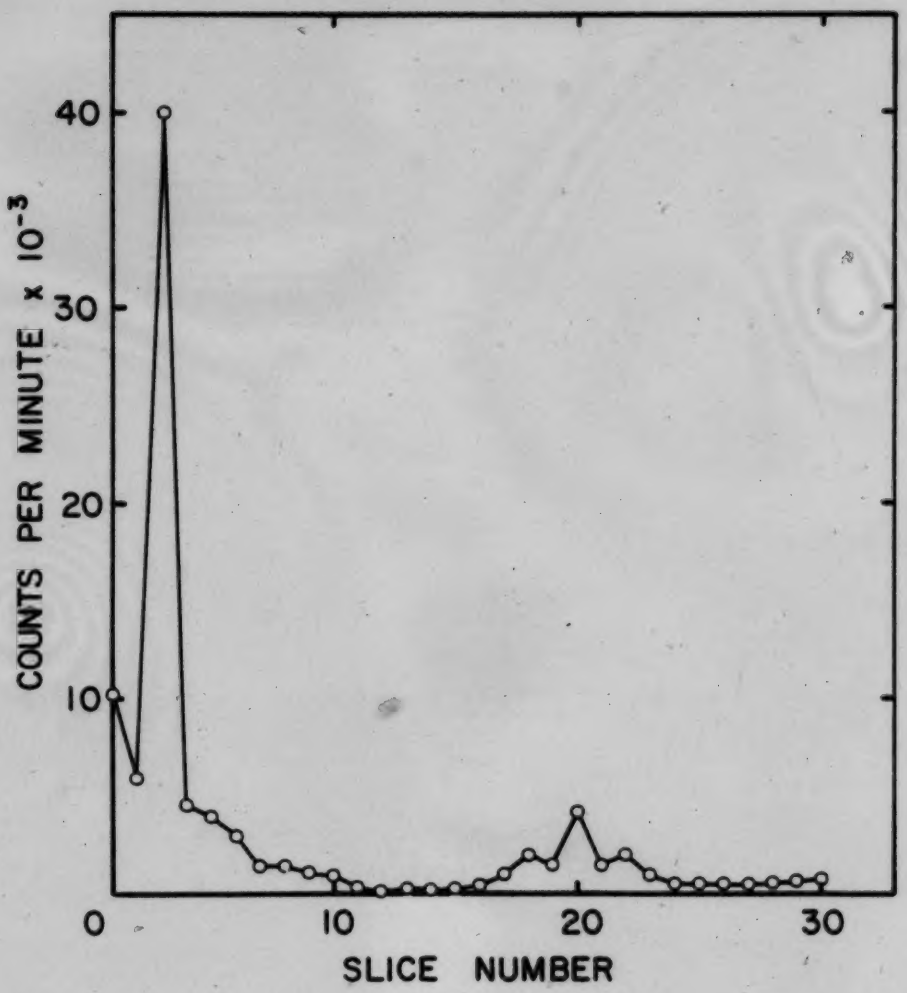

Figure 10. Lactoperoxidase catalysed ^{125}I-iodination of G3PD in Brij buffer. A stock of sodium (^{125}I) iodide was neutralized and reduced as described in Chapter V. To 100 μl of G3PD (0.5 mg/ml) was added 1 mCi of sodium iodide, H_2O_2 to 0.2 mM (prepared by dissolving 30 μl of 30% H_2O_2 in 4.5 ml of 0.1M potassium phosphate, pH 7.5) and 1 unit of lactoperoxidase (also prepared in 0.1 M potassium phosphate, pH 7.5). The reaction was allowed to go for 60 mins at room temperature and stopped by the addition of 50 μl of 0.4% acetic acid. After extensive dialysis to remove free iodide, the sample was electrophoresised according to the method of Jovin *et al* (91) in 10 cm long tube gels. After staining and destaining the gels were sliced into 3 mm pieces and counted in an LKB 1270 Rackgamma II.

weight polypeptide to dimeric G3PD. The possibility that G3PD existed as a trimer seemed unlikely in view of the sedimentation equilibrium and gel filtration data; no species other than the dimeric form was detected by either approach. In summary, the cross-linking data suggested that activation by Brij 58 did not involve any rearrangement of quaternary structure.

3) Effect of Activation on Secondary Structure.

One of the most likely mechanisms of activation was that of conformational change. In order to test this possibility I examined the effect of activation on the secondary structure of G3PD. Circular dichroic spectra for the Brij and perchlorate forms of G3PD were measured in the far ultraviolet. The percentages of α-helix, β-sheet and random coil determined from the spectra were respectively, 25.7, 10.4, and 63.9% in the absence of Brij 58 and 23.9, 16.2, and 59.9% in the presence of Brij 58. The most sensitive index of conformational change is the change in α-helix and a difference of 1.8% is of borderline significance. Therefore, I concluded that activation of the PMS/MTT reductase activity is not accompanied by any large change in secondary structure. However, I could not definitely rule out the possibility of a small change in secondary structure resulting in activation.

4) Effect of Activation on Substrate Binding.

Advantage was taken of the flavoprotein nature of G3PD to measure substrate binding to the Brij and perchlorate

forms of the enzyme. Quenching of flavin fluorescence at 500 nm was followed as a function of DL-glycerol-3 phosphate concentration. The quenching profiles were almost identical for both forms of the enzyme, Figure 11. Apparent dissociation constants of 19.5 and 17.1 μM were measured for the Brij and perchlorate forms respectively. This result suggested that amphipaths were not activating by altering the affinity of the enzyme for its substrate.

5) Effect of pH on the Reductase Activities of Activated G3PD.

Since amphipaths were not acting by altering the affinity of the perchlorate form of the enzyme for its substrate it was postulated that activation might involve an increase in the affinity of G3PD for the electron acceptor PMS. Such a mechanism might involve a small conformational change, not detectable by circular dichroic measurements, which would more readily facilitate PMS binding. If indeed the binding sites for the electron acceptors PMS and ferricyanide were different and if different amino acids were involved in acceptor binding and reduction at these sites, then the pH profiles for the PMS and ferricyanide reductase activities might be expected to be different. In order to test this hypothesis, the pH dependence of both reductase activities was measured in the range 6-9. The results of these measurements are shown in Figure 12. No difference was found between the pH dependence of the PMS/MTT and ferricyanide reductase activities. This result

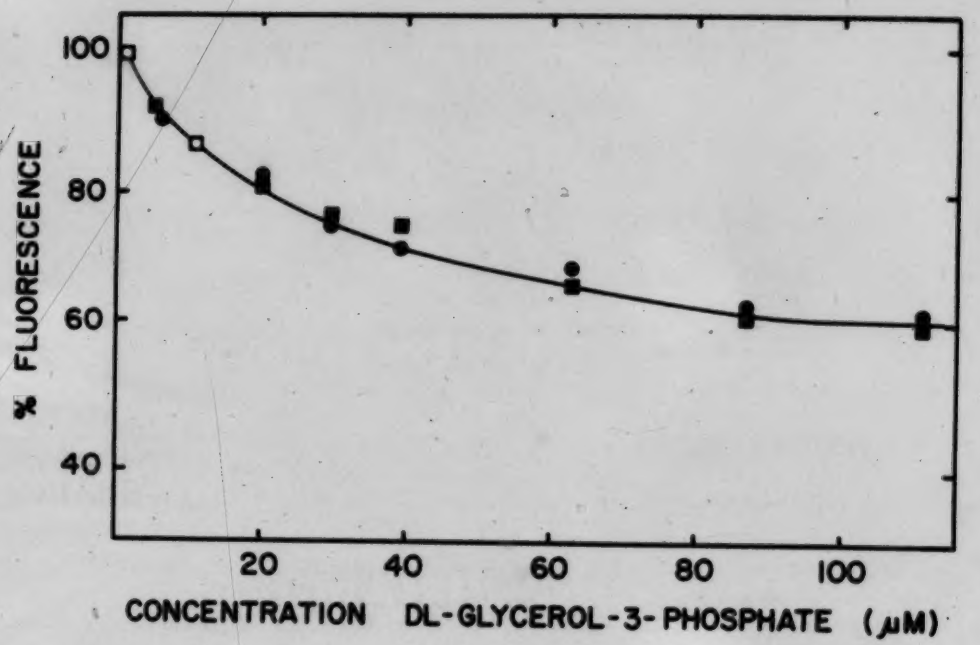

Figure 11. Fluorescence titration curves of G3PD. Fluorescence measurements were carried out as described in the methods section with increasing amounts of DL-glycerol-3-phosphate. The quenching of fluorescence at 500 nm is plotted for the Brij ●-● and perchlorate ■-■ forms of G3PD.

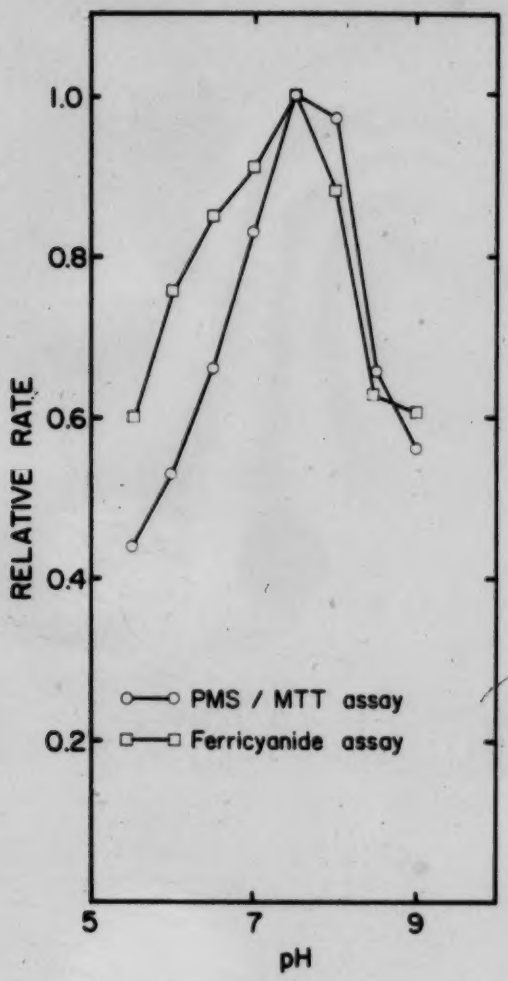

Figure 12. The pH dependence of the PMS/MTT and ferricyanide reductase activities of G3PD. Enzyme in Brij buffer was used and assays were performed as described in Chapter II in the presence of 0.01% (w/v) Brij 58 except that the assay buffer was varied as described below. All buffers used were at a concentration of 50 mM. Tris-HCl, pH 7-9; Hepes, pH 7-8; Imidazole-HCl, pH 6-7.5; Cacidylate, pH 5-6.5.

suggested that the nature of the amino acids involved in the reductase reactions are probably the same for both electron acceptors. However, the possibility of PMS and ferricyanide binding at different sites could not be ruled out.

6) Selective Inhibition of the PMS/MTT and Ferricyanide Reductase Activities.

In order to persue the possibility of different binding sites for PMS and ferricyanide an attempt was made to inhibit one of the two reductase activities of the activated enzyme. In one approach a broad range of heavy metal ions was tested for their effectiveness as inhibitors. Cupric sulfate was found to inhibit the PMS/MTT reductase activity while zinc sulfate inhibited the ferricyanide reductase activity of the activated G3PD. Figures 13 and 14 show the effects of titrating the activated enzyme with either cupric sulfate or zinc sulphate. Concentrations of cupric sulfate as low as 3 μM caused 88% inhibition of the PMS/MTT reducing activity while the ferricyanide reducing activity was unaltered by concentrations as high as 10 μM. On the other hand, Figure 14 shows that 50 μM zinc sulfate completely inhibited the ferricyanide reducing activity while the PMS/MTT reducing activity was only inhibited 27%. Similar ion inhibitions were found for the enzyme in the absence of activating amphipath, although the PMS coupled reduction of MTT was very low. The possibility that these specific ion inhibitions may be related to an inhibition of substrate (glycerol-3-phosphate) binding was eliminated by measuring

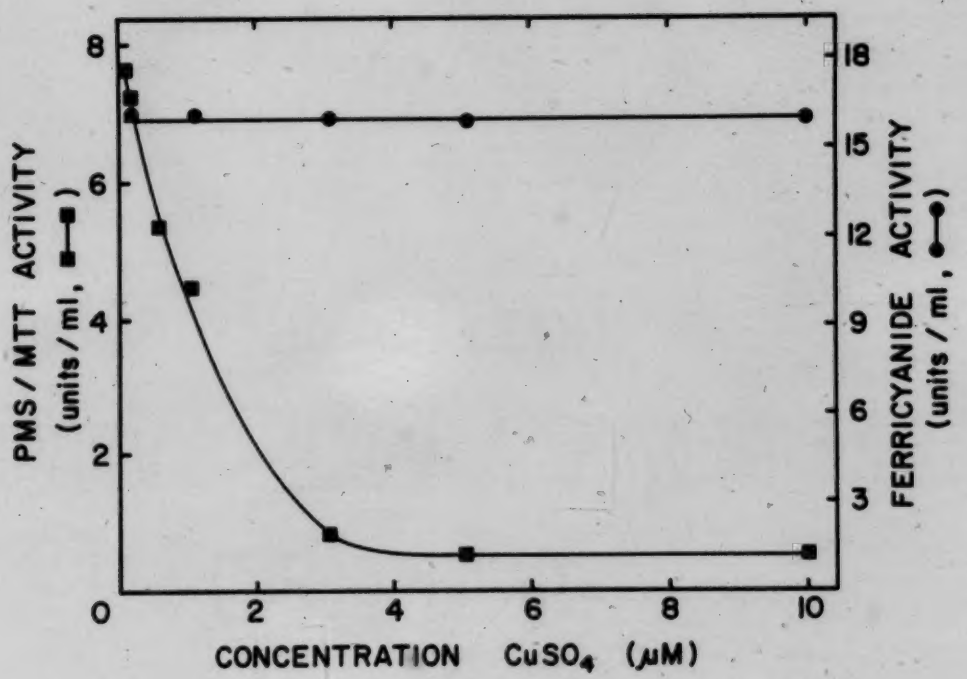

Figure 13. Inhibition of activity by cupric sulfate. Activity was measured in the presence of 0.01% (w/v) Brij 58 as described in Chapter II.

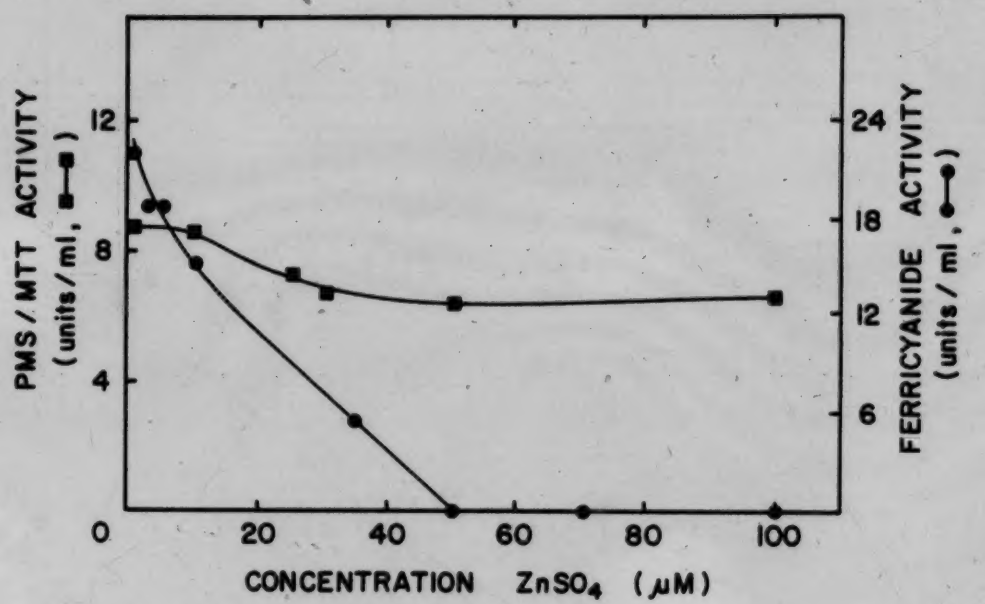

Figure 14. Inhibition of activity by zinc sulfate. Activity was measured as described in the Chapter II in the presence of 0.01% (w/v) Brij 58. Two μg of enzyme in Brij buffer was used per assay.

the apparent dissociation constants for the activated enzyme in the presence or absence of 40 μM cupric sulfate. Values of 19.6 and 17.5 μM were obtained in the presence and absence of inhibitory cation respectively. Both reducing activities could be protected from the inhibitory effects of copper and zinc ions in the assay mixture. The presence of 500 μM cysteine overcame 52% of the inhibition by cupric sulphate. Higher concentrations of cysteine caused reduction of the PMS and MTT. The presence of 50 μM cysteine overcame 78% of the zinc inhibition of the ferricyanide reducing activity. The addition of DL-glycerol-3 phosphate, PMS or ferricyanide to the assay mixture before addition of cupric or zinc ions did not protect against inhibition. The differential effect of copper and zinc ions suggested that G3PD may have different binding sites for the electron acceptors PMS and ferricyanide.

A number of control experiments were performed to show that the ion inhibitions were not due to interference with the assays.

a) When the PMS/MTT reduction assay was used to measure the activity of D-lactate dehydrogenase in Kaback vesicles, 50 μM cupric sulfate was required to produce 88% inhibition. This indicated that the inhibition of G3PD by 3 μM cupric sulfate was not due to interference with the assay.

b) Since potassium ferrocyanide chelates cupric ions (102) it was possible that the lack of inhibition of the ferricyanide reductase activity by cupric sulfate was due to

chelation of the cupric ions by potassium ferrocyanide which is produced by reduction of potassium ferricyanide. This possibility was eliminated by (1) the lack of any turbidity in the assay mixture upon reduction of potassium ferricyanide in the presence of cupric sulfate and (2) when the succinate dehydrogenase activity of fumarate reductase was measured by the ferricyanide reduction assay, 10 and 30 μM cupric sulfate caused 30 and 50% inhibition, respectively. These results make it unlikely that the potassium ferrocyanide produced during the assay chelates the cupric ions presence.

c) When the ferricyanide assay was used to measure the succinate dehydrogenase activity of fumarate reductase, 30 and 100 μM zinc sulfate caused 12 and 43% inhibition respectively. This result indicated that zinc sulfate was not interfering with the ferricyanide assay. Interestingly, the succinate dehydrogenase activity of fumarate reductase, as assayed by the ferricyanide assay, was inhibited by both copper and zinc ions. This finding strongly suggested that the selective inhibition of the reductase activities of G3PD was not due to interference with the assays caused by copper and zinc ions.

d) The above controls make it unlikely that the selective inhibitions were due to chelation of the Cu^{+2} or Zn^{+2} ions by PMS or ferricyanide.

7) Effect of Activation on the Apparent Michaelis-Menten Constants.

Table 3 lists the apparent Km and Vmax values for DL-glycerol-3 phosphate in the presence or absence of Brij 58. The maximal velocity, as measured by the PMS/MTT reduction assay, was increased three-fold by the presence of Brij 58 while the Vmax for the ferricyanide assay was essentially unaffected by amphipaths. Interestingly, the apparent Km values for DL-glycerol-3-phosphate were quite different when determined by the ferricyanide and PMS/MTT reduction assays. One possible explanation for the difference in apparent Km was that the binding sites for PMS and ferricyanide were different. However, it was also possible that both electron acceptors bound to the same site but with different affinities.

Measurement of the apparent Km for PMS is difficult because of the auto-oxidation of reduced PMS by oxygen. In other words there is no quantitative transfer of electrons from PMS to MTT. Therefore, measuring the rate of MTT reduction as a function of PMS concentration does not generate a conventional apparent Km. However, if we assume that the percentage of reduced PMS oxidized by air is independent of PMS concentration, then what I have called K'm is a useful measure of the dependence of enzyme turnover on PMS concentration. Not suprisingly, the K'm for PMS is reduced by activation; this result is in agreement with the postulate that amphipaths act by increasing the

Table 3

The Effects of Amphipaths on the Kinetic Constants of G3PD.

Enzyme Assay	Vmax (u/mg)	Km(mM) DL-G3P	Km(mM) Ferricyanide	K'm(mM) PMS
PMS-MTT	2.5±0.2	1.89±0.4	-	0.21±0.04
PMS-MTT+ Brij 58	7.3±0.5	2.4±0.6	-	0.08±0.01
Ferricyanide	15±1.7	11.4±1.6	0.12±0.03	-
Ferricyanide +Brij 58	12±1.6	10.2±2.4	0.13±0.04	-

DL-G3P = DL-Glycerol-3-Phosphate'.

The concentration of Brij 58 was 0.01% (w/v).

'Only the racemic mixture of glycerol-3-phosphate was commercially available. It has been shown that D-glycerol-3-phosphate does not affect the activity of G3PD (Weiner, J.H., unpublished data)

accessibility of some enzyme binding site for PMS. The apparent Km for ferricyanide was not altered by activation. However, the Km values measured for ferricyanide are subject to considerable error. The assay is performed at 420 nm and we measure directly the reduction of ferricyanide. Since the extinction coefficient for ferricyanide is 1 mM^{-1} cm^{-1} as we decrease the concentration of ferricyanide the difference in optical density at the beginning and end of the reaction decreases and therefore the accuracy of the measurement also decreases. Although some caution must be exercised in interpreting some of the data in Table 3, these results support the hypothesis that activation results in an increased interaction between G3PD and PMS.

D. Discussion.

As our concepts of the structure of biological membranes have changed from the largely static unit membrane model of Davson and Danielli (103) to the dynamic fluid mosaic model of Singer and Nicholson (104), an awareness of the role of lipid-protein interactions in membrane function has developed. The Singer Nicholson model envisages a biological membrane as a sea of lipid molecules into which are embedded proteins. According to this model, membrane proteins can be divided into two classes depending on the conditions required for their extraction: intrinsic or integral proteins which require drastic disruption of membrane structure for their release and extrinsic or

peripheral proteins which can be removed without destruction of the lipid bilayer. The important contribution of this model is that it depicts biological membranes as dynamic structures in which lateral motions of both lipid and protein molecules can occur as well as interactions between these components.

Even before this model was proposed, membrane biochemists had recognized a dependence of membrane-associated activities upon the physical state of membrane lipids. By comparing the Arrhenius plots of succinate dehydrogenase activity in acetone extracted *E.coli* membranes before and after incubations with dispersions of lipids, Esfahani *et al* (105) showed that the break points in Arrhenius plots were dependent upon phospholipid composition. Experiments of this type have been performed by many investigators(106,107,108) and suggest that the physical state of membrane lipids affects the catalytic activity of membrane-bound enzymes. The fact that many purified membrane proteins are found to have phospholipid associated with them lends further support to the suggestion that lipid-protein interactions occur within membranes. However, the most direct evidence for lipid protein interactions comes from experiments in which purified proteins, membranes or cellular organelles are depleted of lipid with a resultant loss of enzymatic activity (105,109,110). Readdition of lipid generally results in a return of activity.

Experiments of the type outlined above have resulted in wide acceptance of the concept that lipids regulate membrane function through their interactions with membrane proteins. However, as the methodology used to probe lipid protein interactions has become more sophisticated, a controversy has developed over the possible existance of boundary lipid(111,112,113,114). The term "boundary lipid" is used to describe a discrete species of lipid which may occur within biological membranes and is distinct from the bulk lipid in that it interacts directly with proteins embedded within the bilayer and as a result is less mobile than the bulk lipid. The existance of boundary lipid has been probed using sophisticated physical techniques such as electron spin resonance (esr) and nuclear magnetic resonance (nmr) spectroscopy. These techniques will not be described here; it suffices to say that esr studies tend to support the existance of boundary lipid while nmr generally fails to detect an immobile lipid phase in biological membranes (112,113).

However, despite the controversy over boundary lipid few biochemists would dispute a role for lipid in regulating the activities of membrane proteins. When one considers the activation of enzymes by amphipaths a number of possible mechanisms come to mind: a) Amphipaths may be acting by solubilizing either the substrate or product of the reaction. Substrate solubility has been reported to be a problem when studying enzymes of lipid or glycolipid

biosynthesis. It has been shown that glycosyltransferases, involved in the biosynthesis of lipopolysaccharides in the cell envelope of the gram-negative bacterium *Salmonella typhimurium*, are activated by phospholipids. However, this activation seems to involve an interaction between the lipopolysaccharide substrate and the phospholipid rather than an interaction between the glycosyltransferase and the phospholipid activator (115). Thus it seems that substrate solubilization is responsible for the apparent activation of enzymic activity. The substrate for G3PD is L-glycerol-3-phosphate which is readily water soluble. The possibility of product solubilization by amphipaths was ruled out by replacing MTT with the readily water soluble electron acceptor DCPIP. This latter experiment was performed by Elke Lohmeier. b) Enzyme solubilization by amphipath is another possible mechanism of activation. This mechanism is supported by the observation that many detergents activate at concentrations close to their critical micellar concentrations (116). Phospholipids on the other hand, activate at concentrations of 0.1-2 mM which are considerably above their critical micellar concentrations (116). *E.coli* pyruvate oxidase appears to be an exception to this rule; phospholipids and detergents bind to high affinity sites in monomeric form and probably act as allosteric affectors (117,118,119). Umbreit and Strominger (120) have shown that D-alanine carboxypeptidase, isolated from *B.subtilis* membranes, could be activated by detergents.

The relative effectiveness of detergents as activators corresponded to the effectiveness of the detergents in solubilizing membrane-bound enzyme activity. However, the authors did not try to correlate activation with a change in quaternary structure. This mechanism seems unlikely in the case of the aerobic G3PD since its quaternary structure, as measured by cross-linking, is not affected by Brij 58. The fact that different nonionic detergents activate to different extents suggests that a simple rearrangement of quaternary structure was not involved in activation. Also, the hydrophilic lipophilic balance number of Brij 58 indicates that it is a poorer solubilizer than Triton X-100 (70). c) The third and most obvious possibility, but unfortunately the most difficult to measure, is that of conformational change. In only a very few cases has it been possible to directly demonstrate a conformational change upon activation (121). However, conformational change has been inferred from indirect evidence such as an increase in thermal stability (93), or a change in the apparent Km (93,121).

In this study I examined a number of properties of the Brij and perchlorate forms of G3PD. The quenching of tryptophan fluorescence upon activation may be due to a conformational change which exposes a buried tryptophan to a more polar environment. The differential inhibition of the two reductase activities by cupric and zinc ions suggests that the binding sites for PMS and ferricyanide may be

different. Interestingly, the differential inhibition by cyanide of the different reductase activities of formate dehydrogenase from *E.coli* has led Enoch and Lester (54) to conclude that this enzyme has a distinct binding site for each of its artificial electron acceptors. The possibility of different binding sites for PMS and ferricyanide is further supported by the different apparent Michaelis-Menten constants for DL-glycerol-3-phosphate as determined by the PMS/MTT and ferricyanide assays. Finally the decrease in K'm for PMS upon activation suggests that amphipaths increase the interaction between PMS and G3PD. Taken together the results described in this chapter indicate that amphipaths act at the level of the electron acceptor PMS, and suggest that activation is mediated by a conformational change which increases the interaction between PMS and G3PD.

In a previous study the apparent Km for DL-glycerol-3 phosphate was measured by following proline uptake in Kaback vesicles (48). An apparent Km of 2 mM was obtained. This indirect measurement suggests that the apparent Km for DL-glycerol-3-phosphate determined by the PMS/MTT assay may be a physiologically relevant number. It is therefore possible that amphipaths are generating a physiologically relevant binding site for an electron acceptor. This suggestion is not inconsistent with the results of other workers. Ragan and Racker (122) have shown that when mitochondrial complex 1 is depleted of more than 50% of its phospholipid it loses its coenzyme Q reductase activity

while the ferricyanide reductase activity is uneffected. Reconstitution of the depleted complex with phospholipid regenerated the coenzyme Q reductase activity. Similarly, Rossi *et al* (123) have shown that extraction of coenzyme Q_{10} from the inner mitochondrial membrane results in a loss of PMS/MTT reductase activity of succinate dehydrogenase at one of the two binding sites for this electron acceptor. They concluded that the presence of coenzyme Q_{10} is required for the normal functioning of one of the two binding sites for phenazine methosulphate. These results suggest that amphipaths may affect physiologically relevant activities and that the phenazine methosulphate binding site may be of physiological significance.

IV. Molecular Properties of Fumarate Reductase.

A. Introduction.

As part of our overall goal of reconstituting the glycerol/fumarate electron transport chain of *E.coli*, fumarate reductase has been purified and partially characterized in this laboratory (70,71,72). However, the previous studies were somewhat incomplete and did not address such questions as the quantitation of the interaction of the purified enzyme with detergents, the iron-sulfur content or the nature of the amino acid residues essential for activity. I felt that a more extensive characterization was required before any successful reconstitution of an electron transport chain involving fumarate reductase could be attempted. I have therefore extended the previous studies and my results are presented in this chapter.

B. Methods.

1) Dimethyl Suberimidate Cross-Linking of Fumarate Reductase.

Cross-linking was performed as described by Davies and Stark (96). Fumarate reductase, in 400 mM potassium phosphate, pH 6.8, was made 60% (by saturation) in ammonium sulphate, and the precipitated protein redissolved in 200 mM triethanolamine-HCl, pH 8.5, and dialysed against this buffer for 17 hrs at 4°C to remove ammonium sulphate.

Dimethyl suberimidate was taken up in 200 mM triethanolamine titrated to pH 8.5 with and allowed to react with an equal volume of fumarate reductase at room temperature for 3 hrs. The enzyme was cross-linked at a final concentration of 5 mg/ml while the final concentration of dimethyl suberimidate was also 5 mg/ml.

2) Isolation of Subunits for Amino Acid Analysis.

The enzyme subunits were isolated by Kelly Dabbs using the procedure of Ziola and Scraba (124). Samples containing fumarate reductase labelled with Remazol Brilliant Blue by the procedure of Griffith (125) were used to follow migration of the subunits during the isolation steps.

3) Amino Acid Analysis.

Samples of the separated subunits were dialysed at 24°C for 24 hrs against 50 mM ammonium bicarbonate, pH 7.5, to remove SDS. Aliquots containing 1 nmole of individual subunits were lyophylized in 10x75 mm pyrex tubes. The samples were subjected to acid hydrolysis in 6N HCl at 110°C in evacuated, sealed tubes for periods of 24, 48, 72 and 96 hrs (126). Samples containing 2 nmoles of subunit were subjected to performic acid oxidation followed by 24 hrs acid hydrolysis for determination of cysteine (127). The hydrolysates were evaporated to dryness, dissolved in 0.1 ml of 0.2 M sodium citrate, pH 2.2, and chromatographed on a Durrum Model D-500 Amino Acid Analyser. The values of serine threonine, valine and isoleucine were determined by extrapolation of the amino acid/leucine or amino

acid/alanine ratios to zero time. In each case the values were in good agreement. The number of tryptophan residues were determined, by Kelly Dabbs, as described by Edelhoch (128).

N-Terminal analysis of the separated subunits of fumarate reductase was performed by Automated Edman Degradation using a Beckman Model 890B sequenator. This work was performed by Mike Carpenter in the laboratory of Dr L.Smillie.

4) Two Dimensional Polyacrylamide Gel Electrophoresis.

The first dimension electrofocusing was performed in slab gels as described by O'Farrell (129) using 15x16 cm glass plates. The composition of the gel was as follows: acrylamide 5.3% (w/v), bis-acrylamide 0.16% (w/v); urea 8M; Nonidet P-40, 2% (v/v); ampholytes, pH 6-8, 1.6% (w/v), pH 3-5, 0.4% (w/v); ammonium persulphate 0.01% (w/v) and TEMED 0.07% (v/v). Twenty five μl of purified, cholate-depleted fumarate reductase (1 mg/ml) was made 8M in urea and added to an equal volume of lysis buffer (urea 8M; Nonidet P-40 2% (v/v); ampholytes, pH 6-8, 1.6% (w/v), pH 3.5-10, 0.4% (w/v); and β-merçaptoethanol, 5% (v/v)). Fifty μl of lysis buffer were added to each well and the gel was pre-run at 200V for 15 mins, 300V for 30 mins and 400V for 30 mins. After pre-running, the wells were emptied and the samples applied. The gel was then run at 360V for 16 hrs and at 450V for 1 hr. The cathode electrolyte was 0.02 M sodium hydroxide, which had been degassed by stirring under reduced

pressure for 6 hrs. The anode electrolyte was 0.01 M phosphoric acid. After electrophoresis one strip of gel was cut out and frozen at -80°C. The pH gradient was measured as follows: a strip of gel was cut into 3 mm pieces and incubated in 1 ml of degassed water at room temperature for 18 hours and the pH was measured. The rest of the gel was fixed by shaking for 20 hrs at 37°C in 1 litre of 10% (w/v) trichloroacetic acid. This treatment was followed by staining for 1 hr at 37°C in 1 litre of Coomassie Brilliant Blue R-250 (1 mg/ml) in ethanol-acetic acid-water (9:2:9 v/v) and the gel was destained in ethanol-acetic acid-water (25:10:60 v/v). For identification of the bands, the strip of gel which had been frozen was thawed, incubated in electrophoresis buffer for 20 mins at room temperature and placed on top of a Laemmli gel (15% (w/v) acrylamide in the running gel and 5% (w/v) in the stacking gel). The strip of electrofocusing gel was held in place with stacking gel. The gel was run, stained and destained as described in Chapter II.

5) Triton X-100 Binding.

^{3}H-Triton X-100 binding was determined as described by Clarke (130) using 5-20% (w/v) sucrose gradients. Two hundred μl of cholate-depleted fumarate reductase (0.56 mg of protein) in 0.4 M potassium phosphate, pH 6.8, was made 2% (v/v) in Triton X-100 and dialysed against 0.1 M sodium sulfate, 0.01 M Tris-SO_4, pH 7.5, and 2% (v/v) Triton X-100 for 24 hrs at 4°C. After dialysis the sample was diluted to

600 µl with dialysis buffer and 150 µl aliquots (0.14 mg of protein) applied to 3.9 ml continuous sucrose gradients containing 5-20% (w/v) sucrose; 0.1 M sodium phosphate; 0.01 M Tris-SO_4, pH 7.5, and 0.05%, (v/v) ^{3}H-Triton X -100. Centrifugation was at 210,000g for 15 hr at 4°C in a Beckman SW-56 rotor. The gradients were fractionated into 15 drop fractions and 50 µl counted for tritium using 5 ml of Aquasol, in a Beckman LS-230 liquid scintillation counter. A counting efficiency of 53.8% was determined using tritiated proline. Using the internal standard method no difference in quenching was found as a function of sucrose concentration. Protein was determined by the method of Lowry *et al* (131) using Biorad protein standard.

6) Treatment of Fumarate Reductase with Sulfhydryl Reagents.

Twenty millimolar and 0.04 mM stock solutions of iodoacetamide and DTNB respectively, were prepared in 100 mM potassium phosphate, pH 8.0. One hundred µl aliquots of these stocks were added to equal volumes of cholate-depleted fumarate reductase (2 mg/ml) in 0.4 M potassium phosphate, pH 6.8, and incubated at 36°C. Five µl aliquots were withdrawn at the indicated times and assayed for fumarate reductase activity.

Quantitation of the sensitive sulfhydryl group(s) was performed as follows: 0.21 mg of cholate-depleted enzyme in 130 µl of 0.2 M sodium phosphate, pH 6.8, was added to an equal volume of 0.4 mM DTNB in 0.2 M sodium phosphate, pH 6.8, in 0.5 ml quartz cuvettes. The reagents were mixed by

rapid inversion and the cuvette was placed in a Gilford 250 spectrophotometer. The absorbance at 412 nm (132) was set to zero within 10 sec of mixing and the increase in absorbance was followed with time. It was assumed that the increase in absorbance during the first 10 secs of the reaction was the same as that recorded during the second 10 secs and this assumption enabled the change in absorbance to be measured from zero time. The calculation of sulfhydryl groups modified was performed as described by Ellman (132) using an extinction coefficient for the anion of DTNB of 13.6 10^3 M^{-1} cm^{-1}. In an identical experiment to that described above 0.21 mg of enzyme in 130 µl of sodium phosphate, pH 6.8, was mixed with an equal volume of 0.4 mM DTNB in 0.2 M sodium phosphate, pH 8.0, and incubated at room temperature. Three µl aliquots were diluted into assay buffer at the indicated times and assayed for fumarate reductase activity.

7) Identification of the Subunit containing the Essential Sulfhydryl Group.

For identification of the subunit containing the essential sulfhydryl group, 0.21 mg of cholate-depleted enzyme in 130 µl of 0.2 M sodium phosphate, pH 6.8, was added to an equal volume of 0.4 mM DTNB in 0.2 M sodium phosphate, pH 8.0. The reaction mixture was incubated at room temperature for 2 min and then passed down a 2 ml Sephadex G-25 column under pressure to rapidly separate the DTNB-modified enzyme from the unreacted DTNB. The column was

pre-equilibrated in 20 mM Tris-HCl, 200 mM sodium phosphate, pH 9.0, and eluted with the same buffer. Six micromoles of sodium ^{14}C-cyanide (7.9 mCi/mmole) in 50 μl equilibration buffer was then added to the DTNB-modified protein and the reaction mixture was incubated at room temperature. After 30 mins incubation the reaction mixture was applied to the 2 ml Sephadex G-25 column in order to separate free from bound ^{14}C-cyanide. An aliquot of the eluted protein was then subjected to electrophoresis on the fast running gel system of Jovin *et al* (91) as described in Chapter II except that a) dithiothreitol was omitted from the solubilizing buffer and b) solubilization was by incubation for 60 mins at room temperature. Following electrophoresis strips of gel were sliced into 3 mm pieces and incubated at 50°C for 4 hrs in 0.5 ml of 94% NCS Tissue Solubilizer. After incubation, 17 μl of glacial acetic acid and 10 ml of Aquasol were added and the samples were counted for ^{14}C. The remainder of the gel was stained and destained as described in Chapter II. In control experiments 0.21 mg of fumarate reductase was treated exactly as described above except that instead of dilution with 0.4 mM DTNB in 0.2 M sodium phosphate, pH 8.0, the sample was diluted with buffer alone. The results are presented as the ^{14}C-labelling profile in the sample treated with DTNB minus the baseline ^{14}C values established with the control experiments. The baseline value was, on average, 120 cpm.

8) Effect of p-Chloromercuriphenylsulfonate on the Visible Absorption Spectrum of Fumarate Reductase.

The visible absorption spectrum of the cholate-depleted enzyme (0.78 mg/ml) in 0.9 ml of 0.2 M sodium phosphate, pH 6.8, was measured at room temperature in a Gilford 2600 spectrophotometer equipped with a Hewlett Packard 7225A plotter using 0.2 M sodium phosphate, pH 6.8, as a blank. Seventy-five μl of 20 mM p-chloromercuriphenylsulfonate in 0.1 M sodium phosphate, pH 8.0, was then added and the reaction mixture incubated at room temperature for 2 mins. After incubation, the spectrum was again measured using 1.5 mM p-chloromercuriphenylsulphonate in 0.2 M sodium phosphate, pH 6.8, as the blank.

9) Iron-Sulfur Content.

Non-heme iron was determined as described in method A of Brumby and Massey (133). Acid labile sulfur was determined, by Kelly Dabbs, as described by King and Morris (134).

C. Results.

1) Quaternary Structure of Fumarate Reductase.

One of the first questions of interest was the quaternary structure of the native enzyme. To probe this I used the bifunctional cross-linking reagent dimethyl suberimidate. Following cross-linking a single new band appeared on PAGE-SDS gels corresponding to a molecular weight of 100,000, Figure 15. Since the staining ratio of

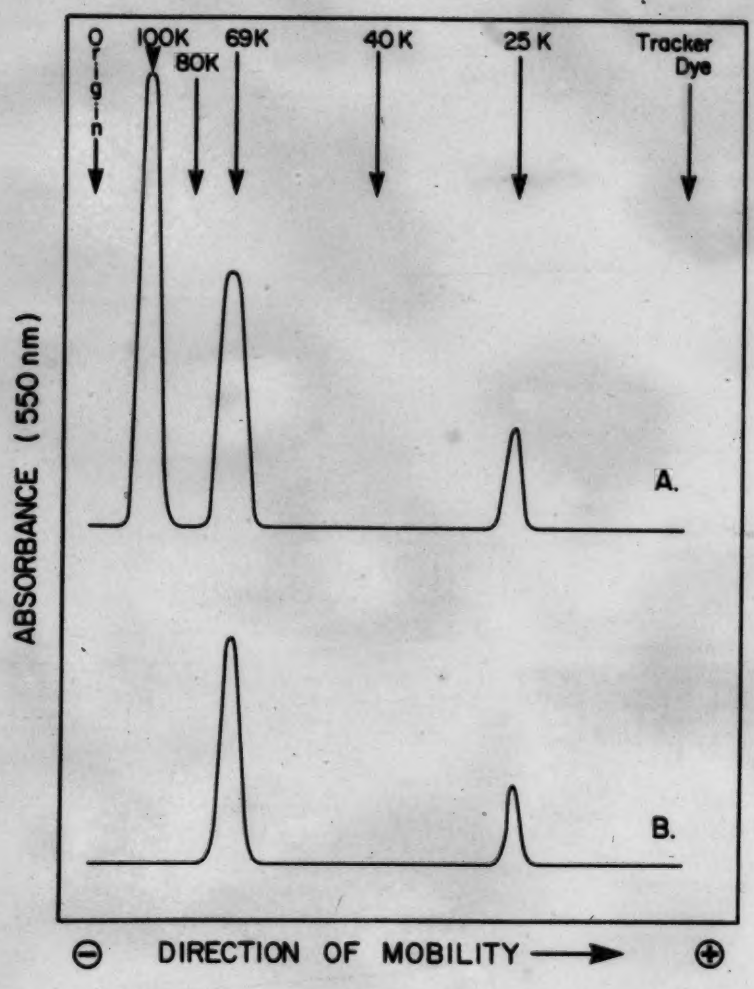

Figure 15. Densitometric scan of the SDS-PAGE electrophoretic pattern of cross-linked (A) and non cross-linked (B) cholate-depleted fumarate reductase. The final concentration of both cross-linker and protein was 5 mg/ml.

the 69,000 and 25,000 dalton bands (approximately 3/1) remained unaltered following cross-linking, the 100,000 dalton species must consist of the 69,000 and 25,000 dalton species in a 1:1 molar ratio. Sedimentation equilibrium studies yielded a molecular weight of 97,700 for the native enzyme while analytical gel filtration experiments, performed by Peter Dickie, indicated a native molecular weight of 100,000 for the cholate form of the enzyme.

2) Amino Acid Composition and N-Termini of the Separated Subunits.

The amino acid compositions of the separated subunits of fumarate reductase along with the amino acid compositions of the corresponding subunits of succinate dehydrogenases from beef heart mitochondria and *Rhodospirillum rubrum* are listed in Table 4. The proportions of hydrophobic amino acids (from Capaldi, 135) are 48.2 and 49.3% for the large and small subunits of fumarate reductase respectively. These proportions are not significantly different from the hydrophobic content of soluble or other membrane proteins which usually contain 45-55% hydrophobic amino acids (135). N-Terminal analysis of the 69,000 and 25,000 dalton subunits was performed by Automated Edman degradation in collaboration with the laboratory of Dr L. Smillie. Figure 16 shows the N-terminal sequence of the small subunit. The unknown amino acid X was shown to be lysine by sequence analysis of the fumarate reductase gene (74). Attempts at sequencing the large subunit were unsuccessful suggesting

TABLE 4

Amino Acid Composition

Amino Acid Composition Was Determined As Described In The Methods Section

	Large Subunits			Small Subunits		
	E. coli FX (residues/ 69,000 grams)	R. rubrum SDH (residues/ 60,000 grams)	Beef Heart SDH (residues/ 70,000 grams)	E. coli FX (residues/ 23,000 grams)	R. rubrum SDH (residues/ 25,000 grams)	Beef Heart (residues/ 27,000 grams)
Aspartate/ Asparagine	62	52	57	23	24	28
Threonine	38	40	38	11	11	14
Serine	23	21	37	12	9	14
Glutamate/ Glutamine	77	53	67	25	21	24
Proline	25	25	30	13	17	14
Glycine	67	53	65	15	16	14
Alanine	67	66	59	23	21	20
Valine	39	38	45	12	14	7
Methionine	20	13	14	6	4	6
Isoleucine	22	25	31	10	12	17
Leucine	53	44	55	20	21	20
Tyrosine	14	16	21	7	5	11
Phenylalanine	20	19	22	7	7	6
Lysine	32	20	26	14	13	20
Histidine	19	18	17	5	3	3
Arginine	39	34	41	7	14	12
Cysteine	9	14	14	11	9	7
Tryptophane	7	6	6	2	6	4

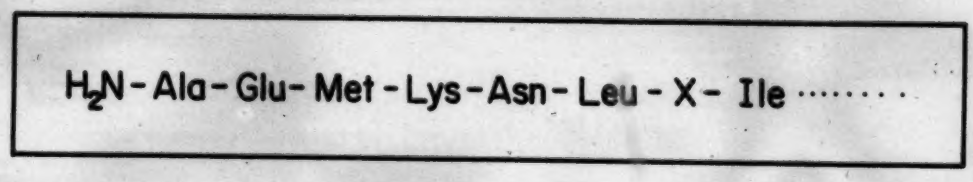

Figure 16. Amino terminal sequence of the 25,000 dalton subunit of fumarate reductase. The sequence was determined by automated Edmân degradation of the purified subunit.

that the N-terminus was blocked. This conclusion was confirmed by gene sequence analysis (73) which indicated that the N-terminal amino acid of the large subunit was methionine followed by glutamine. The methionine was probably cleaved off as a post-translational step leaving glutamine as the N-terminal amino acid in the purified enzyme. Under mildly acid conditions glutamine can cyclize to form a pyrrolidine derivative (136) and a blocked N-terminus.

3) Two Dimensional Electrophoretic Analysis of Fumarate Reductase.

Isoelectric focusing analysis of fumarate reductase in the presence of urea and the nonionic detergent Nonidet P-40 gave 2 major bands of isoelectric points 6.0 and 6.5, Figure 17. The pH gradient was from 7.7 to 5.0. The band of pI 6.0 was yellow in color suggesting that it was the 69,000 dalton subunit. Positive identification was made by electrophoresis of the bands from the first dimension electrofocusing gel into a second dimensional PAGE-SDS gel. The band of pI 6.0 was identified as the 69,000 dalton subunit while the band of pI 6.5 was identified as the 25,000 dalton subunit. The electrofocusing analysis indicated that the native enzyme could be dissociated into its subunits by 8M urea and 2% (v/v) NP-40. On staining a strip of the electrofocusing gel for activity, using the PMS/MTT assay for the succinate dehydrogenase activity of fumarate reductase, no activity could be detected. This result suggested that either the

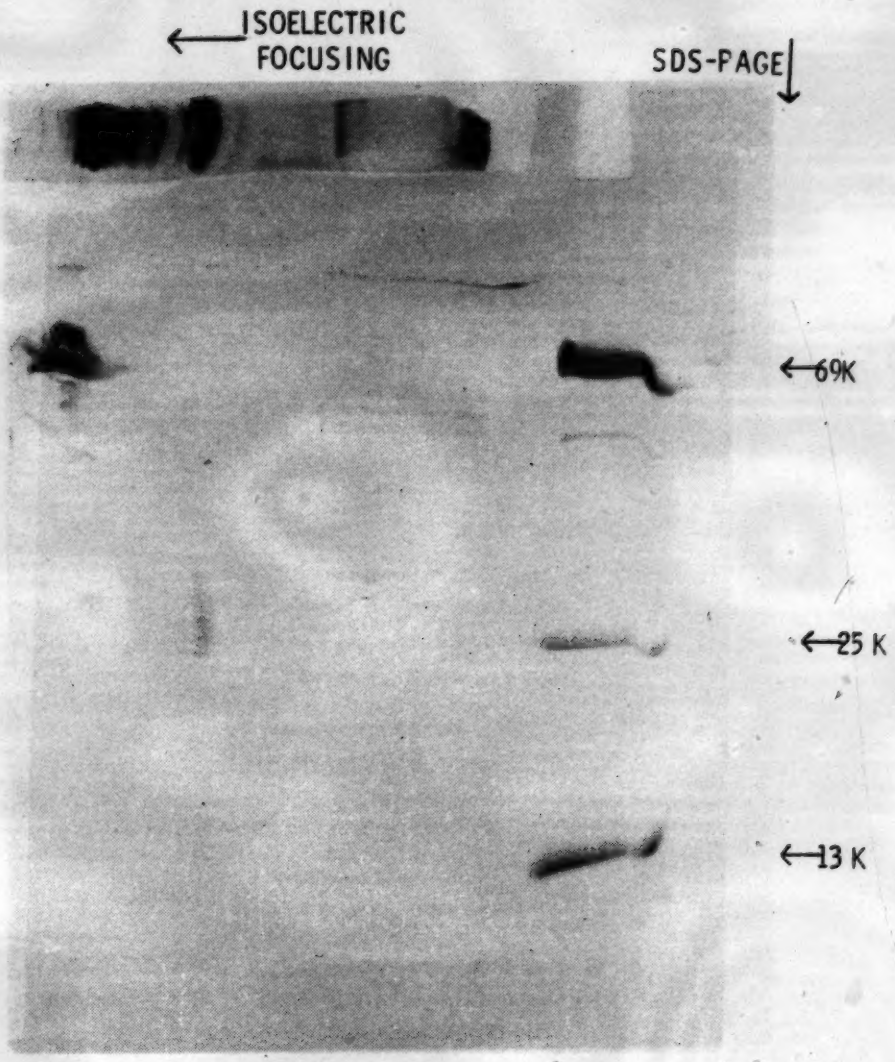

Figure 17. Two dimensional electrophoresis of purified fumarate reductase. The first dimension electrophoresis was performed as described in the methods section. The pH gradient was from 7.7 to 5.0. The second dimension was a 15% (w/v) Laemmli gel (90). The molecular weight standards were the α and β subunits of purified fumarate reductase, 69,000 and 25,000 daltons respectively and RNase at 13,000 daltons.

dissociated subunits were inactive or that the 8 M urea had denatured the separated subunits with resultant loss of catalytic activity.

4) Triton X-100 Binding.

As discussed in Chapter I, the fumarate reductase operon codes for four polypeptides. In addition to the 69,000 and 25,000 dalton catalytic subunits there are 2 hydrophobic polypeptides of molecular weights 15,000 and 13,000 daltons. In this section the results of a study of the binding of Triton X-100 to the 69,000 and 25,000 dalton subunits are presented. The results suggest that the catalytic subunits are largely extrinsic to the hydrophobic bilayer. The approach taken was that of Clarke (130). Enzyme was made 2% (w/v) in Triton X-100 and dialysed against buffer containing 2% (w/v) detergent for 24 hrs at 4°C. The dialysis was to ensure that the interaction between protein and detergent had reached equilibrium. The sample was then applied to a 5-20% (w/v) sucrose gradient which was 0.05% (w/v) in ^{3}H-Triton X-100. Figure 18 shows a typical sedimentation profile. A single major peak of protein was found which was coincident with a peak of radioactivity. Both the 69,000 and 25,000 dalton subunits were present in the major peak. Quantitation from four gradients indicated that 0.15±0.03 mg of detergent was bound per mg of protein. Since the concentration of detergent was above its critical micellar concentration of 0.016% (130) this must represent the maximal level of binding possible.

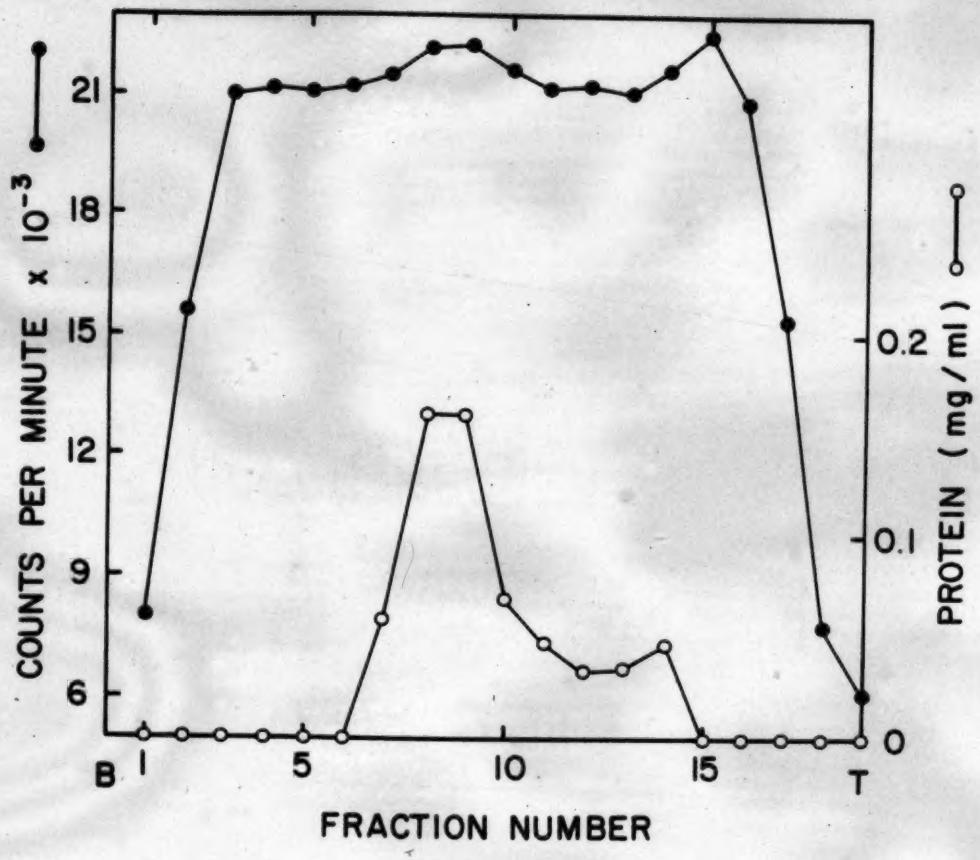

Figure 18. Binding of Triton X-100 to cholate-depleted fumarate reductase after sucrose gradient sedimentation. Triton X-100 binding was determined using 5-20% (w/v) sucrose gradients as described in the methods section.

Clarke (130) has examined Triton X-100 binding to a number of membrane proteins and found a range from 0.2-1.1 mg of detergent/mg of protein. The level of binding found for fumarate reductase is therefore at the lower limit. The possibility that Triton X-100 binding is hindered by cholate which may remain bound even after depletion seems unlikely in view of the large excess of Triton X-100 used. This possibility is further diminished by the finding of Clarke that an excess of Triton X-100 can displace bound SDS from the minor red cell glycoprotein found in band 3. The results of this section are consistent with the postulate that the catalytic subunits are not embedded in the hydrophobic bilayer.

5) Inhibition of Fumarate Reductase by Sulfhydryl Reagents.

The sulfhydryl sensitivity of fumarate reductase was examined using iodoacetamide and 5,5'-dithiobis(-2-nitro benzoic acid) (DTNB). As shown in Figure 19, fumarate reductase activity can be quantitatively inhibited by 10 mM iodoacetamide or 0.02 mM DTNB. In a series of experiments the percent inhibition obtained with 0.02 mM DTNB varied between 85 and 100%. Semi-logarithmic plots of activity versus time were linear indicating first order kinetics, Figure 20. In substrate protection experiments 5 mM fumarate gave only moderate protection against inhibition by 0.02 mM DTNB. The time required for 50% inhibition was increased two-fold by the presence of substrate. This moderate protection may mean that the sensitive sulfhydryl group(s)

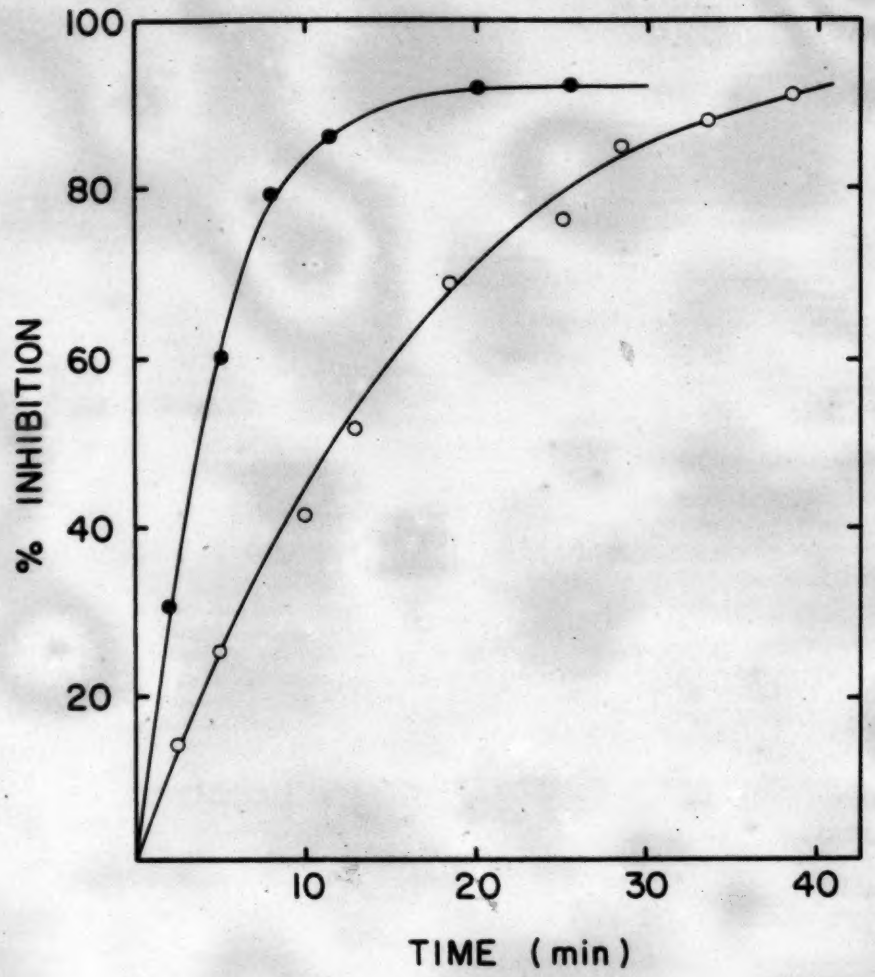

Figure 19. Sulfhydryl sensitivity of fumarate reductase. Cholate-depleted fumarate reductase was incubated with p-CMB or DTNB at 36°C as described in the methods section. The activity of the untreated enzyme was 550 units/mg. ●-●, DTNB treated enzyme; o-o, p-CMB treated enzyme.

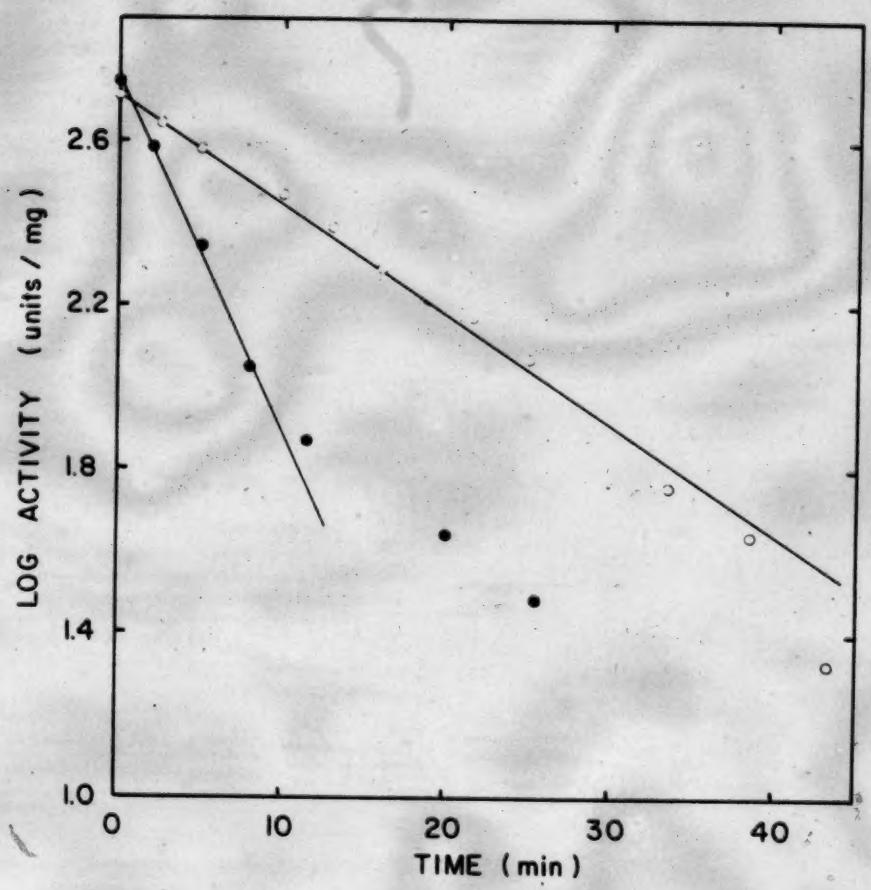

Figure 20. Sulfhydryl sensitivity of fumarate reductase. Cholate-depleted fumarate reductase was treated with p-CMB or DTNB at 36°C as described in the methods section. The activity of the uninhibited enzyme was 550 units/mg. ●-●, DTNB treated enzyme; o-o, p-CMB treated enzyme.

is located at the active site but is not directly involved in the binding of fumarate. The inhibition by DTNB could be reversed by dithiothreitol. When fumarate reductase, which had been inhibited 93% by 0.2 mM DTNB, was incubated with 2 mM dithiothreitol at room temperature for 10 mins, 88% of the original activity returned.

6) Quantitation of Sulfhydryl Groups Essential for Activity.

Since the modification of sulfhydryl groups with DTNB can be quantitated by monitoring the increase in optical density at 412 nm (132) I decided to follow the disappearence of enzymatic activity as a function of sulfhydryl group modification. In identical experiments the titration of fumarate reductase with 0.02 mM DTNB was followed by monitoring either enzyme activity or sulfhydryl group modification, Figure 21. A strong correlation was found between the modification of one sulfhydryl group and loss of 85% of the enzyme activity. When sulfhydryl group modification was measured over a longer period of time it was seen that the essential sulfhydryl group was far more reactive towards DTNB than the other sulfhydryl groups which were apparently not required for activity.

7) Subunit Localization of the Essential Sulfhydryl.

When DTNB-modified proteins are reacted with cyanide, the cyanide anion can displace the DTNB from it's binding site on these proteins (137). I have used this reaction to determine the subunit localization of the single sensitive sulfhydryl group. When fumarate reductase, which had been

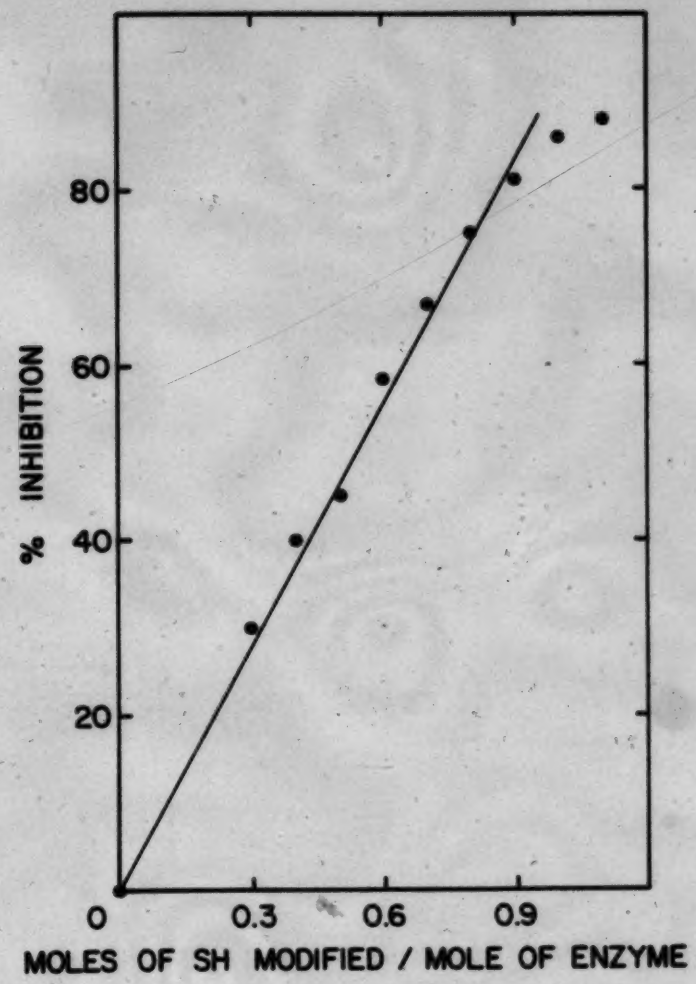

Figure 21. Quantitation of the sensitive sulfhydryl group of cholate-depleted fumarate reductase. Enzyme (0.21 mg) was incubated with an equal volume of 0.4 mM DTNB, at room temperature, as described in the methods section. One hundred percent activity was 540 units/mg.

treated with DTNB under conditions which labelled only the essential sulfhydryl, was reacted with sodium ^{14}C-cyanide and fractionated by polyacrylamide gel electrophoresis in the presence of SDS a peak of radioactivity coincident with the 69,000 dalton subunit was seen, Figure 22. No labelling of the 25,000 dalton subunit occured. However, a second peak of radioactivity was seen which was coincident with a Coomassie Brilliant Blue staining band of approximate molecular weight 38,000. This band was probably a cleavage product of the large subunit since incubation of cyanide modified protein at alkaline pH results in the cleavage of the peptide bond at the amino terminal side of the modified cysteine residue (137). This cleavage product was reproducibly seen when the DTNB-modified protein was treated with either cold or ^{14}C-labelled sodium cyanide. In control experiments in which fumarate reductase, which had not been treated with DTNB, was incubated with either cold or ^{14}C-labelled sodium cyanide no cleavage product was seen on stained gels nor were there any counts above the background level seen in the 69,000 or 25,000 dalton subunits.

8) Visible Absorption Spectrum and Iron-Sulfur Content.

The visible absorption spectrum of native fumarate reductase is shown in Figure 23. The structureless nature of the spectrum between 400 and 470 nm (trace A) suggests the existance of overlapping iron-sulfur and FAD chromatophores (138). In agreement with the spectral data, assays of non-heme iron and acid labile sulfur gave values of 4.5±0.2

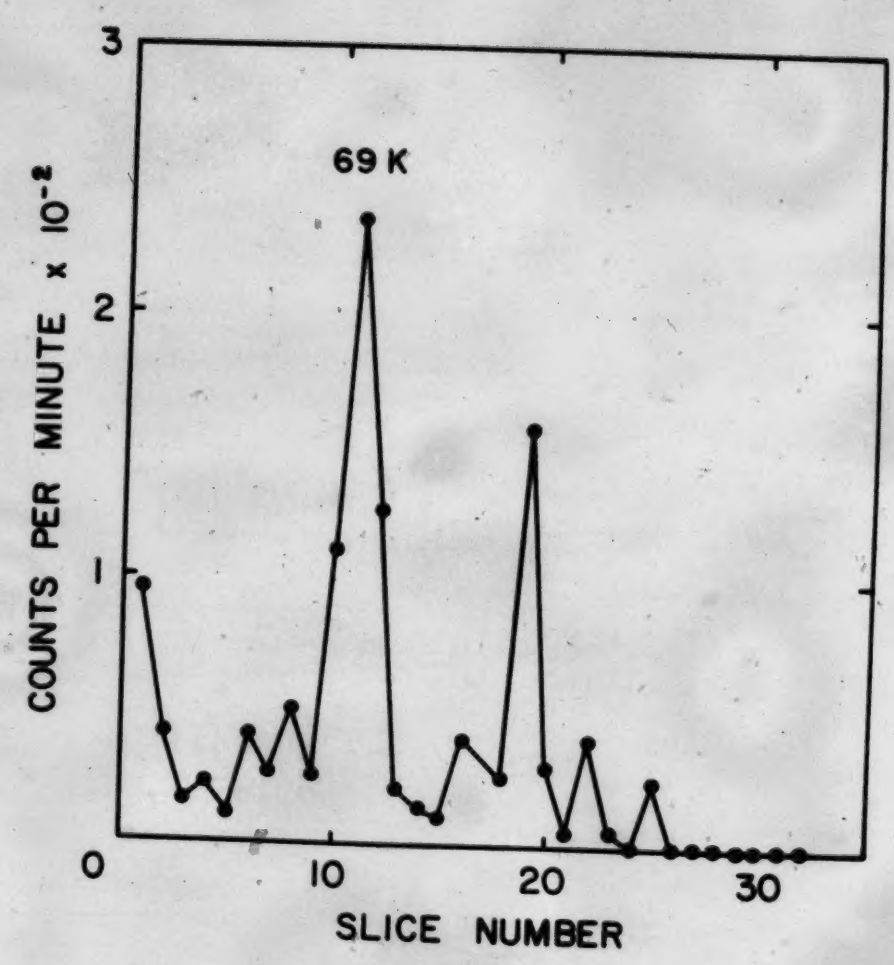

Figure 22. Localization of the sensitive sulfhydryl group of fumarate reductase. Cholate-depleted enzyme was labelled with ^{14}C-cyanide and the radioactive label identified by SDS-PAGE analysis as described in the methods section.

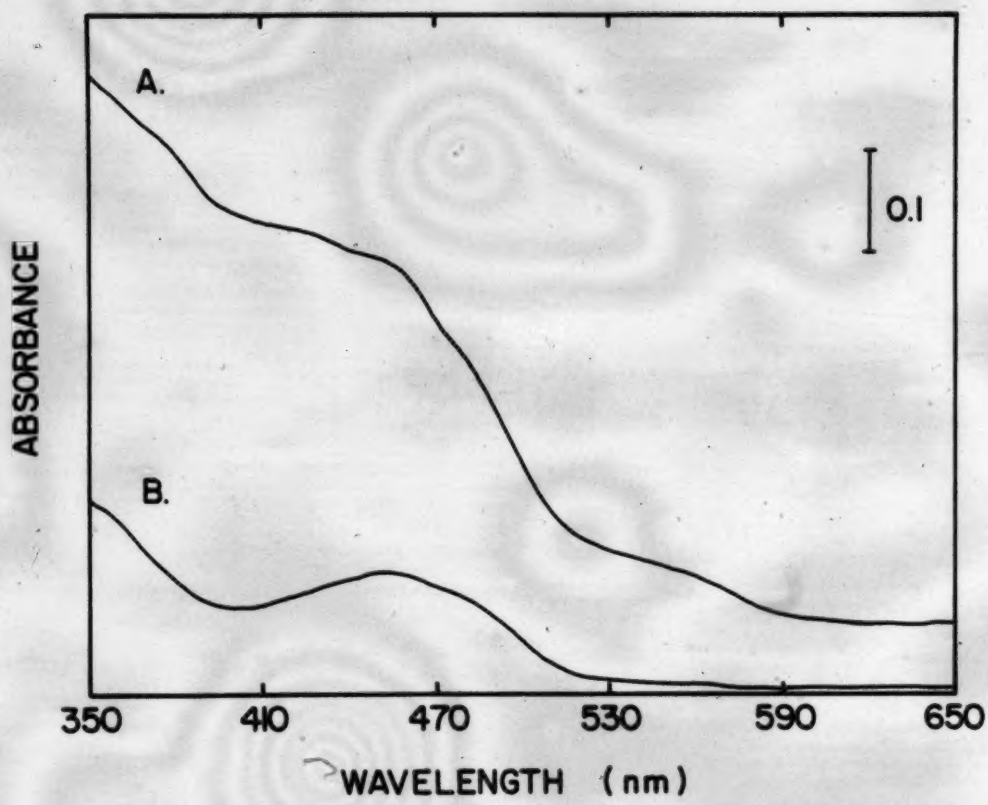

Figure 23. The visible absorption spectrum of cholate-depleted fumarate reductase (A) before and (B) after treatment with 1.5 mM p-chloromercuriphenylsulfonate. Incubation was at room temperature and the reference blank contained 1.5 mM p-chloromercuriphenylsulfonate.

and 4.0±0.1 per mole of enzyme respectively. Further evidence for the existance of an iron-sulfur centre(s) came from a study of the effect of p-chloromercuriphenylsulfonate on the visible absorption spectrum of the enzyme. Upon incubation of fumarate reductase at room temperature for 2 mins with 1.5 mM p-chloromercuriphenylsulfonate the structureless nature of the spectrum disappeared and a peak of flavin absorption appeared, Figure 23 (trace B). Unlike DTNB and iodoacetamide, p-chloromercuriphenylsulphonate destroys iron-sulfur centres in proteins (138) and the appearance of a well resolved absorption peak for the FAD moiety suggests that the iron-sulfur centre(s) had been destroyed. The subunit containing the iron-sulfur centre(s) has not yet been established. However, primary sequence data (73,74) suggests that the centre(s) is located in the 25,000 dalton subunit. While there is a random distribution of cysteine residues in the 69,000 dalton subunit, clustering of cysteine residues, similar to that seen in a ferredoxin from *Peptococcus aerogenes* (139), occurs in the 25,000 dalton subunit, Figure 24. The *P.aerogenes* enzyme contains two centres of the Fe_4S_4 type. One centre is composed of residues 18, 35, 38 and 41 while the second is made up of residues 8, 11, 14 and 45. Although there is considerable conservation of cysteine residues in fumarate reductase and the ferredoxin the replacement of a cysteine residue at position 208 by a valine suggests that fumarate reductase may contain a single centre of the Fe_4S_4 type.

P. aerogenes Ferredoxin

```
      8          11         14              18
-SER-CYS-ILE-ALA-CYS-GLY-ALA-CYS-LYS-PRO-GLU-CYS-PRO-
      35         38         41              45
- SER-CYS-ILE-ASP-CYS-GLY-SER-CYS-ALA-SER-VAL-CYS-PRO-
```

E. coli Fumarate Reductase (25,000 dalton subunit)

```
      149        152        155             159
-GLY-CYS-ILE-ASN-CYS-GLY-LEU-CYS-TYR-ALA-ALA-CYS-PRO-
      205        208        211             215
-SER-CYS-THR-PHE-VAL-GLY-TYR-CYS-SER-GLU-VAL-CYS-PRO-
```

Figure 24. Comparison of the probable iron-sulfur centres of the 25,000 dalton subunit of fumarate reductase with those of a ferredoxin from *Peptococcus aerogenes*. (139). The numbering is from the amino terminal end of each protein and conserved residues are underlined.

D. Discussion.

In this chapter I reported a number of molecular properties of the purified, cholate-depleted fumarate reductase. The native enzyme exists as an $\alpha\beta$ dimer of 69,000 and 25,000 dalton subunits. The enzyme dissociates into its subunits in the presence of 8M urea and 2% (v/v) Nonidet P-40. The isoelectric point of the large subunit is 6.0 while that of the small subunit is 6.5. The enzyme binds only 15% of it's own weight of Triton X-100 suggesting that it is located extrinsic to the hydrophobic bilayer. The active site of the enzyme, which contains a single sensitive cysteine residue, is located in the large subunit while an iron-sulfur centre(s) appears to be located in the small subunit.

During our characterization of the *E.coli* fumarate reductase two reports appeared describing the properties of fumarate reductase from *Vibrio succinogenes* (140,141). The properties reported in these papers show a number of striking similarities to those reported here for the *E.coli* enzyme. The *V.succinogenes* enzyme exists as an $\alpha\beta$ dimer of 79,000 and 31,000 dalton subunits (140). The large subunit contains one mole of covalently-bound FAD (140) as well as a single sensitive sulfhydryl group (141). Although extraction from the membrane requires Triton X-100, the purified enzyme binds only 0.1 mg of detergent/mg of protein and both subunits contain non-heme iron and acid labile sulfur. Also the *V.succinogenes* enzyme catalyses a weak succinate

dehydrogenase activity; the ratio of fumarate reduction to succinate oxidation being 0.01 (140).

In addition to similarities to the *V.succinogenes* enzyme *E.coli* fumarate reductase also has a number of properties which are similar to those of the succinate dehydrogenases from beef heart mitochondria (142,143,144) and *Rhodospirillum rubrum* chromatophores (145). A strong similarity was found between the amino acid and subunit compositions of all three enzymes, Table 4. Also, all three enzymes have an FAD moiety covalently-bound to the large subunit (142,145) and all contain non-heme iron and acid labile sulfur (143,145). Similarly to the mitochondrial succinate dehydrogenase (144) the *E.coli* fumarate reductase is markedly stimulated by anions (see Chapter VI). The similarity in structure and properties of the *E.coli* fumarate reductase to those of fumarate reductase from *V.succinogenes* and the succinate dehydrogenases from beef heart mitochondria and *Rhodospirillum rubrum* chromatophores probably reflects the highly specialized function as well as the similar enzymatic activities of these proteins.

V. The Sidedness of Fumarate Reductase in the Cytoplasmic membrane of *Escherichia coli*.

A. Introduction.

The study of the sidedness or orientation of membrane proteins has, in the past few years, become an area of intense investigation. One reason for the interest in sidedness is the proposal of three distinct mechanisms for the biogenesis of membrane proteins; The Signal Hypothesis of Blobel (146), The Membrane Trigger Hypothesis of Wickner (147), and the Hairpin Loop Hypothesis of Englemann and Steitz (148). Clearly, a critical appraisal of these postulated mechanisms requires a knowledge of the sidedness of a number of membrane proteins. One of the earliest investigations of sidedness was that of glycophorin, the major glycoprotein of the red cell membrane (149). In this study a combination of proteolytic enzymes and labelling reagents was used to demonstrate the transmembranal nature of this protein. In general membrane protein sidedness has been probed using a) lactoperoxidase catalysed ^{125}I-labelling (150), b) by labelling with group specific but membrane impermeable reagents such as diazobenzene sulphonate (151), c) by crossed immunoelectrophoresis (150), d) by analysing the binding of ferritin labelled antibodies to membranes (152) and e) by the use of membrane permeable and impermeable electron donors and acceptors (87). The latter technique has been most useful in the investigation

of the sidedness of electron transport proteins.

A knowledge of protein sidedness has been particularly useful in energy transducing membranes such as the inner mitochondrial and bacterial plasma membranes. The now widely accepted Chemiosmotic Coupling Hypothesis of Mitchell (5) requires that electron transport chains consist of alternating hydrogen and electron carriers arranged across the membrane in a loop. The investigation of the sidedness of mitochondrial electron transport proteins has provided strong support for the chemiosmotic hypothesis (17). *E.coli* electron transport chains have also been studied. The transmembranal localization of both hydrogenase and formate dehydrogenase has been demonstrated (150,153). The α and β subunits of nitrate reductase were shown to have a cytoplasmic localization and the γ subunit was shown to be located on the periplasmic side (154). We are now beginning to develop a picture of the sidedness of some of the *E.coli* electron transport components. The anaerobic glycerol/fumarate electron transport chain shown in Figure 5 is based largely on the chemiosmotic hypothesis which predicts the arrangement of electron transport proteins into loops which span the membrane. In this chapter I describe experiments which were designed to probe the sidedness of fumarate reductase in an *E.coli* plasma membrane with amplified enzyme activity.

B. Methods.

1) Preparation of Broken Cells.

MV12/pLC16-43 was grown anaerobically on glycerol /fumarate medium as described in Chapter II. Cells were harvested, washed twice in 200 mM sodium phosphate, pH 6.8, and resuspended in this buffer to a protein concentration of 51.5 mg/ml. A 1.8 ml aliquot was made 1% (w/v) in Brij 58 and sonicated for 5 mins in 30 sec bursts at maximum power with microprobe of a Bronson sonifer. During sonication the cells were kept on ice.

2) Lactoperoxidase Catalysed Iodination.

Everted membrane vesicles were prepared from CSR603/pLC16-43 as described in the general methods chapter and resuspended in 0.1 M potassium phosphate, pH 7.5, containing 23% (w/v) sucrose, to a protein concentration of 18 mg/ml. Spheroplasts were also prepared from CSR603/pLC16-43 as described in the general methods chapter. Following lysozyme-EDTA digestion the spheroplasts were isolated by centrifugation at 1,000g for 5 mins at room temperature and resuspended by gentle swirling in 0.1 M potassium phosphate, pH 7.5, containing 23% (w/v) sucrose, to a protein concentration of 6.1 mg/ml. The intactness of the spheroplasts was judged by a) the ten-fold decrease in optical density, at 600 nm, when the spheroplasts were transferred from 23% (w/v) sucrose to distilled water and b) the lack of noticeable viscosity when the spheroplasts were gently squirted through a Pasteur pipette.

Sodium ^{125}I-iodide was obtained as a solution containing 3 mCi in 30 ul of 0.1 M sodium hydroxide pH 13. This solution was neutralized by the addition of 15 ul of 1 M potassium phosphate, pH 6.6, followed immediately by 45 ul of 10 uM sodium sulphite. The iodine produced by neutralization was reduced with sodium sulphite to give a neutralized solution of sodium ^{125}I-iodide containing 3 mCi in 90 ul. To 100 ul of everted membrane vesicles (0.9 mg of protein) was added 66.6 uCi of sodium 125-iodide, hydrogen peroxide (prepared by dissolving 3 ul of 35% H_2O_2 in 4.5 ml of 0.1 M potassium phosphate, pH 7.5, containing 24% (w/v) sucrose) to a final concentration of 0.2 mM, and one unit of lactoperoxidase (also prepared in 0.1 M potassium phosphate, pH 7.5, containing 24% (w/v) sucrose). The reaction was allowed to go for 60 mins at room temperature and was stopped by the addition of 900 ul of 0.4% (v/v) acetic acid. Spheroplasts were labelled exactly as described for everted membrane vesicles except that 0.6 mg of protein and two units of lactoperoxidase were used. Also, the reaction was allowed to go for 30 rather than 60 mins. The shortened incubation was found necessary because of the tendency of the spheroplasts to lyse after 30 mins incubation. After the reaction was quenched by the addition of acetic acid each sample was dialysed against three litres of 0.05 M sodium acetate, 0.5 M NaCl, 1 mg/ml bovine serum albumin and 0.2 mg/ml sodium azide for two days to remove the unreacted iodide. Following dialysis, each sample was solubilized and

analysed in a 10% (w/v) acrylamide-0.28% (w/v) bisacrylamide tube gel using the fast running system of Jovin *et al* (91) as described in the general methods chapter, stained, destained, sliced and counted in an LKB 1270 RACKGAMMA II.

3) Preparation and Purification of Anti-Fumarate Reductase Gamma Globulin.

Gamma globulin was prepared and purified by Mark Ehrman as described in (155).

4) Titration of Fumarate Reductase with Anti-Fumarate Reductase Gamma Globulin.

To 2.5 ml of 0.2 M sodium phosphate, pH 6.8, were added either 2 *u*g of pure fumarate reductase, 1 *u*g of fumarate reductase in broken cells, 1.3 *u*g of fumarate reductase in Kaback vesicles, 2 *u*g of fumarate reductase in everted membrane vesicles or 2.3 *u*g of fumarate reductase in whole cells followed by varying amounts of anti-fumarate reductase gamma globulin or anti-ATP citrate lyase gamma globulin. For calculation of the amount of membrane-bound fumarate reductase a specific activity of 550 units/mg was used. The stock anti-fumarate reductase gamma globulin was 28.7 mg/ml in protein while the stock anti-ATP citrate lyase gamma globulin was 30.8 mg/ml in protein. After incubation at room temperature for 5 mins, benzyl viologen, sodium dithionite and fumarate were added and the change in optical density at 570 nm was measured using a chart recorder. Incubation of enzyme in the absence of antibody did not result in any loss of activity.

C. Results.

1) Sidedness of the Active Site of Fumarate Reductase.

A common approach to the study of the sidedness of the active site of membrane-bound enzymes involves the use of membrane impermeable substrates (87). Fumarate reductase activity can be measured using the largely impermeable electron donor reduced methyl viologen (87). When the fumarate reductase activity of whole and broken cells was measured using this electron donor, the specific activity increased from 0.17 to 1.3 units/mg upon breakage of the cells. Since the molecular weight of methyl viologen is 257, it can pass freely through the outer cell wall and the increase in specific activity upon breakage is due to removal of the barrier imposed by the intact inner membrane. Hence, the 7.6 fold increase in specific activity suggests that the active site of fumarate reductase is located on the cytoplasmic side of the inner membrane.

As a control the membrane impermeable electron acceptor ferricyanide was used to assay for glycerol-3-phosphate dehydrogenase activity in both whole and broken cells. Both the aerobic and anaerobic enzymes are present in anaerobically grown cells and both enzymes are located on the cytoplasmic side of the membrane (42,48). The specific activity increased from 0.11 to 0.89 units/mg upon breakage of the cells.

2) ^{125}I-Iodide Labelling of Everted Membrane Vesicles and Spheroplasts.

One of the classic approaches to the study of membrane protein sidedness involves the use of membrane impermeable labelling reagents. We have taken advantage of the increased levels of membrane-bound fumarate reductase in *E.coli* strain CSR603/pLC16-43 and used lactoperoxidase catalysed iodination as a probe of the sidedness of fumarate reductase. Since lactoperoxidase is membrane impermeable, only tyrosine residues exposed on the membrane surface accessible to the enzyme will be labelled. At the level of sodium iodide used in this study no significant chemical labelling should occur(156). Figure 25 shows the ^{125}I-iodide labelling pattern of everted membrane vesicles and spheroplasts. Because of the elevated levels of fumarate reductase whole membranes could be fractionated by polyacrylamide gel electrophoresis, in the presence of sodium dodecyl sulphate, and counted for radioactivity. When spheroplasts were used, no significant amounts of label were found in either the 69,000 or 25,000 dalton subunits. On the other hand, both subunits were labelled when everted membrane vesicles were used. Interestingly, no significant labelling of the OmpC and F gene products (porins) occured. This is consistent with the findings of Birdsell and Cota-Robles (157). These workers found that during the preparation of spheroplasts by lysozyme-EDTA digestion the outer cell wall rolls up into a ball which is largely

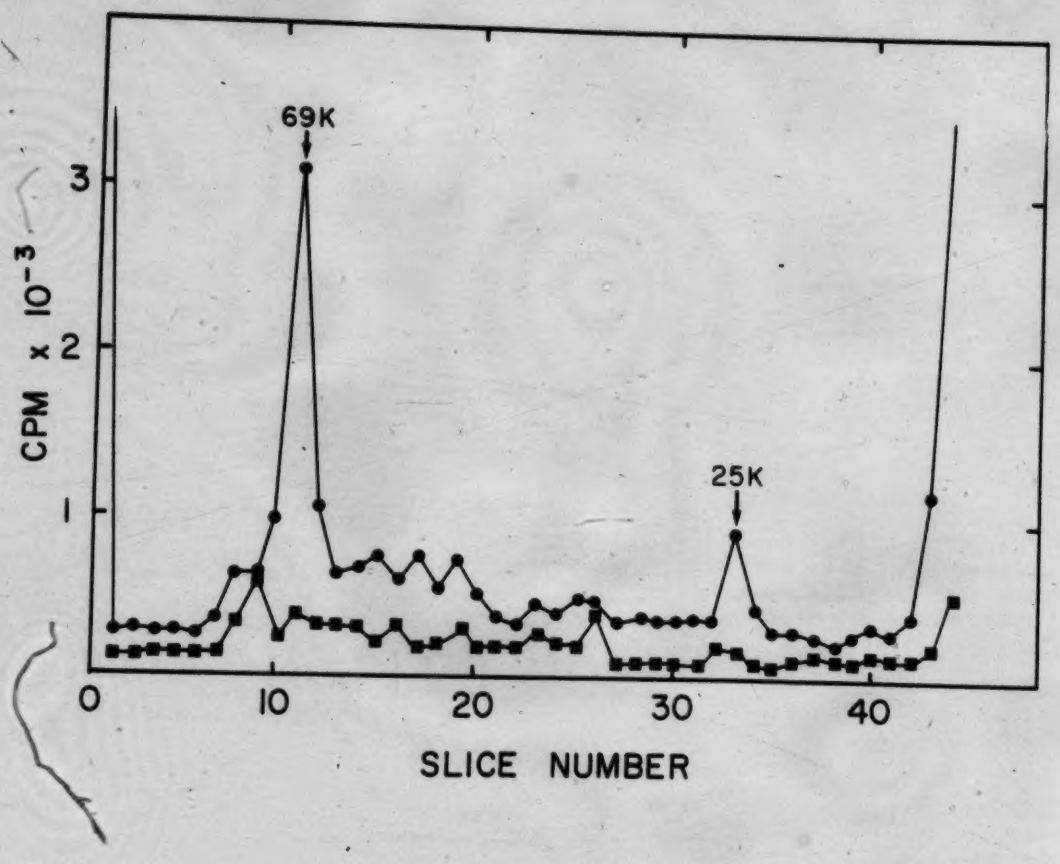

Figure 25. Lactoperoxidase catalysed ^{125}I-iodination of spheroplasts and everted membrane vesicles. Iodination was performed as described in the methods section. ■-■, labelling profile for spheroplasts; ●-●, labelling profile for everted membrane vesicles.

inaccessible to membrane impermeable reagents. A similar mechanism probably accounts for the low levels of label found in the everted membrane vesicles in the 35,000 dalton region.

These results suggest that both subunits are exposed on the cytoplasmic surface and do not span the membrane. This result is supported by the Triton X-100 binding study reported in Chapter IV. Fumarate reductase bound only 0.15±0.03 mg of detergent/mg of protein. A transmembranal protein would be expected to bind considerably more than 15% of its own weight of detergent(130). The lactoperoxidase catalysed iodination approach is subject to the criticism that in order to label a transmembranal protein tyrosine redidues must be exposed on both sides of the membrane. However, since fumarate reductase contains 21 moles of tyrosine per mole of enzyme it seems unlikely that a transmembranal arrangement would not be detected by the iodination approach.

3) Inhibition of Fumarate Reductase Activity by Antibody.

A third approach which has been used to probe the sidedness of fumarate reductase involved the study of the effect of anti-fumarate reductase gamma globulin on membrane-bound enzymatic activity. Figure 26 shows the inhibition profile for fumarate reductase activity in Kaback vesicles, everted membrane vesicles, whole cells, broken cells and pure enzyme. As a control for non-specific inhibition, all preparations were titrated with antibody

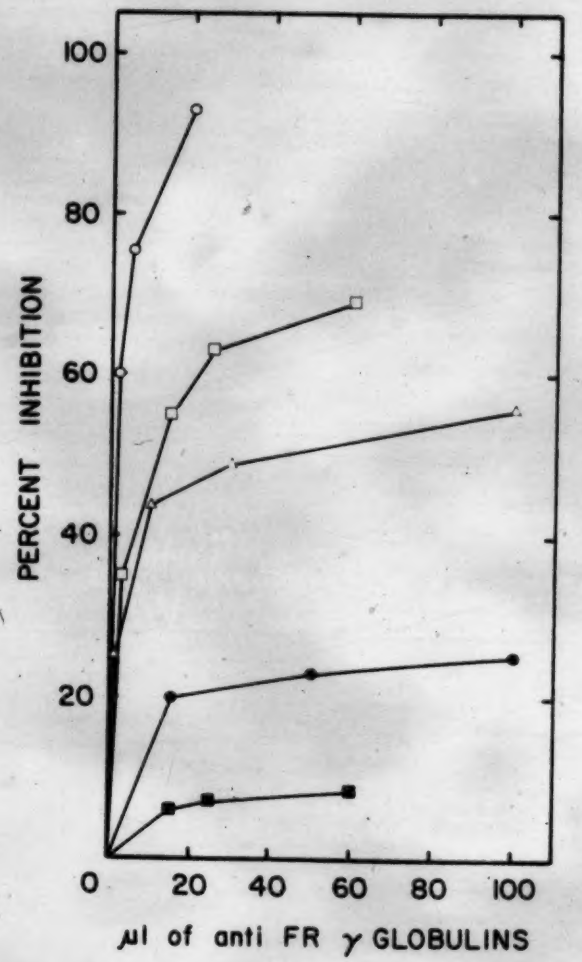

Figure 26. Inhibition of fumarate reductase activity with anti-fumarate reductase antibody. o-o, purified, cholate-depleted enzyme; □-□, broken cells; Δ-Δ, everted membrane vesicles; ●-●, Kaback vesicles; ■-■, whole cells.

against rat liver ATP citrate lyase and any inhibition obtained was subtracted from the inhibition found with anti-fumarate reductase antibody. No greater than 5% inhibition was found with the control antibody. All membrane fractions tested contained approximately the same amount of fumarate reductase. Close to complete inhibition was found with pure enzyme. Broken cells, prepared by sonication of whole cells in the presence of 1% (w/v) Brij 58, were inhibited by 70%. The inability to completely inhibit the activity in broken cells may have been due to protection afforded by the detergent, Brij 58. Everted membrane vesicles were inhibited by only 55%. The less than complete inhibition may have resulted from stabilization of the enzyme by the membrane or alternatively some antigenic sites may not have been accessible to the antibody. Twenty five percent inhibition was found with Kaback vesicles. Kaback vesicles are supposed to have the same orientation as the plasma membrane in the intact cell. However, most workers believe that some "flip-flop" of protein occurs during the preparation of these vesicles(31,48). When the fumarate reductase activity of the Kaback vesicles was measured using the impermeable electron donor methyl viologen, 56% of the activity present in the intact vesicles could be detected. This indicated that considerable "flip-flop" had occured and probably accounts for the 25% inhibition of activity. Approximately 8% inhibition was found with whole cells and this probably resulted from cell lysis. Although the

interpretation of the antibody titration data is the subject of some speculation, in view of the less than complete inhibition of membrane-bound and detergent solubilized activity, it generally supports the conclusions of the two previous sections and suggests that fumarate reductase is located on the cytoplasmic surface of the *E.coli* plasma membrane.

D. Discussion.

Our investigation of the sidedness of fumarate reductase was part of a larger study aimed at understanding the properties of the membrane-bound and soluble forms of this enzyme. In particular our Triton X-100 binding data (Chapter IV) did not support the contentation that fumarate reductase was an integral membrane protein. Also, work by Wikstrom (20) indicated that mitochondrial cytochrome oxidase is a proton pump; a similar function for fumarate reductase would require that it span the membrane. In addition, the chemiosmotic coupling hypothesis requires an asymmetric distribution of alternating hydrogen and electron carriers arranged across the membrane in a loop (5). A proton gradient could never be generated by the anaerobic glycerol/fumarate electron transport chain if the terminal electron acceptor, fumarate reductase, was located on the periplasmic surface of the plasma membrane (see Figure 5). Our results are consistent with the chemiosmotic coupling hypothesis and suggest that fumarate reductase is located on

the cytoplasmic surface of the *E.coli* plasma membrane. During the course of the work described in this chapter, the laboratory of Dr W. Konings independently deduced the sidedness of fumarate reductase (158). Their results are in agreement with those described here.

VI. Effects of Anions on Fumarate Reductase.

A. Introduction.

It is now becoming increasingly clear that a large number of intrinsic membrane proteins require phospholipids or nonionic detergents for activity. This phenomenon was discussed in Chapter III in relation to the aerobic glycerol-3-phosphate dehydrogenase from *E.coli*. During Peter Dickie's initial characterization of purified fumarate reductase, a protein which requires nonionic detergent for extraction from the membrane and is therefore classified as an intrinsic membrane protein, he noticed that amphipaths did not affect the turnover rate of the enzyme. However, a marked increase in activity was observed when enzyme activity was measured in the presence of phosphate. Interestingly, membrane-bound (everted membrane vesicles) fumarate reductase was not stimulated by phosphate. Indeed, based on the quantitation of fumarate reductase activity in the presence of phosphate before and after membrane solubilization, no dramatic increase in activity was seen (see appendix I). This suggests that the membrane-bound enzyme is already in the activated state. We hypothesised that phosphate may be mimicking some membrane component and decided to study the effects of phosphate on a number of properties of cholate-depleted purified fumarate reductase.

B. Methods.

1) Titration of Fumarate Reductase with Anions.

Assays of fumarate reductase were performed as described in Chapter II except that 25 mM Hepes, pH 6.8 , was used instead of 200 mM sodium phosphate, pH 6.8, as the assay buffer. One molar stocks of salts, titrated to pH 6.8, were added to the assay mixture to give the final concentrations indicated. The order of addition was always assay buffer, anion, enzyme, benzyl viologen, dithionite and fumarate. Purified enzyme, which had been cholate depleted and taken up in 25 mM Hepes, pH 6.8, was used. Succinate dehydrogenase activity was measured as described in the general methods chapter except that sodium phosphate, pH 6.8, was used at various concentrations as the assay buffer.

2) Thermostability of Fumarate Reductase.

Cholate-depleted fumarate reductase (2.1 mg/ml) in either 200 mM sodium phosphate, pH 6.8, or 25 mM Hepes, pH 6.8, was incubated at 40, 45 or 50°C. Aliquots were withdrawn at the specified times and assayed for fumarate reductase activity in 200 mM sodium phosphate, pH 6.8.

3) Stability of Fumarate Reductase at Alkaline pH.

Fifty ul of cholate-depleted fumarate reductase (1 mg/ml) in 0.4 M sodium phosphate, pH 6.8, was applied to a 2 ml Pasteur pipette column of Sephadex G-25 equilibrated with 20 mM Tris-HCl at a pH of 7.9, 8.2, 8.6 or 9.0. The column was eluted with the equilibration buffer and fractions containing fumarate reductase combined. These operations

usually took 8-9 mins. At 10 mins an aliquot was assayed for fumarate reductase activity and this value was taken as 100% activity. Aliquots were taken at the specified times and assayed. The percent inhibition was calculated relative to the activity at 10 mins. First order rate constants for inactivation were calculated from the slopes of semi-logarithm plots of activity versus time (see appendix III).

4) Effect of Alkaline pH on the Visible Absorption Spectrum of Fumarate Reductase.

Cholate-depleted fumarate reductase (0.12 mg/ml) in 20 mM Tris-HCl, pH 8.2, was incubated at room temperature and its absorption spectrum between 350 and 600 nm measured after 8, 13, 22, 30, 40, 55, 80, 108 mins incubation. The spectra were measured in a Varian Cary spectrophotometer using 20 mM Tris-HCl, pH 8.2, as a blank.

5) Circular Dichroic Spectra of Fumarate Reductase.

The far ultraviolet spectra of fumarate reductase in 25 mM Hepes, pH 6.8, or 0.4 M sodium phosphate, pH 6.8, were measured at 27°C in a Cary 60 spectrophotometer equipped with a 6001 CD attachment. The appropriate buffer blanks were used to establish the baselines for the spectra. Molar ellipticities were measured as described by Oikawa *et al* (97) and and the α-helical, β-sheet and random coil components determined as described by Chen *et al* (98), (see appendix II).

6) Titration of Fumarate Reductase with DTNB.

Cholate-depleted fumarate reductase (300 ug in 0.15 ml of 25 mM Hepes, pH 6.8, or 270 ug in 0.15 ml of 0.4 M sodium phosphate, pH 6.8) was added to an equal volume of 40 uM DTNB in 25 mM Hepes, pH 6.8, and incubated at room temperature. Aliquots were withdrawn at the specified times and assayed for fumarate reductase activity. Rate constants for the modification of fumarate reductase by DTNB were calculated from the slopes of semi-logarithm plots of activity versus time (see appendix III).

7) Measurement of the Michaelis-Menten Constants and Maximal Velocities.

Apparent Km and Vmax values were determined from the Wilkinson (99) statistical fit of initial rate measurements of fumarate reductase or succinate dehydrogenase activity in sodium phosphate, pH 6.8, buffer of varying concentrations. At least 10 different concentrations of substrate were used for each determination.

C. Results.

1) Stimulation of Fumarate Reductase Activity by Anions. .

The original study carried out by Peter Dickie showed that phosphate stimulated fumarate reductase activity. I first wanted to see if other anions could replace phosphate. Table 5 lists the stimulatory effects of a broad range of mono- and divalent anions at concentrations of 50 and 200 mM and in the presence of the reducing agent dithiothreitol.

Table 5

Activation of Fumarate Reductase by Anions.

Activator	Fold Stimulation 50 mM	200 mM
Sodium Phosphate	5.20	5.86
Sodium Azide	5.20	5.80
Sodium Citrate	4.20	5.80
Sodium Acetate	3.44	5.23
Sodium Sulfate	4.16	4.73
Sodium Chloride	2.25	3.74
Potassium Nitrate	ND	3.52
Sodium Formate	2.58	3.50
Sodium Nitrite	2.90	2.40
Sodium Sulfite	1.00	1.32
Sodium Borate	1.00	1.00

ND = not determined.

2 ug of enzyme, which had been taken up in 25 mM Hepes, pH 6.8, following cholate depletion, was used per assay. Stock salt solutions, titrated to pH 6.8, were added directly to the assay buffer before the enzyme to the indicated final concentration. The assay buffer was 25 mM Hepes, pH 6.8 which contained 0.5 mM DTT.

Although most anions tested could activate fumarate reductase, the chaotropic anion perchlorate gave 68% inhibition at a concentration of 500 mM, while potassium cyanide gave 54% inhibition at a concentration of 4 mM. The data in Table 5 indicated that activation was not a simple ionic strength effect (cf phosphate and sulfate). Since phosphate was found to be one of the best activators it was chosen for further detailed study. Figure 27 presents the stimulation of fumarate reductase as a function of phosphate concentration in the presence and absence of 0.5 mM dithiothreitol. In the absence of reducing agent 300 mM phosphate was required for maximal stimulation. However, when dithiothreitol was present, maximal activation was achieved by 50-100 mM phosphate. Interestingly, dithiothreitol alone did not activate the enzyme indicating that it acts to potentiate the anion effect. In independent experiments Peter Dickie showed that other reducing agents, glutathione and β-mercaptoethanol at 0.05 and 10 mM respectively, could also potentiate the stimulatory effects of anions. It can also be seen in Figure 27 that phosphate had no significant stimulatory effect on membrane-bound fumarate reductase in the presence or absence of 0.5 mM dithiothreitol.

Stimulation by anions was virtually instantaneous (within 20 sec) and was not affected by the presence of 0.1% (v/v) Triton X-100 in the assay mixture. Also activation was reversible; enzyme in 0.4 M sodium phosphate, pH 6.8,

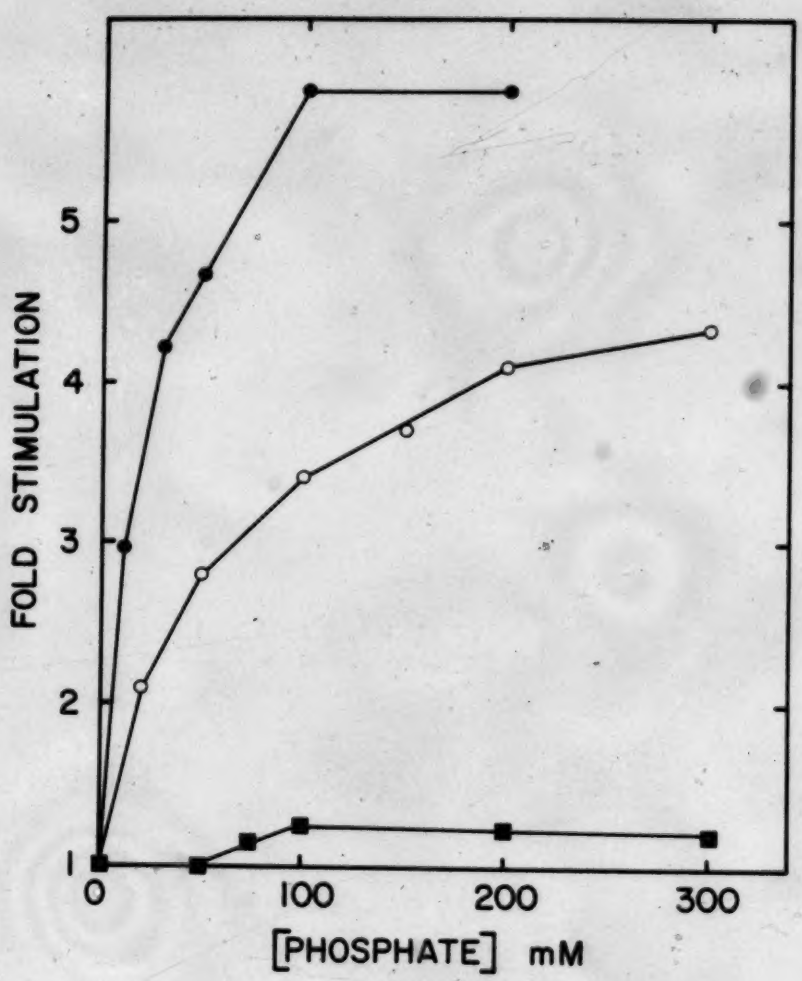

Figure 27. Stimulation of fumarate reductase activity by phosphate and dithiothreitol. The assay buffer was 25 mM Hepes, pH 6.8. One molar potassium phosphate, pH 6.8, was added to the assay mixture to the indicated final concentrations. ■-■, activity in everted membrane vesicles, prepared from MV12/pLC16-43, in the presence and absence of 0.5 mM dithiothreitol. *O-O*, activity of cholate-depleted, purified enzyme in the absence of 0.5 mM dithiothreitol. ●-●, activity of cholate-depleted, purified enzyme in the presence of 0.5 mM dithiothreitol. Activity is expressed as the fold stimulation above a basal value of 40 and 100 units/mg for the membrane-bound and purified enzymes respectively.

diluted into Hepes buffer gave a level of activity characteristic of the anion deficient enzyme. The inability of Hepes to activate is probably related to the pH at which assays were performed; at a pH of 6.8 Hepes (pKa= 7.55) would be largely in the protonated form. The order of addition of components to the assay mixture was important; the following order was found to give maximum activation and was used throughout this study, buffer, anion, enzyme, benzyl viologen, dithionite and fumarate, Table 6. Although the extent of activation depended on the order of addition, phosphate gave significant activation even when added last to the assay mixture. Fumarate, on the other hand, showed a more rigid dependence upon the order of addition; when fumarate was added last only a 1.8 fold activation occurred at a concentration of 200 mM. However, when added before the enzyme, fumarate was a good activator giving 4.4 and 5.7 fold activation at 50 and 200 mM respectively.

I next investigated the ability of a series of phosphate esters to activate. The best activator found was pyrophosphate, Figure 28. A 6.5 fold stimulation occured at 7 mM. The adenine nucleotides AMP, ADP and ATP were also found to be effective activators. The order of potency as activators was ATP>ADP>AMP. Interestingly, o-phosphorylethanolamine, the anionic head group of the major phospholipid class in *E.coli*, gave 5.2 fold stimulation at a concentration of 19 mM. The results in Figure 28 suggest that activation depends upon the charge

Table 6

The Dependence of Activation on the Order of Addition to the Assay Mixture.

Order of Addition	Fold Stimulation
Hepes,P(200mM),FR,BV,Dith,Fum.	5.5
Hepes,FR,P(200mM),BV,Dith,Fum.	4.9
Hepes,FR,BV,Dith,P(200mM),Fum.	4.4
Hepes,FR,BV,Dith,Fum,P(200mM).	3.2
Hepes,Fum(200mM),FR,BV,Dith.	5.7
Hepes,FR,BV,Dith,Fum(200mM).	1.8
Hepes,FR,Fum(30mM),BV,Dith.	3.4
Hepes,FR,BV,Dith,Fum.	1.0

Hepes = 25 mM Hepes, pH 6.8.

P = Sodium Phosphate, pH 6.8.

FR = Fumarate Reductase.

BV = Benzyl Viologen.

Dith = Sodium Dithionite.

Fum = Sodium Fumarate, pH 6.8.

The concentrations of dithionite, benzyl viologen and fumarate were as described in Chapter II unless specified otherwise. Two ug of enzyme was used per assay.

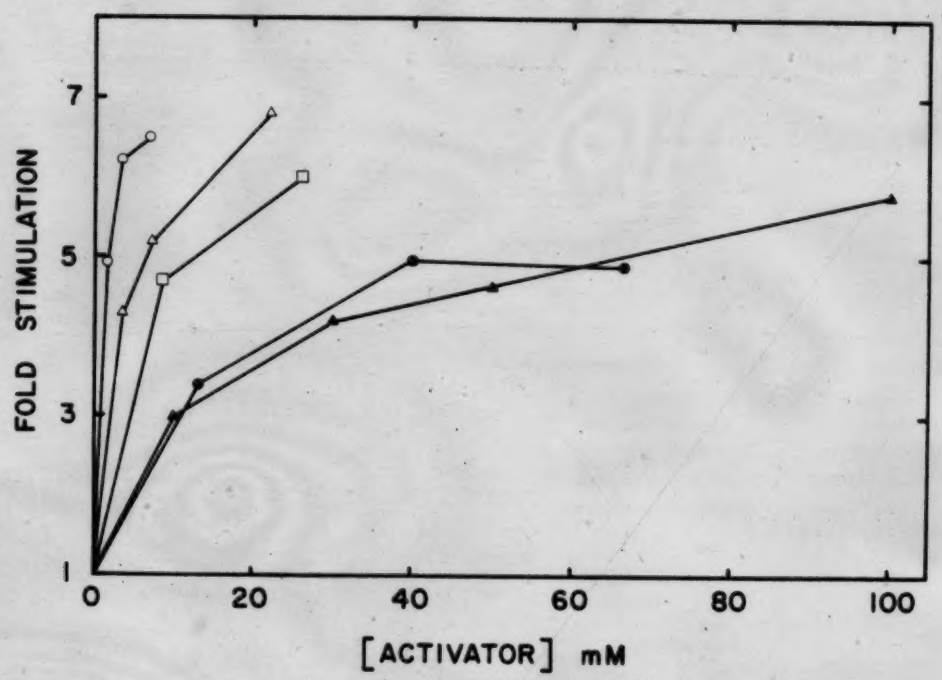

Figure 28. Stimulation of cholate-depleted fumarate reductase by phosphate esters. The assay buffer was 25 mM Hepes, pH 6.8, which contained 0.5 mM dithiothreitol. Phosphate esters, titrated to a pH of 6.8, were added directly to the assay mixtures to the indicated final concentrations. Activity was measured during titration with; o-o, sodium pyrophosphate; Δ-Δ, ATP; □-□, ADP; ●-●, AMP; and ▲-▲, potassium phosphate. Activity is expressed as the fold stimulation above a basal level of 100 units/mg.

density of the activator. The polyanion dextran sulfate was unable to stimulate reductase activity at concentrations of bound sulfate equivalent to concentrations of sodium sulfate which gave activation. Anion stimulation therefore seems to be a function of the size of the non-anionic portion of the molecule relative to that of the anionic portion as well as the total number of negative charges on the activator.

Although anions clearly enhance fumarate reductase activity, the use of an artificial electron donor such as reduced benzyl viologen may be causing artifacts in the assay. To address this possibility fumarate reductase from the pig intestinal parasite *Ascaris lumbricoides*, which had been partially purified by Bernie Lemire, was assayed using another artificial electron donor, reduced methyl viologen. No more than a 20% stimulation of activity was found in the presence of 200 mM concentrations of various anions. However, with the *E.coli* enzyme activation by anions occurred whether methyl- or benzyl viologen was used. Also, the finding that membrane-bound fumarate reductase was not activated by anions strongly suggests that anion activation of the *E.coli* enzyme is not an artifact of the use of benzyl viologen. I have also found that the cholate form of the enzyme shows the same dependence of activity upon anions as does the cholate-depleted form. Although cholate is anionic at pH 6.8 its bulky cyclohexane rings probably preclude it from acting as an activator.

2) Effect of Anions on Thermostability.

In order to see if anion activation resulted in a modulation of the physical properties of fumarate reductase, I examined a number of physical properties in the presence and absence of anions. One of the first properties I examined was the ability to resist thermal denaturation. A striking difference was seen when the thermostabilities of purified fumarate reductase in 200 mM potassium phosphate, pH 6.8, and 25 mM Hepes, pH 6.8, were compared, Figure 29. Fifty percent inhibition occured after 2.5, 23 and 65 mins at 50, 45 and 40°C respectively in Hepes. In 200 mM potassium phosphate, pH 6.8, conditions under which activation is approximately 70%, no significant loss of activity occured upon incubation for at least 60 mins at temperatures of up to 46°C. It therefore seems that activation by anions is accompanied by a dramatic increase in thermal stability.

3) Effect of Anions on the Stability of Fumarate Reductase at Alkaline pH.

During the cyanide labelling experiments described in Chapter IV, I noticed that enzyme activity was lost very rapidly upon incubation at room temperature in 20 mM Tris-HCl, pH 9.0. I therefore decided to examine the effect of phosphate on the rate of loss of activity at alkaline pH. The stability of fumarate reductase activity in the pH range 7.9 to 8.6 was examined in the presence and absence of 200 mM sodium phosphate. Figure 30 compares the rates of loss of

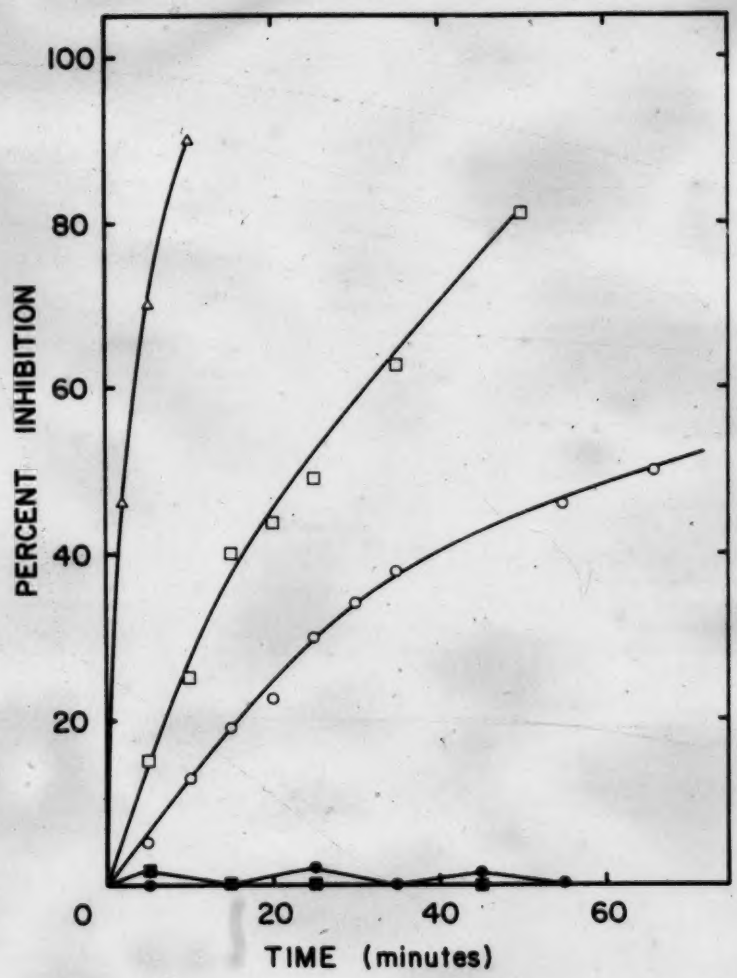

Figure 29. Thermostability of fumarate reductase. Cholate-depleted fumarate reductase was incubated in either 25 mM Hepes, pH 6.8, at 40(o), 45(□) or 50°C(Δ) or in 200 mM sodium phosphate, pH 6.8, at 40(●) or 45°C(■).

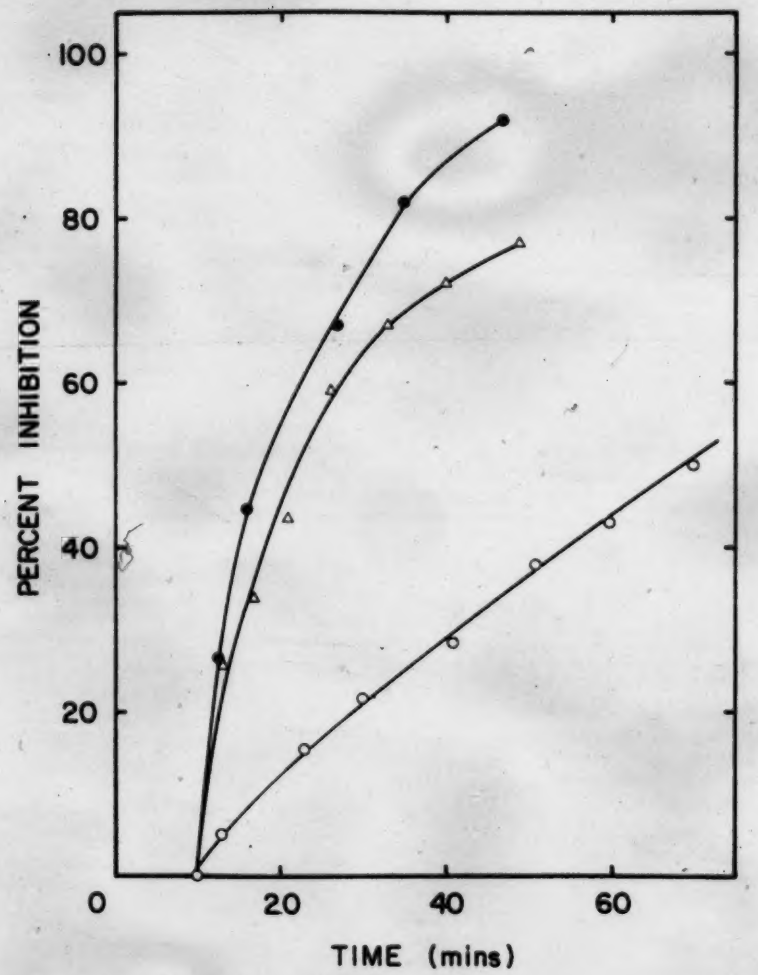

Figure 30. Stability of fumarate reductase at alkaline pH. Cholate-depleted fumarate reductase was incubated at room temperature in 20 mM Tris-HCl, at pH 7.9(o), 8.2(Δ) or 8.6(●). Assays were performed as described in Chapter II.

reductase activity in 20 mM Tris-HCl at pH values of 7.9, 8.2 and 8.6 (when activity was assayed in 20 mM Tris-HCl, pH 7.0, a level of activity characteristic of the deactivated enzyme was found). Since it took 8-9 mins to get the enzyme into the appropriate buffer, the data in Figure 30 are based on an activity of 100% at 10 mins. By extrapolation of semi-logarithm plots of activity versus time it was estimated that the following losses of activity had occured by 10 mins: 9.8, 30.6 and 48.3% at pH values of 7.9, 8.2 and 8.6 respectively. From the data in Figure 30 it can be seen that the rate of loss of activity increased markedly when the pH was increased from 7.9 to 8.2 while the increase was less dramatic in the pH range from 8.2 to 8.6. Rate constants for inhibition were extracted from semi-logarithm plots of activity versus time (see appendix III) and these are presented in Table 7 along with the half-times of inhibition. When 200 mM sodium phosphate was present in the Tris buffer no loss of activity occured upon incubation at room temperature for up to 60 mins at pH values as high as 9.0.

In order to further examine the stabilizing effects of anions experiments were performed to examine the following possible mechanisms of inactivation:

a) At alkaline pH essential sulfhydryl groups may be oxidized. The oxidized sulfhydryls may then chelate heavy metal cations which would be inhibitory to enzyme activity. In order to test this hypothesis enzyme was incubated at a

Table 7

Stability of Fumarate Reductase at Alkaline pH in the Absence of Anions.

pH	Half-Life(mins)	k(sec^{-1})
7.9	64	1.8×10^{-4}
8.2	18	6.4×10^{-4}
8.6	10	11.3×10^{-4}

Half-Life is the time required for loss of 50% of the starting activity.

pH of 7.9 or 8.6 in 20 mM Tris-HCl which contained 1 mM dithiothreitol to reduce any oxidized sulfhydryls. Again first order kinetics of inhibition were found with rate constants of 2.2 10^{-4} and 12.1 10^{-4} sec^{-1} at pH 7.9 and 8.6 respectively. Therefore oxidation of sulfhydryl groups seems not to be responsible for inhibition at alkaline pH.

b) The iron-sulfur centre(s) may be destroyed by alkaline pH. This possibility was examined as follows; fumarate reductase was incubated at room temperature in 20 mM Tris-HCl, pH 9.0, in the presence or absence of 200 mM sodium phosphate. After 35 mins incubation the sample incubated in the absence of phosphate had lost 95% of its reductase activity while the sample incubated in the presence of phosphate retained 100% of its activity. The samples were then chromatographed on a 2 ml column of Sephadex G-25 to separate the iron, which would have been released upon destruction of the iron-sulfur centre(s), from the protein. An assay for non-heme iron on both samples indicated that the samples incubated in the presence of phosphate had 4.5 moles of iron per mole of enzyme while the sample incubated in the absence of phosphate had 4.6 moles of iron per mole of enzyme. It therefore seems that inactivation is not due to destruction of the iron-sulfur centre(s). This result was confirmed by measurement of the visible absorption spectrum of enzyme incubated in 20 mM Tris-HCl, pH 8.2. Figure 31 shows the visible absorption spectrum between 350 and 600 nm as a function of time of

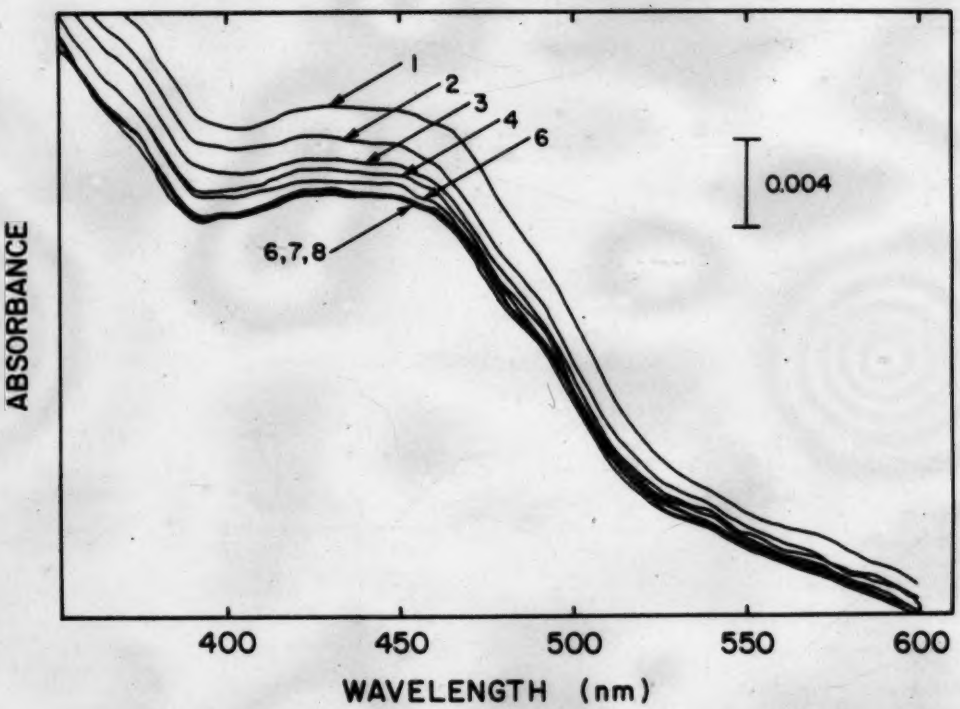

Figure 31. Effect of alkaline pH on the visible absorption spectrum of fumarate reductase. Cholate-depleted fumarate reductase was incubated at room temperature in 20 mM Tris-HCl, pH 8.2, for 8(1), 13(2), 22(3), 30(4), 40(5), 55(6), 80(7), and 108(8) minutes. Spectra were mwasured in a Varian Cary spectrophotometer using 20 mM Tris-HCl, pH 8.2, as a reference blank.

incubation. During the first 55 mins of incubation absorption between 400 and 470 nm decreased by about 10% and then remained constant for up to 60 mins further incubation. Although the absorbance decreased on the same time scale as inactivation occured, the structureless nature of the spectrum remained. This result suggests that destruction of the iron-sulfur centre(s) and FAD moiety are not responsible for inactivation. However, the decrease in absorbance upon inactivation may be due to a change in the environment of the FAD and iron-sulfur chromatophores.

c) Another possible mechanism was inactivation resulting from destruction of the active conformation of the protein. Such a mechanism is plausible since deprotonation of essential residues could have occured at alkaline pH. To probe this possibility we measured the far ultraviolet circular dichroic spectrum of enzyme incubated in 20 mM Tris-HCl, pH 9.0, for 50 mins in the presence or absence of 200 mM sodium phosphate. The percentages of α-helix, β-sheet and random coil respectively were 29.5, 10.5 and 60% in the presence of phosphate and 26.0, 11.7 and 62.3% in the absence of phosphate. As a control for any conformational change due to Tris-HCl, a sample was incubated in 200 mM sodium phosphate, pH 6.8, at room temperature for 50 mins and its far ultraviolet circular dichroic spectrum was measured. The percentages of α-helix, β-sheet and random coil respectively were 29.6, 11.2 and 59.2%. Thus it seems that inactivation is not accompanied by any large change in

conformation. However, the 3.6% decrease in α-helical content may be significant. In this regard it was interesting to examine the effect of fumarate on the rate of inactivation. I measured the first order rate constant for inactivation of fumarate reductase during incubation in 20 mM Tris-HCl, pH 8.6, in the presence and absence of 1 mM fumarate. At this concentration fumarate is acting as an substrate rather than as an activating anion. The rate constant decreased from 11.3 10^{-4} to 2.1 10^{-4} sec^{-1} upon inclusion of substrate during the incubation. This result may be interpreted to mean that substrate helps to stabilize the enzyme in its active conformation. A similar role can probably be attributed to activating anions.

4) Effect of Anions on the Circular Dichroic Spectrum of Fumarate Reductase.

In order to examine the possibility of anions activating by inducing a conformational change in the protein, the far ultraviolet circular dichroic spectra of the enzyme in 400 mM sodium phosphate, pH 6.8, or 25 mM Hepes, pH 6.8, were measured, Figure 32. The percentages of α-helix, β-sheet and random coil respectively calculated from these spectra were 30.1, 12.9 and 57% for the activated enzyme and 34.8, 17.4 and 47.8% for the deactivated enzyme. Thus, upon activation, the α-helical content decreased by 4.7%. This result is suggestive of a conformational change occuring upon activation.

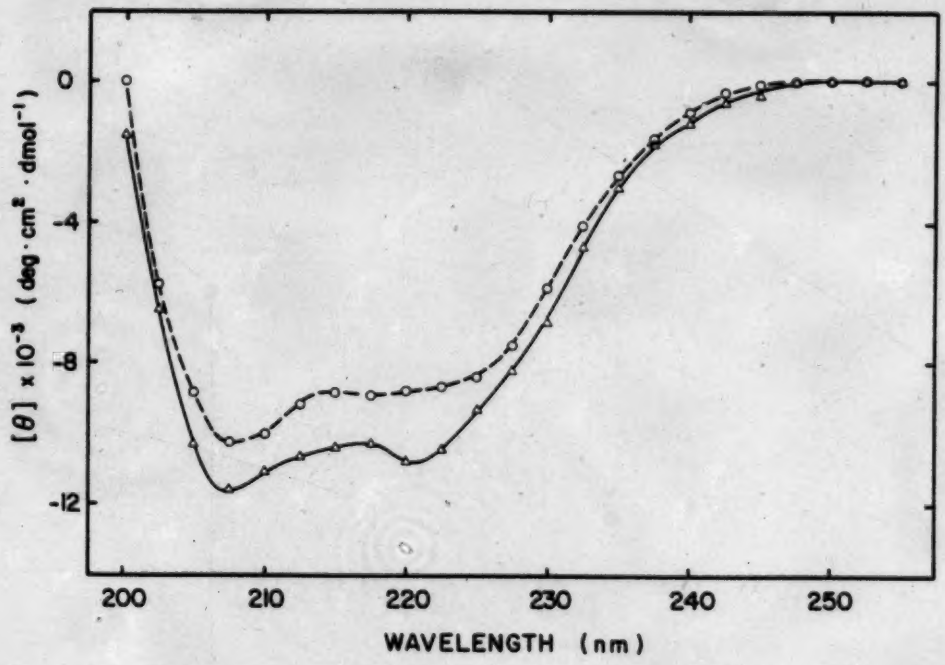

Figure 32. The far ultraviolet circular dichroic spectrum of cholate-depleted fumarate reductase in 25 mM Hepes, pH 6.8, (Δ-Δ), or 400 mM sodium phosphate, pH 6.8, (o-o). The appropriate buffer blanks were used to establish the baselines.

5) Effect of Anions on the Sulfhydryl Sensitivity of Fumarate Reductase.

Although the results of the previous section were suggestive of a conformational change being induced by anions they were not conclusive. I therefore decided to use another approach to probe the conformation of the activated and deactivated enzymes. The approach chosen derived from the work presented in Chapter IV which demonstrated the existance of a single sulfhydryl group which was essential for fumarate reductase activity. Essentially I decided to examine the sensitivity of the activated and deactivated enzymes to inactivation by the sulfhydryl reagent DTNB.

Figure 33 shows the linear first order kinetics of the inactivation of reductase activity by 0.02 mM DTNB. The first order kinetics were surprising since DTNB was present in only a two-fold molar excess over protein. However, it was interesting to find that the rate of inactivation in 25 mM Hepes was significantly faster than the rate in 200 mM sodium phosphate. In three independent experiments the rate of loss of activity of the deactivated enzyme was 2.3 to 2.8 fold faster than the loss of activity of the activated enzyme. From the data in Figure 33 pseudo-first order rate constants for inactivation were calculated to be 5.6 10^{1} M^{-1} sec^{-1} for the deactivated and 2.1 10^{1} M^{-1} sec^{-1} for the activated enzymes (see appendix III). In a similar experiment to that shown in Figure 33 the rate of modification of sulfhydryl groups was followed. Identical

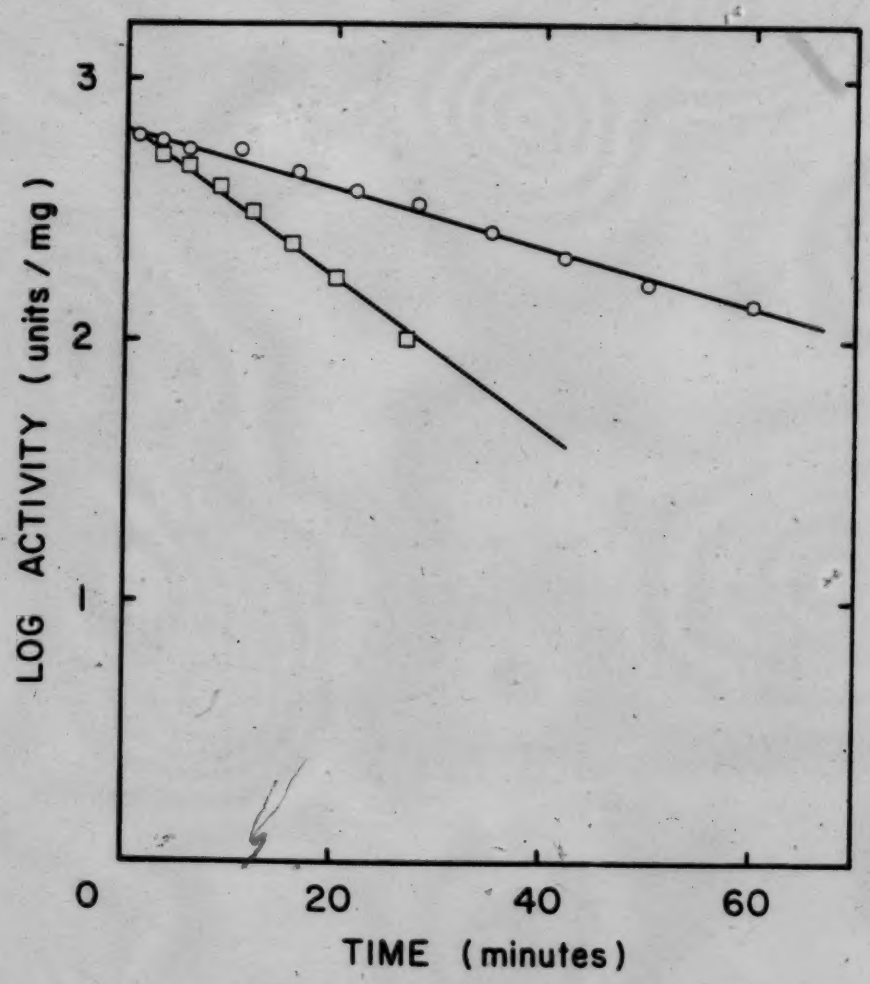

Figure 33. Sensitivity of fumarate reductase to inhibition by 0.02 mM DTNB. Cholate-depleted fumarate reductase in either 25 mM Hepes, pH 6.8, (□-□), or 400 mM sodium phosphate, pH 6.8, (o-o), was added to an equal volume of 0.04 mM DTNB. Incubation was at room temperature and assays were performed as described in Chapter II.

rates were found for the enzyme in 25 mM Hepes and 200 mM sodium phosphate. This result is not surprising since there are probably a number of surface exposed cysteine residues in both forms of the enzyme. The equal rates of cysteine modification suggest that the different rates of inhibition are not an artifact of differences in DTNB reactivity because of the different ionic strengths of the incubation mixtures. Quantitation of sulfhydryl group modification indicated that at 20 μM DTNB the deactivated enzyme was inhibited 85% after one mole of sulfhydryl had been modified per mole of enzyme. However, for the activated enzyme 85% inhibition occured after two moles of sulfhydryl had been modified per mole of enzyme. These results are consistent with the hypothesis that in the deactivated enzyme the sensitive cysteine is accessible to DTNB and competes effectively with the other accessible sulfhydryls for the low levels of DTNB available. In the activated enzyme the sensitive cysteine is less accesible to DTNB and competes less effectively with the other accesible cysteine residues and as a result is modified at a slower rate. The results presented above are consistent with the idea that anions induce a conformational change in fumarate reductase. However, the possibility that anions bind at the active site and protect the essential sulfhydryl cannot be ruled out.

6) Effect of Anions on the Catalytic Parameters of Fumarate Reductase.

To further pursue the effects of anions on the catalytic activity of fumarate reductase, I measured the Michaelis-Menten constants for both fumarate (fumarate reductase activity) and succinate (succinate dehydrogenase activity) as a function of phosphate concentration. The Km for fumarate was found to be independent of phosphate concentration, Table 8. An average value of 420 μM was determined. However, the Km for succinate was dependent on phosphate concentration Figure 34 and Table 8. The Km for succinate showed the same dependence on phosphate concentration as did activation of fumarate reductase activity in the absence of reducing agent (cf Figure 27). The Km increased from 20±3 to 1514±110 μM as the phosphate concentration increased from 0 to 400 mM respectively. The maximal velocity of the succinate dehydrogenase activity remained relatively constant as the phosphate concentration was increased. The succinate dehydrogenase assays at 0 and 700 mM were performed by Peter Dickie.

The significance of the increase in the Km for succinate is uncertain. Although membrane-bound fumarate reductase is not activated by anions, I have found that its Km for succinate increases from 531±102 μM in 50 mM phosphate to 1763±161 μM in 200 mM phosphate. This result suggests that the effects of phosphate on the maximal velocity of fumarate reductase activity and the Km for succinate are probably distinct and unrelated to one another.

Table 8

The Effect of Phosphate on the Km and Vmax for Succinate and Fumarate.

Phosphate(mM)	Succinate Km(μM)	Succinate Vmax	Fumarate Km(μM)	Fumarate Vmax
0	20±3	3.3±0.12	400±40	110±25
50	400±20	4.6±0.08	440±60	415±47
200	958±100	3.6±0.13	400±35	570±50
400	1514±110	3.7±0.12	414±34	524±34
700	1660±120	5.0±0.17	ND	ND

*V*max is in units/mg.

The zero phosphate assay was done in 25 mM Hepes, pH 6.8.

ND = not determined.

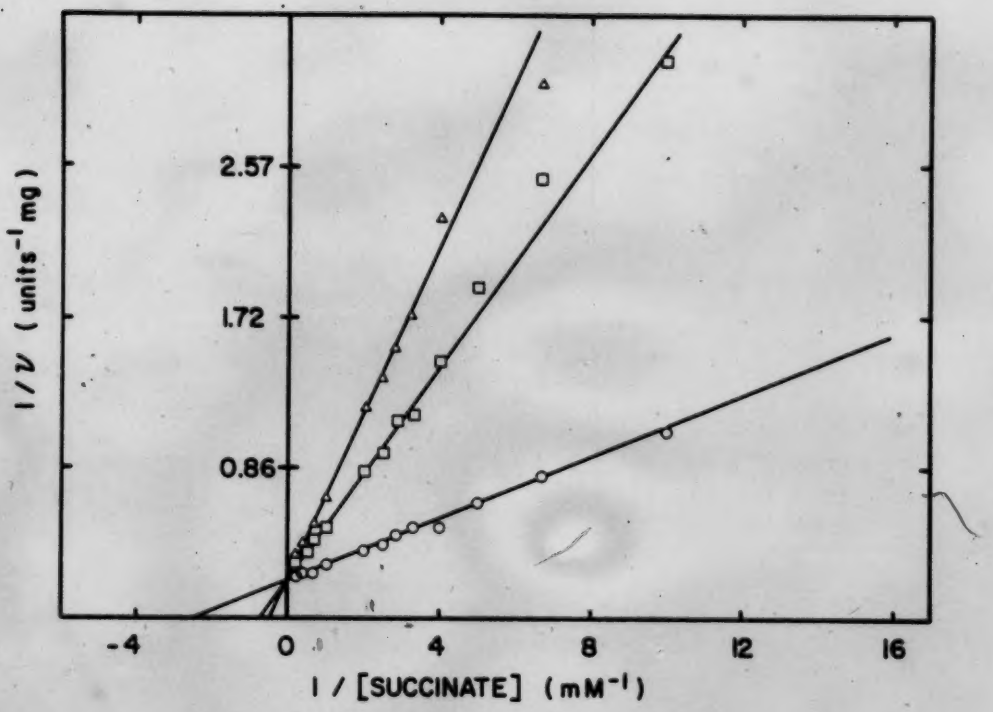

Figure 34. Lineweaver-Burk plots of the succinate dehydrogenase activity of fumarate reductase at various concentrations of sodium phosphate, pH 6.8. o-o, 50 mM sodium phosphate; □-□, 200 mM sodium phosphate; Δ-Δ, 400 mM sodium phosphate.

D. Discussion.

There are only a small number of reports in the literature which describe a modulating role for anions in enzymatically catalysed reactions. It has been shown that yeast phosphoglycerate kinase binds anions and as a result has a decreased susceptibility to inhibition by DTNB (159). In this study it was shown that the enzyme contains a single anion binding site and that the affinity of anions for this site depends on their charge. The more highly charged the anion the tighter the binding. The authors suggest that anion binding induces a conformational change which reduces the accessibility of a single thiol group to modification by DTNB. Anions also result in an increased rate of substrate turnover (160) and a decreased susceptibility of the enzyme to proteolysis (161). However, in contrast to the results with fumarate reductase, the modulating effects of anions on yeast phosphoglycerate kinase occur at concentrations of 0.01-1 mM for the most effective anions.

Beef heart succinate dehydrogenase has also been shown to be activated by anions. Kearney *et al* (144) showed that, in contrast to our work with fumarate reductase, both membrane-bound (electron transport particles) and purified succinate dehydrogenases were activated by anions and pH. Membrane-bound succinate dehydrogenase could be activated by lowering the pH from 7.4 to various values in the range 5.8 to 7.0. This activation was enhanced by the presence of monovalent anions. In contrast the purified enzyme could not

be activated by lowering the pH in the absence of added anions. In a subsequent communication, Ackrell *et al* (162) showed that the lack of activation of purified succinate dehydrogenase was due to the presence of bound oxaloacetate which was displaced by added anions. However, these authors also showed that activation occured twice as fast as oxaloacetate release suggesting that anion activation is not mediated through a release of bound oxaloacetate. Interestingly, activation of both purified and membrane-bound succinate dehydrogenase was time dependent whereas with fumarate reductase activation was instantaneous.

In this chapter I described the effects of anions on a number of properties of cholate-depleted fumarate reductase. The most obvious and easily measured effect of anions is activation of fumarate reductase activity. This activation is rather non-specific in that a range of different anions activate, although to varying extents. Total charge density seems to be the main criterion for activation; the more highly charged anions being the best activators. Anions also have a dramatic stabilizing effect on the enzyme. Both resistance to thermal denaturation and inactivation at alkaline pH are increased by anions. Anions therefore seem to maintain the enzyme in an active conformation. Another effect of anions is the dramatic increase in the apparent Km for succinate. This effect seems to be distinct from the other effects of anions since it occurs with the

membrane-bound as well as the purified enzyme. The circular dichroic and DTNB titration data suggest that activation may be mediated through a conformational change in the protein.

The activation of many intrinsic membrane proteins by amphipaths is easily reconcileable with the hydrophobic environment in which they function *in vivo*. However, fumarate reductase is not activated by amphipaths and only binds 0.15 mg of Triton X-100/mg of protein. During the purification of fumarate reductase, which involves Triton X-100 solubilization and Phenyl Sepharose CL-4B chromatography, there is no dramatic increase in the total number of units of fumarate reductase as assayed in the presence of 200 mM sodium phosphate, pH 6.8, and 0.5 mM dithiothreitol (see appendix I). This result coupled with the finding that the membrane-bound enzyme is not stimulated by phosphate, suggests that the membrane-bound form of the enzyme is in the activated state and that anions may be altering the properties of the purified enzyme in such a way that it more closely resembles the membrane-bound form. Anions may be mimicking the effect of some membrane component other than the hydrophobic environment. One possibility is that the membrane-bound enzyme is activated by an interaction with phospholipid head groups. In this regard the activation of fumarate reductase by o-phosphorylethanolamine is interesting. A second possibility involves the 13,000 and 15,000 dalton polypeptides which are encoded by the fumarate reductase

operon. These polypeptides may interact with the 69,000 and 25,000 dalton catalytic subunits within the membrane and anions may be mimicking this interaction. This possibility will be discussed further in Chapter VII.

VII. The Effects of Anions on Membrane-Bound and Triton X-100 Solubilized Fumarate Reductase.

A. Introduction.

During the characterization of fumarate reductase some conflicting results were obtained. Although the cholate-depleted, purified enzyme was readily soluble in aqueous buffers and bound only 15% (by wgt) Triton X-100, its solubilization from the membrane required nonionic detergents. Also, nonionic detergents did not affect the catalytic activity of the purified enzyme while anions had dramatic effects on the activity and stability of the purified enzyme. A possible explanation for the apparent anomalous behaviour of the 69,000 and 25,000 dalton catalytic subunits became evident as a result of the sequencing of the fumarate reductase operon (73,74,75). The very hydrophobic 13,000 and 15,000 dalton polypeptides may be subunits of the membrane-bound and Triton X-100 solubilized enzymes. Such an interaction may bind the catalytic subunits to the membrane and modulate the physical and catalytic properties of the enzyme.

In this chapter I describe some data on the Triton X-100 solubilized and membrane-bound enzymes. The membranes used in this study were prepared from an *E.coli* strain harboring a plasmid which we have called pfrd63. This strain was produced by inserting the *Hind III* fragment (fumarate reductase operon) from the ColE1 plasmid pLC16-43, into the

cloning vector pBR322. This modified pBR322 was then inserted into a transformable strain of *E.coli* and resulted in a dramatic amplification of the level of fumarate reductase activity in the transformed cells. This cloning work was performed by Joel Weiner.

B. Methods.

1) Preparation of Membrane Vesicles and Triton X-100 Extracts.

Everted membrane vesicles were prepared as described in Chapter II and stored at -80°C in 50 mM Tris-HCl, pH 7.5. Vesicles were transferred to the appropriate buffer by centrifugation at 160,000g for 15 mins at room temperature in a Beckmann Airfuge and resuspended in the appropriate buffer. Triton X-100 extracts were routinely prepared as follows: membrane vesicles were harvested by centrifugation at 160,000g for 15 mins at room temperature and resuspended in either 200 mM sodium phosphate, pH 6.8, or 25 mM Hepes, pH 6.8. The suspension was made 1% (w/v) in Triton X-100 and solubilization was allowed to proceed on ice for 30 mins. Insoluble debris was removed by centrifugation at 160,000g for 15 mins and the supernatant was passed down a 2 ml Pasteur pipette column of Sephadex G-25 equilibrated in the appropriate buffer. The eluted protein was then used to study the effects of anions on enzymatic activity and thermal stability.

To study the stability of membrane-bound enzymatic activity at alkaline pH, vesicles were harvested by centrifugation and resuspended in 20 mM Tris-HCl, pH 8.6, incubated at room temperature and assayed at various times for fumarate reductase activity. To study the stability of Triton X-100 extracted enzyme at alkaline pH, membrane vesicles were resuspended in 25 mM Hepes, pH 6.8, extracted as described above and passed down a 2 ml Pasteur pipette column of Sephadex G-25 equilibrated in 20 mM Tris-HCl, pH 8.6, and eluted with this buffer. Zero time was taken when the sample was applied to the column and the first assay was usually performed within 6 mins. All assays were performed using 200 mM sodium phosphate, pH 6.8, as the assay buffer unless otherwise stated.

2) Growth of *E.coli* HB101/pfrd63.

HB101/pfrd63 was grown anaerobically in 12 ml cultures on glycerol/fumarate medium as described in Chapter II except that no subculture was prepared and the cells were inoculated directly from thawed, frozen cultures into the growth medium. Cultures were harvested after different periods of growth and the membrane and supernatant fractions separated and assayed for fumarate reductase activity and protein. For aerobic growth, cells were inoculated directly into 20 ml of glycerol/fumarate medium in 100 ml Ehrlenmeyer flasks and growth was allowed to proceed in a shaking water bath. In all cases growth was at 37°C.

3) Chemical Cross-Linking.

Everted membrane vesicles were harvested by centrifugation at 160,000g for 15 mins at room temperature, resuspended in 200 mM triethanolamine-HCl, pH 8.5, made 0.5% (w/v) in Triton X-100 and incubated on ice for 30 mins. Insoluble debris was removed by centrifugation and various aliquots of a 20 mg/ml stock of dithiobis(succimidyl propionate) in dimethyl sulfoxide were added to 100 µl aliquots of supernatant and the reaction was allowed to go for 1.5 mins at room temperature. The final concentration of cross-linker was either 2.2 or 0.9 mg/ml while the final protein concentration was 4 mg/ml. The reaction was stopped by the addition of an excess of 1 M Tris-HCl, pH 6.8. The cross-linked material was precipitated with $(NH_4)_2SO_4$ and the pellet taken up in Laemmli solubilization solution (see Chapter II) and dialysed for 60 mins at room temperature against this solution to remove the $(NH_4)_2SO_4$. The sample was solubilized by boiling for 3 mins and analysed on a 5-15% (w/v) acrylamide Laemmli gel as described in Chapter II. A frozen strip of first dimension gel, which had not been stained, was thawed, incubated at room temperature for 10 mins in Laemmli electrophoresis buffer (90) which contained 50 mM DTT and placed on top of a 15% (w/v) Laemmli gel. The second dimension contained a 2 cm stacking gel, prepared as described in (90) except that the acrylamide-bisacrylamide was replaced with 1% (w/v) agarose and DTT was added to 50 mM. Electrophoresis, staining and

destaining were performed as described in Chapter II.

C. Results.

1) Anaerobic and Aerobic Expression of Fumarate Reductase in *E.coli* HB101/pfrd63.

Table 9 lists the levels of fumarate reductase activity found in the membrane and supernatant fractions prepared from anaerobically or aerobically grown *E.coli* HB101/pfrd63. During anaerobic growth the membrane became saturated when a specific activity of 70 was attained. Following saturation of the membrane, fumarate reductase activity began to appear in the cytoplasm. It therefore seems that the membrane can tolerate a 16 fold increase in fumarate reductase over that found in the wild type before becoming saturated. Interestingly, aerobic growth of HB101/pfrd63 resulted in a derepression of fumarate reductase synthesis and the appearance of fumarate reductase activity in the membrane fraction. A similar result was obtained by Cole and Guest (163). They found that a 13 fold amplification of fumarate reductase activity resulted in aerobic expression of enzyme activity. However, these workers found an aerobic level that was 50% of the anaerobic level (based on specific activity) while I have found that the aerobic level is only 10% of the anaerobic level. The aerobic expression is probably a result of a gene dosage effect which results in the titration of the repressor.

Table 9.

Aerobic and Anaerobic Expression of Fumarate Reductase in HB101/pfrd63.

Strain	OD	Membrane Fraction Total Units	SA	Supernatant Total Units	SA
(A)					
HB101/ pfrd63	0.28	2.6	4.8	2.4	5.2
	0.56	13.7	70	3.4	4.3
	1.12	14.3	70	14.7	10.1
HB101/ pBR322	1.00	2.4	4.3	0	0
(B)					
HB101/ pfrd63	1.10	1.3	7.1	0	0
HB101/ pBR322	0.81	0	0	0	0

HB101/pfrd63 is strain HB101 which has been transformed with pBR322 containing the fumarate reductase operon.

SA = Specific Activity.

(A) = Anaerobic Growth.

(B) = Aerobic Growth.

2) PAGE-SDS Analysis of a Triton X-100 Extract of HB101/pfrd63 Plasma Membranes.

Figure 35 is a densitometric scan of a 8-22% (w/v) gradient Laemmli gel of a Triton X-100 extract of HB101/pfrd63 plasma membranes. Four major polypeptides of molecular weights 69,000, 25,000, 15,000 and 14,100 were present in a molar ratio of 1:1.2:0.8:1.4 respectively. When two other gel slices, from the same gel, were scanned and the peaks quantitated, molar ratios of 1:1.3:0.8:1.3 and 1:1:0.8:1.1 were found for the 69,000, 25,000, 15,000 and 14,100 daltons bands respectively. We have analysed Triton extracts on a number of different gel systems: a) when a 15% Laemmli gel was used, three major bands corresponding to molecular weights of 69,000, 25,000 and 13-15,000 were found in a molar ratio of 1:1:2 respectively. b) When a 10-25% (w/v) Ornstein-Davis gel (164) was used, three major bands corresponding to molecular weights of 69,000, 25,000 and 15,000 were present in a molar ratio of 1:1:1.7 respectively. c) When a 10-25% (w/v) fast running gel system of Jovin *et al* (91) was used, three major bands corresponding to molecular weights of 69,000, 25,000 and 15,000 were found in a molar ratio of 1:1:1 respectively. For some unknown reason the low molecular weight polypeptides behave anamolously on the latter gel system. In general these results suggest that amplification of fumarate reductase activity results in the amplification of four polypeptides of molecular weights 69,000, 25,000, 15,000 and

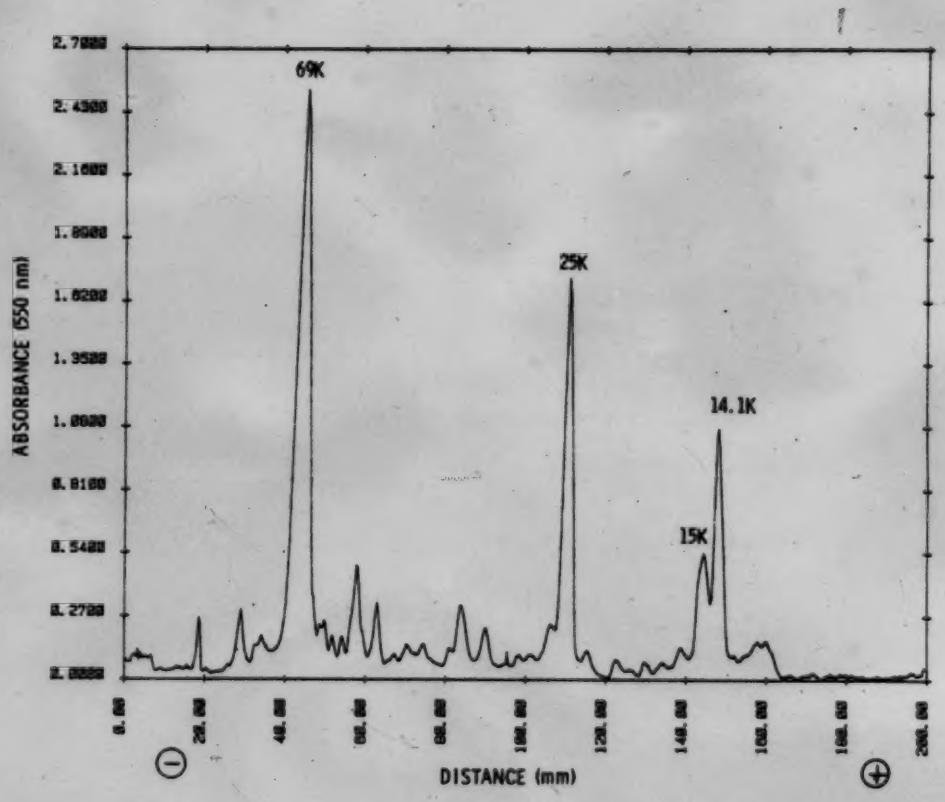

Figure 35. Densitometric scan of an 8-22% (w/v) gradient Laemmli gel of a Triton X-100 extract of HB101/pfrd63 plasma membranes. Molecular weights were calculated from semi-logarithm plots of molecular weight (using the molecular weight standards listed in Chapter II) versus Rf.

14,100 present in an approximate molar ratio of 1:1:1:1. Most gel systems tested were unable to separate the 15,000 and 14,100 dalton polypeptides.

3) Chemical Cross-Linking of the Triton X-100 Extract.

One of the first questions of interest was the quaternary structure of fumarate reductase in the Triton extract. To address this question I cross-linked the Triton X-100 extracted material with the cleavable reagent dithiobis(succimidyl propionate), (DTSP). This reagent cross-links primary and secondary amino groups separated by 12 Å or less. Figure 36 shows the first and second dimension gels. Although considerable streaking of cross-linked material occurred, a broad band, ranging in molecular weight from 109,600 to 127,600 was found on the first dimension gel. When the cross-linked material was cleaved with dithiothreitol and run on a second dimension gel three major bands, corresponding to molecular weights of 69,000, 25,000 and 13,000 were found to be components of the cross-linked material. When the strip of second dimension gel, immediately beneath the cross-linked complex on the first dimension gel, was scanned for Coomassie Brilliant Blue stained protein a molar ratio of 1:0.85:1.2 (69,000:25,000:13,000) was found. In a second independent experiment a molar ratio of 1:0.72:0.85 was found. These results were obtained using 2.2 mg/ml DTSP and 4 mg/ml protein. An identical result was obtained when the cross-linker concentration was decreased to 0.9 mg/ml while

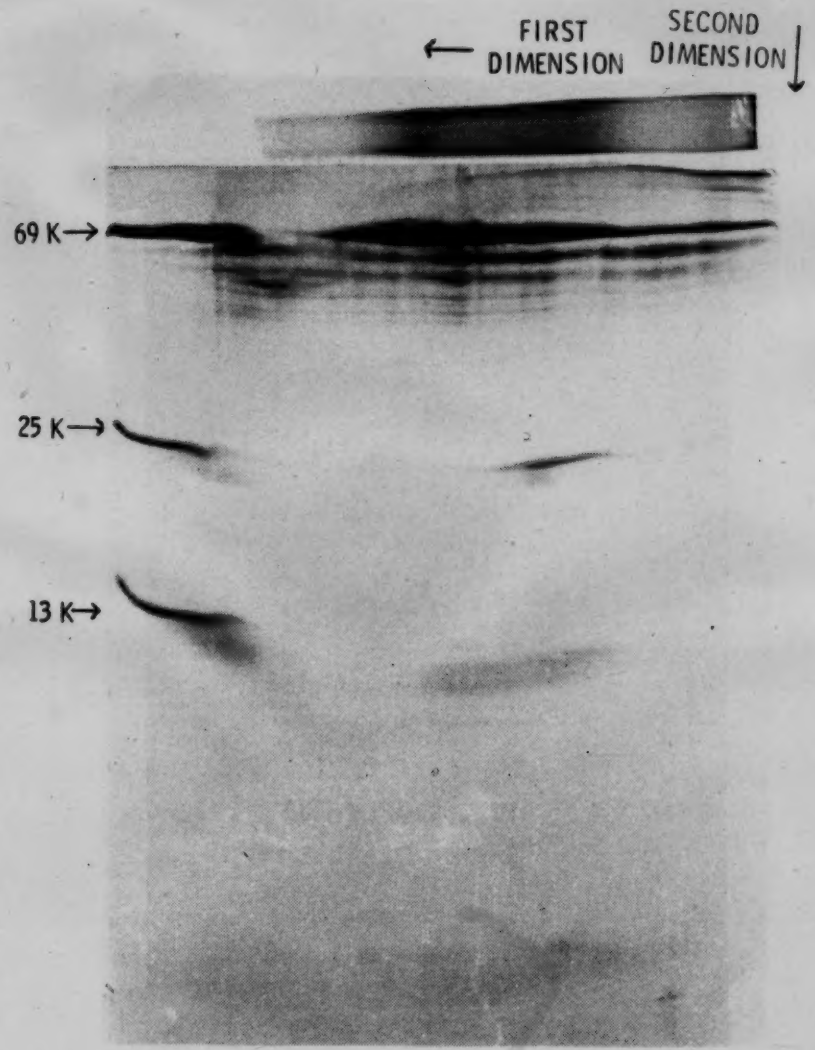

Figure 36. First and second dimension gels of the cross-linked Triton X-100 extract of HB101/pfrd63 plasma membranes. The molecular weight standards were; the α and β subunits of purified fumarate reductase, 69,000 and 25,000 daltons respectively , and RNase at 13,000 daltons.

the protein concentration was kept at 4 mg/ml. These results suggest that the Triton X-100 extracted material consists of a complex of the 69,000 and 25,000 dalton subunits and a third subunit(s) of approximate molecular weight 13,000 present in a molar ratio of 1:1:1 respectively. At present the relationship between the 13,000 dalton band and the 15,000 and 14,100 dalton bands seen on 8-22% (w/v) Laemmli gels is uncertain. The 13,000 dalton band may be composed of one or both of the 15,000 and 14,100 dalton polypeptides.

4) Effect of Anions on Catalytic Activity.

Since anions dramatically activate the purified, two subunit form of fumarate reductase it was of interest to examine the effect of phosphate on the catalytic activity of the Triton X-100 extracted enzyme, Table 10. The effect of phosphate on the membrane-bound enzyme was included for completeness. It can be clearly seen that the presence of the 15,000 and 14,100 dalton polypeptides abolishes the ability of phosphate to activate enzyme activity. It is tempting to speculate that anions interact with the catalytic subunits in such a way as to mimick the interaction of these subunits with the 15,000 and/or 14,100 dalton polypeptides.

5) Effect of Anions on Stability at Alkaline pH.

Another property of the two subunit form of fumarate reductase which is dramatically altered by anions is its stability at alkaline pH. When enzyme activity in Triton X-100 extracts or membrane vesicles was measured as a

Table 10

The Effect of Anions on the Catalytic Activity of Membrane-Bound and Triton X-100 Solubilized Fumarate Reductase.

Assay Buffer	Enzyme	SA(u/mg)
Hepes	Triton X-100 Extract	172
Phosphate	Triton X-100 Extract	164
Hepes	Membrane-Bound	62
Phosphate	Membrane-Bound	68

Hepes = 25 mM Hepes, pH 6.8.

Phosphate = 200 mM sodium phosphate, pH 6.8.

SA = Specific Activity (units/mg).

Both the Triton X-100 extract and the membrane vesicles were prepared in 25 mM Hepes, pH 6.8, before assay.

function of time of incubation in 20 mM Tris-HCl, pH 8.6, no loss of activity occured, Figure 37. Again, this result suggests that the low molecular weight polypeptide(s) alter the pH stability of the catalytic subunits in such a way that it is quite similar to the anion activated two subunit enzyme. at alkaline pH.

6) Effect of Anions on Thermostability.

I next investigated the thermostability of the Triton X-100 extracted and membrane-bound enzymes in 25 mM Hepes, pH 6.8, or 200 mM sodium phosphate, pH 6.8, Figure 38. As expected the membrane-bound enzyme was completely stable for up to 60 mins at 46°C in the absence of anions. Suprisingly, Triton X-100 extracted enzyme was thermolabile at 46°C in the absence of anions. Fifty percent of the activity was lost after 19 mins at 46°C and this rate of loss of activity is similar to the loss of activity of the two subunit form of the enzyme in the absence of anions (50% of the activity was lost after 23 mins at 45°C). In the presence of 200 mM sodium phosphate, pH 6.8, no loss of activity occured after 60 mins at 46°C.

D. Discussion.

In Chapter VI I reported the marked activating and stabilizing effects of anions on the purified, catalytically active two subunit form of fumarate reductase. In addition, I suggested that anions may be mimicking an interaction between the catalytic subunits and some membrane component

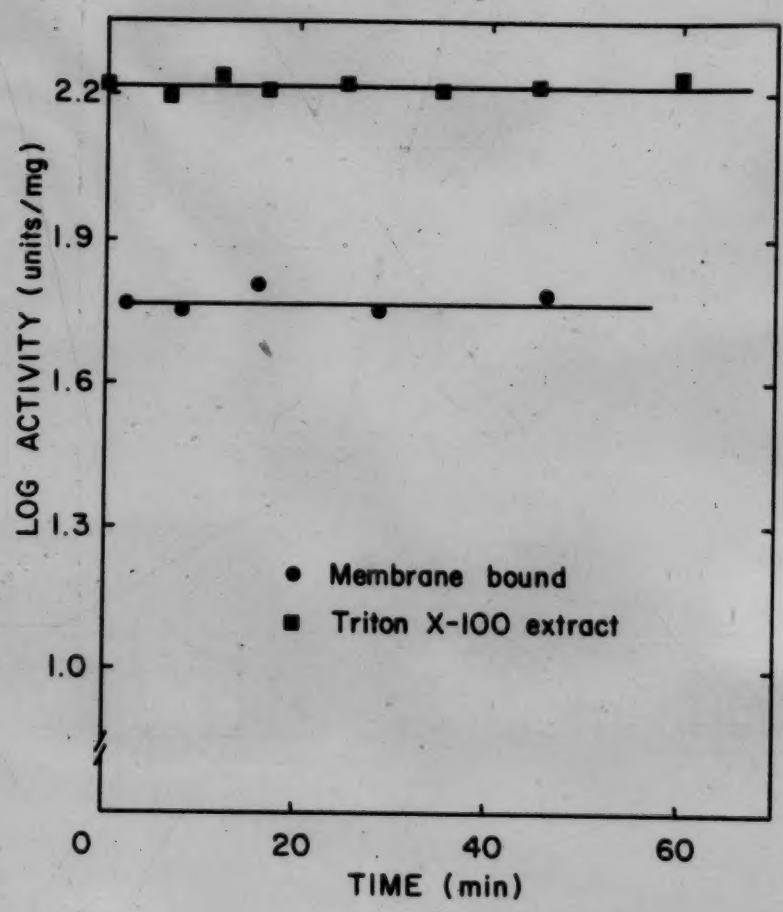

Figure 37. Stability of membrane-bound or Triton X-100 extracted fumarate reductase at alkaline pH. Incubation was at room temperature in 20 mM Tris-HCl, pH 8.6. The membrane vesicles were 6.6 mg/ml in protein and had a specific activity of 59 units/mg. The Triton X-100 extract was 1.65 mg/ml in protein and had a specific activity of 167 units/mg.

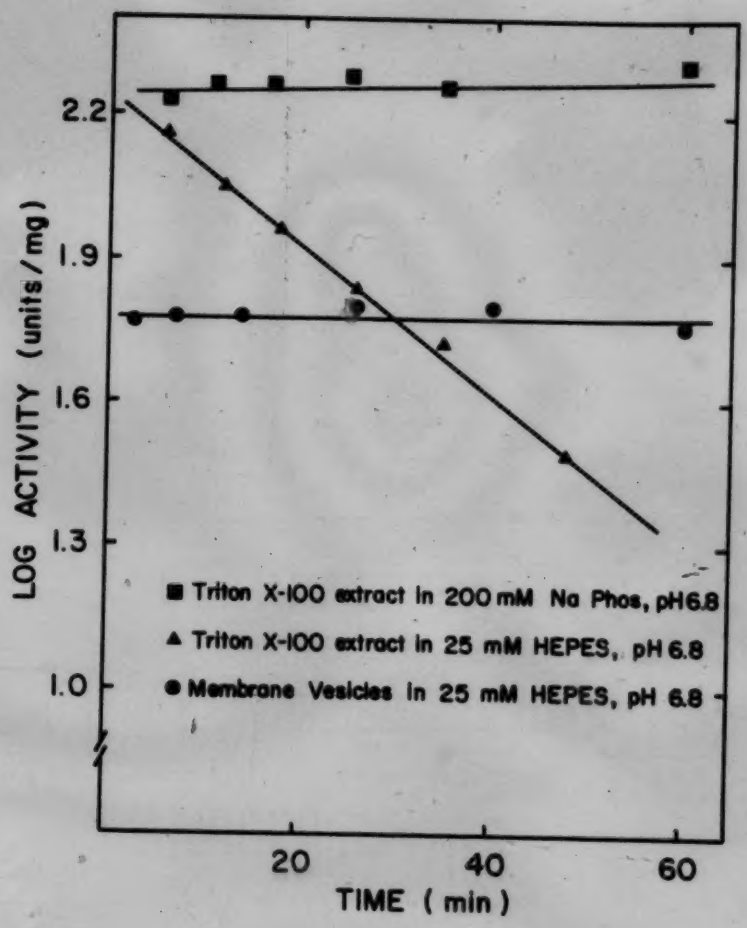

Figure 38. Thermostability of membrane-bound and Triton X-100 extracted fumarate reductase. The membrane vesicles were 6.7 mg/ml in protein and had a specific activity of 58 units/mg. The Triton X-100 extract in 25 mM Hepes, pH 6.8, was 1.43 mg/ml in protein and had a specific activity of 180 units/mg while the Triton X-100 extract in 200 mM sodium phosphate, pH 6.8, was 0.72 mg/ml in protein and had a specific activity of 171 units/mg. All incubations were at 45°C.

other than the hydrophobic environment. The 13,000 and 15,000 dalton polypeptides are an obvious possibility; they are encoded by the same operon as the 69,000 and 25,000 dalton subunits and contain 70% hydrophobic amino acids.

In this chapter I described the effects of phosphate on some properties of the membrane-bound and Triton X-100 solubilized fumarate reductase. Extraction of HB101/pfrd63 everted membrane vesicles with 0.5% (w/v) Triton X-100 resulted in a fraction highly enriched in fumarate reductase activity (see Figure 35). We estimate that fumarate reductase is 75% pure (based on a four subunit enzyme) in the Triton extracts. However, the specific activity of the Triton extracts was only 170 (units/mg) while that of the pure enzyme was 550 (units/mg). This may mean that some of the membrane-bound enzyme is inactive. This could arise from an inability of cells to attach the covalent FAD or the non-heme iron to all of the amplified enzyme. The Triton extracts contain four major polypeptides of molecular weights 69,000, 25,000, 15,000 and 14,100 present in a molar ratio of approximately 1:1:1:1 respectively. However, when the extract is cross-linked with DTSP, the cross-linked complex contains three major polypeptides of molecular weights 69,000, 25,000 and approximately 13,000 present in a molar ratio of 1:1:1 respectively. This result is a little surprising since it suggests that the Triton extracted material exists as a $\alpha\beta\gamma$ trimer while the extract actually contains four rather than three distinct polypeptides. It is

possible that cross-linking of the two low molecular weight, hydrophobic polypeptides to the catalytic subunits was not quantitative due to the presence of tightly bound lipid. Whatever the explanation it seems certain that Triton X-100 extracted fumarate reductase has a more complex quaternary structure than the purified $\alpha\beta$ dimeric form.

I next investigated the effects of anions on the activity and stability of membrane-bound and Triton X-100 extracted fumarate reductase. Phosphate was ineffective at activating the membrane-bound and Triton solubilized enzymes, both of which were quite stable at alkaline pH in the absence of phosphate. However, while the membrane-bound enzyme was stable for up to 60 mins at 46°C in the absence of phosphate, the Triton solubilized enzyme was unstable at 46°C in the absence of phosphate. Activity was lost at about the same rate as that seen for the anion-depleted two subunit enzyme. The presence of 200 mM sodium phosphate, pH 6.8, stabilized the Triton solubilized enzyme against thermal denaturation.

The results of this chapter suggest that Triton X-100 solubilized and perhaps membrane-bound fumarate reductase exists as a complex of dissimilar subunits of molecular weights 69,000, 25,000, 15,000 and/or 14,100. The purified dimeric form arises as a result of dissociation of the low molecular weight polypeptide(s) subunit from the catalytic subunits during purification. At present it is not known whether the 13,000 dalton species, seen on the second

dimension gel of cross-linked fumarate reductase, consists of one or both of the small molecular weight polypeptides encoded by the fumarate reductase operon. The stability at alkaline pH and the lack of stimulation of enzymatic activity by phosphate suggests that a similarity may exist between the membrane-bound and Triton X-100 extracted fumarate reductase and the anion activated $\alpha\beta$ dimeric form.

VIII. Conclusions.

The studies reported in this thesis were directed towards developing an understanding of the properties of two *E.coli* electron transport proteins, the aerobic glycerol-3-phosphate dehydrogenase and fumarate reductase. In my early studies I examined the effect of amphipaths on the activity of G3PD. This enzyme was particularly interesting since its PMS/MTT reductase activity was activated by amphipaths while its ferricyanide reductase was unaffected. The results suggested that amphipaths may be generating a site of interaction between G3PD and PMS. DL-glycerol-3-phosphate dependent quenching of flavin fluorescence suggested that activation did not involve a change in the affinity of the enzyme for its substrate L-glycerol-3-phosphate. This conclusion was confirmed by the inability of Brij 58 to significantly change the Km for DL-glycerol-3-phosphate, as determined by the PMS/MTT assay. However, the Km for DL-glycerol-3-phosphate, as determined by the PMS/MTT assay, was significantly different from the Km determined by the ferricyanide reductase assay. This suggested that the sites of interaction of PMS and ferricyanide with G3PD may be different. This postulate was supported by the differential inhibition of the two reductase activities by Cu^{+2} and Zn^{+2} ions. In summary the results of this study suggested that amphipaths activate G3PD by increasing the interaction between the enzyme and the electron acceptor PMS. To date research in the area of

amphipathic modulation of membrane proteins has generated no general rules or mechanisms of activation. A plausible general mechanism would involve a conformational change which alters the affinity of the enzyme for its substrate(s) and/or product(s). The limiting factor to date has probably been the lack of technology for measuring small conformational changes in proteins.

The bulk of this thesis reports the results of studies on the terminal electron transferring enzyme, fumarate reductase. Characterization studies indicated that the purified enzyme consisted of two dissimilar subunits of molecular weights 69,000 and 25,000 present in a molar ratio of 1:1. The purified enzyme contained 4 to 5 moles each of nonheme iron and acid labile sulfur, probably present as an iron-sulfur centre of the Fe_4S_4 type in the small subunit. However, identification of the precise nature of the iron-sulfur center(s) will require further work. The purified enzyme was also shown to contain a single sensitive sulfhydryl residue which was located in the large subunit.

A picture of the roles of the subunits is now beginning to emerge. The 25,000 dalton subunit probably interacts with other components of the electron transport chain and serves to channel electrons from the chain to the active site of fumarate reductase which is probably located in the large subunit. This model is similar to that proposed for beef heart mitochondrial succinate dehydrogenase (164,165,166) (other similarities between these enzymes were discussed in

Chapter IV). Succinate dehydrogenase has three iron-sulfur centres: two, S1 and S2, are located in the FAD containing large subunit while the third, S3, is located in the small subunit. Reducing equivalents are passed from the active site, in the large subunit, via FAD, S1 and S2 to the S3 centre in the small subunit and from there down the electron transport chain.

Further characterization of the purified enzyme indicated that the catalytic activity and stability of fumarate reductase were markedly enhanced by anions. The membrane-bound and Triton X-100 solubilized enzymes showed similar properties to the purified, anion activated enzyme. Interestingly, amplification of fumarate reductase activity was accompanied by an increase in the level of four polypeptides, of molecular weights 69,000, 25,000, 15,000 and 14,100, in the membrane fraction. Cross-linking studies suggested that the Triton solubilized enzyme had a more complex quaternary structure than the purified enzyme. However, at this time we do not know whether one or both of the low molecular weight polypeptides are associated with the 69,000 and 25,000 dalton subunits.

The 15,000 and 14,100 dalton polypeptides appear to be required for the binding of the catalytic subunits to the plasma membrane. Bernie Lemire has produced a clone, HB101/pfrd117, which contains pBR322 into which a piece of the fumarate reductase operon, which codes for the catalytic subunits, has been inserted. When HB101/pfrd117 was grown

anaerobically whole cell fumarate reductase activity was elevated several fold. However, only the wild type level of activity was found in the membrane fraction. The remainder was found in the supernatant fraction. This result strongly suggests that the catalytic subunits are not capable of binding to the membrane in the absence of the low molecular weight polypeptides. We are now developing a picture of membrane-bound fumarate reductase; the catalytic subunits are largely exposed to the cytoplasm and are anchored to the membrane through an interaction with one or both of the low molecular weight polypeptides. This model is supported by the topology study reported in Chapter V as well as the very hydrophobic nature of the low molecular weight polypeptides and the finding that the catalytic subunits bound only 15% of their own weight of Triton X-100. Again, a similar model is emerging for beef heart mitochondrial succinate dehydrogenase. Merli *et al* (167) and Girdlestone *et al* (168) suggest that the 70,000 dalton subunit of succinate dehydrogenase is largely exposed to the cytoplasm and is anchored to the membrane through an interaction with the 27,000 dalton subunit. The small subunit is in turn anchored to the membrane through an interaction with two other low molecular weight polypeptides which are components of complex II and at least one of which appears to be required for succinate-ubiquinone reductase activity (169).

Future research should be directed towards gaining a detailed understanding of the interaction between the anchor

polypeptide(s) and the catalytic subunits. Methods need to be developed to purify the low molecular weight polypeptides in a non denatured form. Once this is achieved there are a number of interesting experiments which can be undertaken: a) it should be possible to reconstitute an anion insensitive fumarate reductase activity by reconstituting a 3 or 4 subunit enzyme from the anion sensitive catalytic subunits and the purified low molecular weight polypeptides, b) it should be possible to reconstitute the multi-subunit enzyme into liposomes as a first step in reconstituting a coupled electron transport chain and c) a detailed cross-linking study should be undertaken to precisely establish the quaternary structure of the multi-subunit enzyme. Experiments should also be undertaken to try to establish whether or not the low molecular weight polypeptides merely anchor the catalytic subunits to the membrane or whether they also mediate electron transfer from menaquinone or cytochrome b to the catalytic subunits. At present the cytochrome b component of the glycerol-fumarate electron transport chain is being purified in Dr Weiner's laboratory. The membrane-bound enzyme should also be studied to develop a detailed picture of the topology of the multi-subunit enzyme. The question of topology is important since a transmembranal arrangement would open the way for experiments to establish whether or not fumarate reductase, like mitochondrial cytochrome oxidase (20), is a proton pump.

BIBLIOGRAPHY

1. Slater, E.C., 1976 *in Reflections on Biochemistry.* (Kornberg, A., Horecker, B.L., Cornudella, L., and Oro, J., ed) p 45-55, Pergamon Press Ltd.

2. Gale, E.F., and Paine, T.F., 1951. *Biochem. J.* **48**. 298-301.

3. Kaback, H.R., 1960. *Fed. Proc.* **19**, 130.

4. Mitchell, P., 1961. *Nature* **191**, 144-148.

5. Mitchell, P., 1975. *Biochem. Soc. Trans.* **4**, 399-430.

6. Moyle, J., and Mitchell, P., 1973. *FEBS Letters* **30**, 317-320.

7. Thayer, W.S., and Hinkle, P.C., 1973. *J. Biol. Chem.* **248**, 5395-5402.

8. Downie, J.A., Gibson, F., and Cox, G.B., 1979. *Ann. Rev. Biochem.* **48**, 103-131.

9. Ryrie, I.J., and Blackmore, P.F., 1976. *Arch. Biochem. Biophys.* **176**, 127-135.

10. Mitchell, P., and Moyle, J., 1965. *Nature* **208**, 147-151.

11. Mitchell, P., and Moyle, J., 1967. *Biochem. J.* **105**, 1147-1162.

12. Harold, F.M., 1976. *Curr Topics in Bioenergetics.* **6**, 83-149.

13. Rosen, B.P., and Kashket, E.R., 1978. *in Bacterial Transport* (Rosen, B.P., ed.) p 559-620. Marcel Decker Inc.

14. Mitchell, P., 1973. *J. Bioenergetics.* **4**, 63-91.

15. Kaback, H.R., 1977. *J. Cell. Physiol.* **89**, 575-594.

16. Racker, E., and Stockenius, W., 1974. *J. Biol. Chem.* **249** 662-663.

17. Racker, E., 1976. *in A New Look at Mechanisms in Bioenergetics.* p 89-106, Academic Press.

18. Mitchell, P., 1975. *FEBS Letters* **56**, 1-6.

19. Stockenius, W., and Lozier, R.H., 1974. *J. Supramol. Struct.* 2, 769-774.

20. Wikstrom, M.K.F., 1977. *Nature* 266, 271-273.

21. Boyer, P.D., 1977. *Ann. Rev. Biochem.* 46, 957-966.

22. Brand, M.D., Reynafarje, B., and Lehninger, A.L., 1977. *J. Cell. Physiol.* 89, 595-602.

23. Mitchell, P., 1974. *FEBS Letters* 43, 189-194.

24. Racker, E., 1977. *Ann. Rev. Biochem.* 46, 1006-1014.

25. Rosing, J., Kayalar, C., and Boyer, P.D., 1977. *J. Biol. Chem.* 252, 2478-2485.

26. Kayalar, C., Rosing, J., and Boyer, P.D., 1977. *J. Biol. Chem.* 252, 2486-2491.

27. Boyer, P.D., 1977. *TIBS.* 2, 38-41.

28. Boyer, P.D., 1965. *In Oxidases and Related Redox Systems* (King, T.E., Mason, H.S., and Morrison, M., eds) *2*, p 994-1008, New York Wiley.

29. Slater, E.C., 1953. *Nature* 172, 975-978.

30. Williams, R.J.P., 1978. *FEBS Letters* 85, 9-19.

31. Bragg, P.D., 1979. *In Membrane Proteins in Energy Transduction* (Capaldi, R.A., ed) *2*, p 341-449, Marcel Decker Inc.

32. Haddock, B.A., Downie, J.A., and Garland, P.B., 1979. *Biochem. J.* 154,285-294.

33. Poole, R.K., and Haddock, B.A., 1975. *Biochem. J.* 152, 537-546.

34. Haddock, B.A., and Jones, C.W., 1977. *Bacteriol. Rev.* 41, 47-99.

35. Downie, J.A., and Cox, G.E., 1978. *J. Bacteriol.* 133, 477-484.

36. Poole, R.K., and Haddock, B.A., 1974. *Biochem. J.* 144, 77-85.

37. Lawford, H.G., and Haddock, B.A., 1973. *Biochem. J.* 136, 217-220.

38. Thauer, R.K., Jungermann, K., and Decker, K., 1977.

Bacteriol. Rev. 41, 100-180.

39. Garland, P.B., Downie, J.A., and Haddock, B.A., 1975. *Biochem. J.* 152, 547-559.

40. Enoch, H.G., and Lester, R.L., 1974. *Biochim. Biophys. Res. Comm.* 61, 1234-1241.

41. Kemp, M.B., Haddock, B.A., and Garland, P.B., 1975. *Biochem. J.* 148, 329-333.

42. Schryvers, A.B., and Weiner, J.H., 1981. *J. Biol. Chem.* 256, 9959-9965.

43. Miki, K., and Lin, E.C.C., 1973. *Bacteriol. J.* 114, 767-771.

44. Singh, A.P., and Bragg, P.D., 1975. *Biochim. Biophys. Acta.* 396, 229-241.

45. Singh, A.P., and Bragg, P.D., 1976. *Biochim. Biophys. Acta.* 423, 450-461.

46. Miki, K., and Wilson, T.H., 1978. *Biochim. Biophys. Res. Comm.* 83, 1570-1575.

47. Weiner, J.H., and Heppel, L.A., 1972. *Biochem. Biophys. Res. Comm.* 47, 1360-1365.

48. Weiner, J.H., 1974. *J. Membr. Biol.* 15, 1-14.

49. Schryvers, A.B., Lohmeier, E., and Weiner, J.H., 1978. *J. Biol. Chem.* 253, 783-788.

50. Kristler, W.S., and Lin, E.C.C., 1971. *J. Bacteriol.* 108, 1224-1234.

51. Kistler, W.S., and Lin, E.C.C., 1972. *J. Bacteriol.*

52. Jaworski, A., Campbell, H.D., Poulis, M.I., and Young, I.G., 1981. *Biochemistry* 20, 2041-2047.

53. Jaworski, A., Mayo, G., Shaw, D.C., Campbell, H.D., and Young I.G., 1981. *Biochemistry* 20, 3621-3628.

54. Enoch, H.G., and Lester, R.L., 1975. *J. Biol. Chem.* 250, 6693-6705.

55. Bennett, R., Taylor, D.R., and Hurst, A., 1966. *Biochim. Biophys. Acta.* 118, 512-521.

56. Futai, M., and Kimura, H., 1977. *J. Biol. Chem.* 252, 5820-5827.

57. Futai, M., 1973. *Biochemistry* 12, 2468-2474.

58. Kohn, L.D., and Kaback, H.R., 1973. *J. Biol. Chem.* 248, 7012-7017.

59. Pratt, E.A., Fung, L.W.M., Flowers, J.A., and Ho, C., 1979. *Biochemistry* 18, 312-316.

60. Williams, R.F., and Hager, L.P., 1966. *Arch. Biochim. Biophys.* 116, 168-176.

61. O'Brien, T.A., Schrock, H.L., Russell, P., Blake, R., and Gennis, R.B., 1976. *Biochim. Biophys. Acta.* 452, 13-29.

62. Shaw-Goldstein, L.A., Gennis, R.B., and Walsh, C., 1978. *Biochemistry* 17, 5605-5613.

63. Kim, I.C., and Bragg, P.D., 1971. *Can. J. Biochem.* 49, 1098-1104.

64. Jones, R.W., Kranz, R., and Gennis, R.B., 1982. *FEBS Letters* (in press).

65. Owen, P., and Condon, C., 1982. *FEMS Letters* (submitted).

66. Condon, C., and Owen, P., 1982. *FEMS Letters* (submitted).

67. Cole, S.T., and Guest, J.R., 1980. *Mol. Gen. Genet.* 178, 409-418.

68. Cole, S.T., and Guest, J.R., 1980. *Mol. Gen. Genet.* 179, 377-385.

69. Cole, S.T., and Guest, J.R., 1979. *Eur. J. Biochem.* 102, 65-71.

70. Dickie, P., and Weiner, J.H., 1979. *Can. J. Biochem.* 57, 813-821.

71. Weiner, J.H., and Dickie, P., 1979. *J. Biol. Chem.* 254, 8590-8593.

72. Lohmeier, E., Hagen, D.S., Dickie, P., and Weiner, J.H., 1981. *Can. J. Biochem* 59, 158-164.

73. Cole, S.T., 1982. *Eur. J. Biochem.* 122, 479-484.

74. Cole, S.T., Grundstrom, T., Jaurin, B., Robinson, J.J., and Weiner, J.H., 1982. *Eur. J. Biochem.* (submitted).

75. Grundstrom, T., and Jaurin, B., 1982. *Proc. Natl. Acad.*

Sci. USA. 79, 1111-1115.

76. Singer, T.P., Kearney, E.B., and Kenney, W.C., 1973. *Adv. Enzymol.* 37, 189-272.

77. MacGregor, C.H., Schnaitman, C.A., Normansell, D.E., and Hodgins, M.G., 1974. *J. Biol. Chem.* 249, 5321-5327.

78. MacGregor, C.H., Schnaitman, C.A., 1974. *J. Supra. Struct.* 2, 715-727.

79. Clegg, R.A., 1976. *Biochem. J.* 153, 533-541.

80. DeMoss, J., 1977. *J. Biol. Chem.* 252, 1696-1701.

81. MacGregor, C.H., 1975. *J. Bacteriol.* 121, 1102-1110.

82. MacGregor, C.H., 1975. *J. Bacteriol.* 121, 1111-1116.

83. MacGregor, C.H., 1976. *J. Bacteriol.* 126, 122-131.

84. Bonnefoy-Orth, V., Lepelletier, M., Passal, M,C., and Chippaux, M., 1981. *Mol. Gen. Genet.* 181, 535-540.

85. Miller, J.H., 1972. *Experiments in Molecular Genetics.* Cold Spring Harbour Laboratory. New York.

86. Minakami, S., Ringler, L., and Singer, T.P., 1962. *J. Biol. Chem.* 237, 569-576.

87. Jones, R.W., and Garland, P.B., 1977. *Biochem. J.* 164, 199-211.

88. Spencer, M.E., and Guest, J.R., 1973. *J. Bacteriol.* 144, 563-570.

89. Kaback, H.R., 1971. *Meth. Enzymol.* 22, 99-120.

90. Laemmli, U.K., 1970. *Nature* 227, 680-685.

91. Jovin, T.M., Englund, P.T., and Bertsch, L.L., 1969. *J. Biol. Chem.* 244, 2996-3008.

92. Fung, L.M.W., Pratt, E.A., and Ho, C., 1979. *Biochemistry* 18, 317-324.

93. Kawada, N., Takeda, K., and Nosoh, Y., 1981. *J. Biochem.* 89, 1017-1027.

94. Vik, S.B., Georgevich, G., and Capaldi, R.A., 1981. *Proc. Natl. Acad. Sci. USA.* 78, 1456-1460.

95. Blake, R., Hager, L.P., and Gennis, R.B., 1978. *J. Biol. Chem.* 253, 1963-1971.

96. Davies, G.E., and Stark, G.R., 1970. *Proc. Natl. Acad. Sci. USA.* 66, 651-656.

97. Oikawa, K., Kay, C.M., and McCubbin, W.D., 1968. *Biochim. Biophys. Acta.* 168, 164-167.

98. Chen, Y.H., Yang, J.T., and Chau, K.H., 1974. *Biochemistry* 13, 3350-3359.

99. Wilkinson, G.N., 1961. *Biochem. J.* 80, 324-332.

100. Cantor, C.A., and Schimmel, P.R., *in Biophysical Chemistry Part II* p 409-480, W.H. Freeman and Company.

101. Peters, K., and Richards, F.M., 1977. *Ann. Rev. Biochem.* 46, 523-551.

102. Ostwald, W., 1914. *in Principles of Inorganic Chemistry* MacMillan and Company London.

104. Singer, S.J., and Nicholson, G.L., 1972. *Science* 175, 720-731.

105. Esfahani, M., Crowfoot, P.D., and Wakil, S.J., 1972. *J. Biol. Chem.* 247, 7251-7256.

106. Bertoli, E., Finean, J.B., and Griffiths, D.E., 1976. *FEBS Letters* 61, 163-165.

107. Solaini, G., and Bertoli, E., 1981. *FEBS Letters* 132, 127-128.

108. Mavis, R.D., and Vagelos, P.R., 1972. *J. Biol. Chem.* 247, 652-659.

109. Feo, F., Canuto, R.A., and Brossa, O., 1978. *Biochim. Biophys. Acta.* 504, 1-14.

110. Esfahani, M., Rudkin, B.B., Cutler, C.J., and Waldron, P.E., 1977. *J. Biol. Chem.* 252, 3194-3198.

111. Bertoli, E., Finean, J.B., and Griffiths, G.E., 1976. *FEBS Letters* 61, 163-165.

112. Chapman, D., Gomez-Fernandez, J.C., and Goni, F.M., 1979. *FEBS Letters* 98, 211-223.

113. Chapman, D., Gomez-Fernandez, J.C., and Goni, F.M., 1982. *Trends in Biochem Sci* 7, 67-70.

114. Gomez, J.C., Goni, F.M., Bach, D., Restall, C., and Chapman, D., 1979. *FEBS Letters* 98, 224-228.

115. Rothfield, L., and Romeo, D., 1971. *in Structure and Function of Biological Membranes.* (Rothfield, L., ed) p 251-284. Academic Press New York.

116. McElhaney, R.N., 1982. *Curr Topics in Membranes and Transport.* 17, 317-380.

117. Sandermann, H., 1978. *Biochim. Biophys. Acta.* 515, 209-237.

118. Gennis, R.B., and Hager, L.P., 1976. *in The Enzymes of Biological Membranes vol II.* (Martonosi, A., ed) p 493-504, Plenum Press New York and London.

119. O'Brien, T.A., and Gennis, R.B., 1979. *Biochemistry* 18, 804-809.

120. Umbreit, J.N., and Strominger, J.L., 1973. *Proc. Natl. Acad. Sci. USA.* 70, 2997-3001.

121. Kimura, H., and Futai, M., 1978. *J. Biol. Chem.* 253, 1095-1100.

122. Ragan, C.I., and Racker, E., 1973. *J. Biol. Chem.* 248, 6876-6884.

123. Rossi, E., Norling, B., Persson, B., and Ernster, L., 1970. *Eur. J. Biochem.* 16, 508

124. Ziola, B.R., and Scraba, D.G., 1976. *Anal. Biochem.* 72, 366-371.

125. Griffith, I.P., 1972. *Anal. Biochem.* 46, 402-412.

126. Moore, S., and Stein, W.H., 1954. *J. Biol. Chem.* 211, 893-905.

127. Moore, S., 1963. *J. Biol. Chem.* 238, 235-237.

128. Edelhoch, H., 1967. *Biochemistry* 6, 1948-1954.

129. O'Farrell, P.H., 1975. *J. Biol. Chem.* 250, 4007-4021.

130. Clarke, S., 1975. *J. Biol. Chem.* 250, 5459-5469.

131. Lowry, O.H., Rosebrough, N.J., Farr, A.L., and Randall, R.J., 1951. *J. Biol. Chem.* 193, 265-275.

132. Ellman, G.L., 1959. *Arch. Biochim. Biophys.* 82, 70-77.

133. Brumby, P.E., and Massey, V., 1967. *Meth. Enzymol.* 10, 463-474.

134. King, T.E., and Morris, R.O., 1967. *Meth. Enzymol.* 10,

634-641.

135. Capaldi, R.A., 1977. *In Membrane Proteins and Their Interactions with Lipids.* (Capaldi, R.A., ed) p 1-19, Marcel Decker Inc.

136. Schroeder, W.A., 1967. *Meth. Enzymol.* 11, 445-469.

137. Jacobson, G.R., Schaffer, M.H., Stark, G.R., and Vanaman, T.C., 1973. *J. Biol. Chem.* 248, 6583-6591.

138. Malkin, R., 1973. *In Iron Sulfur Proteins vol II.* (Lovenberg, W., ed) p 1-23, Academic Press.

139. Yoch, D.C., and Carithers, R.P., 1979. *Microbiol. Rev.* 43, 384-421.

140. Unden, G., Hackenberg, H., and Kroger, A., 1980. *Biochim. Biophys. Acta.* 591, 275-288.

141. Unden, G., and Kroger, A., 1980. *FEBS Letters* 117, 323-326.

142. Kearney, E.B., 1960. *J. Biol. Chem.* 235, 865-877.

143. Davis, K.A., and Hatefi, Y., 1971. *Biochemistry* 10, 2509-2524.

144. Kearney, E.B., Ackrell, B.A.C., Mayr, M., and Singer, T.P., 1974. *J. Biol. Chem.* 249, 2016-2020.

145. Davis, K.A., Hatefi, Y., Crawford, I.P., and Baltscheffsky, H., 1977. *Arch. Biochim. Biophys.* 180, 459-464.

146. Blobel, G., 1980. *Proc. Natl. Acad. Sci. USA.* 77, 1496-1500.

147. Wickner, W., 1980. *Science* 210, 861-868.

148. Englemann, D.M., and Steitz, T.A., 1981. *Cell* 23, 411-422.

149. Marchesi, V.T., Furthmayr, H., and Tomita, M., 1976. *Ann. Rev. Biochem.* 45, 667-698.

150. Graham, A., 1981. *Biochem. J.* 197, 283-291.

151. Smith, S., and Ragan, I.C., 1980. *Biochem. J.* 185, 315-326.

152. Wientjies, F.B., van't Riet, J., and Naninga, N., 1980. *Arch. Microbiol.* 127, 39-46.

153. Graham, A., and Boxer, D.H., 1981. *Biochem. J.* 195, 627-637.

154. Jones, R.W., Lamont, A., and Garland, P.B., 1980. *Biochem. J.* 190, 79-94.

155. Wickner, W., 1975. *Proc. Natl. Acad. Sci. USA.* 72, 4749-4752.

156. Morrison, M., 1974. *Meth. Enzymol.* 22, 103-109.

157. Birdsell, D.C., and Cota-Robles, E.H., 1967. *J. Bacteriol.* 93, 427-437.

158. van des Plas, J., Hellingwerf, K.J., Seijen, H.G., Guest, J.R., Weiner, J.H., and Konings, W.N., 1982. *Eur. J. Biochem.* (submitted).

159. Wrobel, J.A., and Stinson, R.A., 1978. *Eur. J. Biochem.* 85, 345-350.

160. Larsson-Raznikiewicz, M., and Jansson, J.R., 1973. *FEBS Letters* 34, 243-246.

161. Wrobel, J.A., and Stinson, R.A., 1981. *Biochim. Biophys. Acta.* 662, 236-245.

162. Ackrell, B.A.C., Kearney, E.B., and Mayr, M., 1974. *J. Biol. Chem.* 249, 2021-2027.

163. Cole, S.T., and Guest, J.R., 1979. *FEMS Letters* 5, 65-67.

164. Baginsky, M.L., and Hatefi, Y., 1969. *J. Biol. Chem.* 244, 5313-5319.

165. Ackrell, B.A.C., Kearney, E.B., and Coles, C.J., 1977. *J. Biol. Chem.* 252, 6963-6965.

166. Ohnishi, T., King, T.E., Salerno, J.C., Blum, H., Bowyer, J.R., and Maida, T., 1981. *J. Biol. Chem.* 256, 5577-5582.

167. Merli, A., Capaldi, R.A., Ackrell, B.A.C., and Kearney, E.B., 1979. *Biochemistry* 18, 1393-1940.

168. Girdlestone, J., Bisson, R., and Capaldi, R.A., 1981. *Biochemistry* 20, 152-157.

169. Yu, C-A., and Yu, L., 1980. *Biochemistry* 19, 3579-3585.

Appendix I.

The following flow chart is taken from a typical purification using Pfrd63. All assays were done in 200 mM sodium phosphate, pH 6.8 and 0.5 mM dithiothreitol.

Fraction	Total Units	% Recovery	SA
Crude Cell Envelope	120,000	100	60
Triton X-100 Extract	118,600	98.8	170
Ammonium Acetate Sup	105,400	87.8	180
Phenyl Sepharose	68,000	56.7	550

SA = Specific Activity (units/mg).

Appendix II.

Molar ellipticities were calculated from the observed ellipticities, measured in a Cary 60 spectrophometer equipped with a 6001 CD attachment, using the following equation;

$$[Q] = \frac{Q \times MRW}{10 \times C \times l}$$

[Q] = Molar ellipticity at a given wavelength.

Q = Measured ellipticity at a given wavelength.

MRW = Mean Residue Weight; a value of 115 was used.

l = Length of the light path through the sample. In this case it was 0.05 cm.

C = Protein concentration in mg/ml.

A plot of molar ellipticity versus wavelength was then constructed (cf Figure32).

The percentages of α-helix, β-sheet and random coil were then calculated using the equations given below. Essentially the percentages of α-helix and β-sheet were calculated by inserting the values for the molar ellipticities at different wavelengths into the appropriate equations. This generates three values each for the percentages of α-helix, β-sheet and random coil (by subtraction). The values reported in the text were the average values, all values were in good agreement.

Equation 1. Values of [Q] taken at 210 and 225 nm.

$(((Q_{210}-2200)\times 1276)+((Q_{225}+264)\times 5990))\div 204373560 = \alpha.$

$((Q_{210}-2200)-(\alpha \times 24100))\div 5990 = \beta.$

Equation 2. Values of [Q] taken at 215 and 220 nm.

$(((Q_{215}+669)\times 7860)-((Q_{220}+1880)\times 10009))\div 106021360 = \alpha.$

$((Q_{215}+669)-(26369\times\alpha))\div 10009 = \beta.$

Equation 3. Values of [Q] taken at 220 and 225 nm.

$(((Q_{220}+1800)\times 1276)+((Q_{225}+264)\times 7860))\div 267595840 = \alpha.$

$(Q_{220}+1800)-(31300\times\alpha)\div 7860 = \beta.$

Appendix III.

a) The rate constants for inactivation of fumarate reductase at alkaline pH were calculated as follows; semi-logarithm plots of activity (units/mg) versus time gave straight lines indicating first order kinetics. The slopes of these lines were multiplied by 2.303 to give the first order rate constants shown in Table 7.

b) The pseudo first order rate constants for the inactivation of fumarate reductase with DTNB in the presence and absence of phosphate were calculated as follows; the slopes of linear plots of activity (units/mg) versus time (Figure 33) were multiplied by 2.303 and divided by the concentration of DTNB (20 μM).